

USE OF IONIC STRENGTH RESPONSIVE POLYMERIC MICROGELS FOR  
FOULING REMOVAL IN MEMBRANE FILTRATION

A THESIS SUBMITTED TO  
THE GRADUATE SCHOOL OF NATURAL AND APPLIED SCIENCES  
OF  
MIDDLE EAST TECHNICAL UNIVERSITY

BY

FATMA ÇALILI

IN PARTIAL FULFILLMENT OF THE REQUIREMENTS  
FOR  
THE DEGREE OF MASTER OF SCIENCE  
IN  
CHEMICAL ENGINEERING

FEBRUARY 2019



Approval of the thesis:

**USE OF IONIC STRENGTH RESPONSIVE POLYMERIC MICROGELS  
FOR FOULING REMOVAL IN MEMBRANE FILTRATION**

submitted by **FATMA ÇALILI** in partial fulfillment of the requirements for the degree of **Master of Science in Chemical Engineering Department, Middle East Technical University** by,

Prof. Dr. Halil Kalıpçılar  
Dean, Graduate School of **Natural and Applied Sciences**

\_\_\_\_\_

Prof. Dr. Pınar Çalık  
Head of Department, **Chemical Engineering**

\_\_\_\_\_

Assoc. Prof. Dr. Pınar Zeynep Çulfaz Emecen  
Supervisor, **Chemical Engineering, METU**

\_\_\_\_\_

Assist. Prof. Dr. Ayşe Asatekin  
Co-Supervisor, **Chemical and Biological Eng., Tufts Uni.**

\_\_\_\_\_

**Examining Committee Members:**

Prof. Dr. Nihal Aydoğan  
Chemical Engineering, Hacettepe University

\_\_\_\_\_

Assoc. Prof. Dr. Pınar Zeynep Çulfaz Emecen  
Chemical Engineering, METU

\_\_\_\_\_

Prof. Dr. Levent Yılmaz  
Chemical Engineering, METU

\_\_\_\_\_

Assoc. Prof. Dr. Erhan Bat  
Chemical Engineering, METU

\_\_\_\_\_

Assist. Prof. Dr. Emre Büküşoğlu  
Chemical Engineering, METU

\_\_\_\_\_

Date: 01.02.2019

**I hereby declare that all information in this document has been obtained and presented in accordance with academic rules and ethical conduct. I also declare that, as required by these rules and conduct, I have fully cited and referenced all material and results that are not original to this work.**

Name, Surname: Fatma alı

Signature:

## ABSTRACT

### USE OF IONIC STRENGTH RESPONSIVE POLYMERIC MICROGELS FOR FOULING REMOVAL IN MEMBRANE FILTRATION

Çalılı, Fatma

Master of Science, Chemical Engineering

Supervisor: Assoc. Prof. Dr. Pınar Zeynep Çulfaz Emecen

Co-Supervisor: Assist. Prof. Dr. Ayşe Asatekin

February 2019, 101 pages

Stimuli-responsive polymeric surfaces can improve non-fouling properties of membranes and control their pore size and permeation characteristics upon alteration of stimulus intensity. In this study, zwitterionic poly(sulfobetaine methacrylate) (P(SBMA)) microgels have been added into the feed or deposited on the membrane surfaces to clean foulant deposits formed on the surface of the membranes after the filtration. Salt-responsive P(SBMA) microgels have altered their phase from swollen to shrunk, swollen to more swollen or shrunk to swollen due to the change of ionic strength in the medium. The effect of this size change in loosening and removing the fouling layer on the membrane was investigated.

In the performance tests, PES (polyether sulfone) based ultrafiltration membranes were used. P(SBMA) microgels used in the tests as the ionic strength responsive microgel were synthesized by inverse emulsion free-radical polymerization. Fouling resistances and flux recoveries of membranes were calculated using pure water permeances (PWP) of neat membranes, filtration fluxes and PWP of the membranes after applying the cleaning procedure to compare their cleaning efficiencies. Different foulants, which are Bovine serum albumin (BSA), humic acid in the presence of calcium ions (HA gel) and yeast cells, were used with or without the zwitterionic

microgels in the presence of different sodium chloride (NaCl) concentrations. To remove the cake layer, cleaning was performed via stirring and pure water/salt solution to make them shrink/swell.

P(SBMA) microgels can maximally swell in the presence of 0.5 M NaCl. Due to the formation of highly adsorptive fouling, the microgels could not provide an efficient BSA fouling removal. HA gel fouling in the absence of NaCl was the most irreversible while when NaCl was in the feed, reversibility was similar with or without microgel. This possibly implies a looser cake layer in the presence of NaCl. Yeast fouling, however, was more reversible when P(SBMA) microgels were used, compared to fouling with yeast in pure water or in 0.5 M NaCl.

In conclusion, this study showed how P(SBMA) microgels affect cake layer removal from PES UF membrane surface by adding them in the feed or depositing them on the membrane surface before the filtration. Presence of P(SBMA) microgels in the solution medium during the filtration could render higher flux recovery and cleaning efficiency than microgel-free filtrations for all foulants. Particularly, yeast fouling removal was achieved by adding of these microgels into the feed and depositing them on the membrane surface. These promising physical methods can be applicable to existing membrane processes to remove yeas-like foulants.

Keywords: Membrane fouling, ionic strength responsive microgels, P(SBMA), zwitterionic microgels

## ÖZ

### MEMBRAN FİLTRASYONUNDA KİRLENMEYİ TEMİZLEMELİK AMAÇLI İYONİK GÜCE DUYARLI POLİMERİK MİKROJELLERİN KULLANIMI

Çalı, Fatma  
Yüksek Lisans, Kimya Mühendisliği  
Tez Danışmanı: Doç. Dr. Pınar Zeynep Çulfaz Emecen  
Ortak Tez Danışmanı: Dr. Öğr. Üyesi Ayşe Asatekin

Şubat 2019, 101 sayfa

Uyarana duyarlı polimerik yüzeyler membranların kirlenmeme özelliklerini geliştirebilir ve uyarın şiddetinin değişmesiyle gözenek boyutlarını ve geçirgenlik özelliklerini kontrol edebilirler. Bu çalışmada, çift kutuplu P(SBMA) (poli (sülfobetain metakrilat)) mikrojelleri filtrasyon sırasında membran yüzeyinde oluşan kirlenici tabakalarını temizlemek için beslemeye eklenmiş ya da membrane yüzeyine biriktirilmiştir. Temizlik sırasında tuza duyarlı P(SBMA) mikrojelleri kirlilik tabakasının uzaklaştırılması için iyonik gücün değişmesinden dolayı şişmişten büzüşmüş, şişmişten daha çok şişmiş ve büzüşmüşten şişmiş faz değiştirmiştir. Böylece bu faz değişiminin membran üzerindeki kirlilik tabakasının uzaklaştırılmasına etkisi incelenmiştir.

Performans testlerinde PES (polietersülfon) bazlı ultrafiltrasyon membranlar kullanılmıştır. Testlerde iyonik güce duyarlı mikrojel olarak kullanılan P(SBMA) mikrojelleri ters emülsiyon serbest-radikal polimerizasyonu yöntemiyle sentezlenmiştir. Kirlilik dirençleri ve membranların akı geri kazanımları temizlik verimlerinin karşılaştırılması için membranın filtrasyondan önceki saf su geçirgenliği, filtrasyon akısı ve temizlik sonrası saf su geçirgenliği kullanılarak hesaplanmıştır. Farklı kirleniciler, bovin serum albumin (BSA), kalsiyum iyonları ile birlikte hümitik

asit (HA gel) ve maya hücreleri, çift kutuplu mikrojeller ile ya da mikrojelsiz farklı NaCl (sodyum klorür) konsantrasyonlarında kullanılmıştır. Kek tabakasını uzaklaştırmak için yapılan temizleme işlemi karıştırılarak ve mikrojelleri büzüşmüş/şişmiş hale getirmek için saf su/tuzlu su ile gerçekleştirilmiştir.

P(SBMA) mikrojelleri maksimum 0.5 M NaCl varlığında şişebiliyorlar. Yüksek derecede adsorptif kirlilik oluşumu nedeniyle, mikrojeller BSA kirliliğinin temizlenmesini etkili bir şekilde sağlayamamıştır. NaCl beslemede olduğunda tersinirlik mikrojelli ya da mikrojelsiz benzer iken NaCl yokluğunda tersinmez HA gel kirliliği en fazladır. Bu muhtemelen NaCl varlığında daha gevşek kek tabakası anlamına gelir. Bununla birlikte, maya kirliliği P(SBMA) mikrojelleri kullanıldığında daha temizlenebilir olmuştur.

Sonuç olarak, bu çalışma P(SBMA) mikrojellerinin, beslemeye eklenerek veya filtrasyondan önce membran yüzeyinde biriktirerek PES UF membran yüzeyinden kek tabakasının çıkarılmasını nasıl etkilediğini göstermiştir. Filtrasyon sırasında çözelti ortamında P(SBMA) mikrojellerinin varlığı, tüm kirleticiler için mikrojelsiz filtrasyonlardan daha yüksek akı geri kazanımı ve temizleme verimliliği sağlayabilir. Özellikle, bu mikrojellerin beslemeye eklenmesi ve membran yüzeyine deposit edilmesi yoluyla maya kirliliğinin giderilmesi sağlandı. Bu ümit verici fiziksel yöntemler, maya benzeri kirleticileri gidermek için mevcut membran işlemlerine uygulanabilir.

Anahtar Kelimeler: Membran kirliliği, iyonik güce duyarlı mikrojeller, P(SBMA), çift kutuplu mikrojeller

To My Mom

## ACKNOWLEDGMENTS

Firstly, I would like to express my appreciation to my supervisor Assoc. Prof. Dr. Pınar Zeynep Çulfaz Emecen for her support, guidance and patience. I would like to extend my gratitude to my co-supervisor Asst. Prof. Dr. Ayşe Asatekin to give me an opportunity to work in her laboratory and her research group for their help.

I would like to thank a lot my lab mates in Çulfaz-Emecen research group. I would like also to express my gratitude to Zeynep, Ecem and Canan who are more than lab mates for me. I thank all topic students who were temporary members of Çulfaz-Emecen research group during my master's period. Especially, I would like to acknowledge Khalid Gasimzade who was an ultra-pure water supplier during my last months. Cemil Abi also deserves my thanks for his technical help about setting up plexy membrane modules.

My deepest appreciation goes to my beloved family and Umut Çankır who always respect and support my decisions. I thank my stress ball, Choco who is my ugly but lovely cat. I would like also to thank a new member of my family, Serhat Kırıl, his parents and sister.

I would like to express my gratitude to my second home, METU and İskenderun Technical University (İSTE) where will be my work place in the future. And also, I would like to thank Asst. Prof. Dr. Emin Taner Elmas.

Finally, I would like to thank the Scientific and Technological Research Council of Turkey (TUBİTAK MAG116M047), National Science Foundation of the United States (NSF CBET-1427772 Project) and Coordination Office of Middle East Technical University (METU BAP 03-04-2014-001 Project) for their financial support.

## TABLE OF CONTENTS

ABSTRACT .....	v
ÖZ .....	vii
ACKNOWLEDGMENTS .....	x
TABLE OF CONTENTS .....	xi
LIST OF TABLES .....	xiv
LIST OF FIGURES .....	xvi
LIST OF ABBREVIATIONS .....	xix
LIST OF SYMBOLS .....	xxi
CHAPTERS	
1. INTRODUCTION .....	1
1.1. Ultrafiltration Membranes .....	3
1.2. Concentration Polarization and Membrane Fouling .....	5
1.3. Membrane Cleaning .....	8
1.4. Stimuli-responsive Polymeric Surfaces.....	9
1.5. Poly (sulfobetaine methacrylate) (P(SBMA)) Microgel: an Ionic Strength Polymeric Microgel .....	14
1.6. Foulants .....	16
1.7. Aim of the Study .....	18
2. EXPERIMENTAL METHOD.....	19
2.1. Materials .....	19
2.2. Membrane Production .....	20
2.3. P(SBMA) Microgel Synthesis .....	21

2.4. Scanning Electron Microscopy (SEM) .....	22
2.5. Dynamic Light Scattering (DLS) .....	23
2.6. High Resolution X-Ray Photoelectron Spectroscopy (XPS).....	23
2.7. Performance Tests.....	23
2.8. Adsorption Tests .....	27
2.9. Iron Oxide Decoration of P(SBMA) Microgels.....	28
3. RESULTS AND DISCUSSION .....	31
3.1. PES Based UF Membranes .....	31
3.2. P(SBMA) Microgels .....	33
3.3. Performance Tests.....	36
3.3.1. The Use of P(SBMA) Microgels with PES20 Membrane for BSA Fouling Removal .....	37
3.3.2. The Use of P(SBMA) Microgels with PES25 Membrane for HA Gel Fouling Removal .....	41
3.3.3. The Use of P(SBMA) Microgels with PES20 Membrane for Yeast Fouling Removal.....	48
3.3.4. P(SBMA) Microgel Deposition on PES20 Membrane for Yeast Fouling Removal.....	60
3.4. Adsorption Tests .....	64
3.5. Modification of PSBMA Microgels for Recovery.....	67
4. CONCLUSION .....	71
REFERENCES .....	73
APPENDICES	
A. Static Adsorption Tests.....	81
B. Adsorption Resistance Tests.....	86

C.	Calibration Lines .....	88
D.	XPS Analysis of P(SBMA) Microgels.....	91
E.	Filtration Data .....	92

## LIST OF TABLES

### TABLES

Table 2.1. Concentrations of iron salts and P(SBMA) used in the syntheses of the iron decorated microgels (Rubio-Retama et al., 2010) .....	29
Table 3.1. Comparison of P(SBMA) microgel syntheses according to initiators .....	35
Table 3.2. BSA adsorption on PES20 membrane in the presence of NaCl and/or P(SBMA) .....	65
Table 3.3. HA gel adsorption on PES25 membrane in the absence and presence of NaCl and/or P(SBMA) .....	65
Table 3.4. Yeast adsorption on PES20 membrane in the presence of NaCl.....	65
Table 3.5. Adsorption resistance test results compared with fouling resistances in the filtrations.....	66
Table 3.6. Elemental analysis of magnetic P(SBMA) particle by Energy-dispersive X-Ray (EDX) spectroscopy .....	69
Table A.1. BSA adsorption test results on neat PES20 membrane in the presence of NaCl.....	81
Table A.2. BSA adsorption test results on PES20 membrane with P(SBMA) microgel deposited in the presence of NaCl .....	82
Table A.3. HA gel adsorption test results on neat PES25 membrane in the presence of NaCl.....	83
Table A.4. HA gel adsorption test results on neat PES25 membrane .....	83
Table A.5. HA gel adsorption test results on PES25 membrane with P(SBMA) microgel deposited in the presence of NaCl .....	84
Table A.6. HA gel adsorption test results on PES25 membrane with P(SBMA) microgel deposited.....	84
Table A.7. Yeast adsorption test results on neat PES20 membrane in the presence of NaCl.....	85
Table E.1. BSA filtration data table.....	92
Table E.2. HA gel filtration data table.....	94

Table E.3. Yeast filtration data table (1) .....	96
Table E.4. Yeast filtration data table (2) .....	98
Table E.5. Yeast filtration data table using neat and P(SBMA) microgel deposited PES20 membranes .....	100

## LIST OF FIGURES

### FIGURES

Figure 1.1. Nominal pore size of membranes (Greenlee et al., 2009).....	1
Figure 1.2. Schematic view of the basic membrane module .....	2
Figure 1.3. Schematic view of UF separation mechanism according to shape of molecule.....	3
Figure 1.4. Dead-end and cross-flow filtrations .....	4
Figure 1.5. A schematic representation of concentration polarization .....	5
Figure 1.6. Types of membrane fouling .....	6
Figure 1.7. Chemical Structure of SBMA and P(SBMA) .....	14
Figure 2.1. Chemical structure of Polyether Sulfone (PES) .....	20
Figure 2.2. Scheme representation of polymer solution casting (a) and phase inversion (b).....	21
Figure 2.3. Experimental set-up for performance tests.....	24
Figure 2.4. Schematic representation of microgel sizes during the filtration (top) and cleaning (bottom).....	25
Figure 2.5. Schematic representation of microgel sizes during the filtration and cleaning on P(SBMA) microgel deposited membrane .....	26
Figure 3.1. SEM Images of PES based UF membranes .....	32
Figure 3.2. Hydrodynamic diameter of zwitterionic P(SBMA) microgels synthesized with V-70 in different NaCl concentration .....	34
Figure 3.3. Hydrodynamic diameter of P(SBMA) microgels synthesized with AIBN in different NaCl concentration .....	36
Figure 3.4. Normalized flux graphs of three serial BSA + 0.5 M NaCl (a), BSA+ 0.5 M NaCl +0.01 g/L P(SBMA) microgels (b) and BSA+ 0.5 M NaCl +0.1 g/L P(SBMA) microgels (c) filtrations on PES20 membrane and PWP values after the cleaning...	38
Figure 3.5. Resistance graphs of three serial BSA + 0.5 M NaCl (a), BSA+ 0.5 M NaCl +0.01 g/L P(SBMA) microgels (b) and BSA+ 0.5 M NaCl +0.1 g/L P(SBMA) microgels (c) filtrations on PES20 membrane.....	40

Figure 3.6. Normalized flux (a) and resistance (b) graphs of three serial HA gel filtrations without microgel and salt .....	42
Figure 3.7. Normalized flux graphs of three serial HA gel filtrations with 0.5 M NaCl + 0.1 g/L P(SBMA) microgels (a), 1 M NaCl + 0.1 g/L P(SBMA) microgels (b) and 0.5 M NaCl (c) .....	44
Figure 3.8. Resistance graphs of three serial HA gel filtrations with 0.5 M NaCl + 0.1 g/L P(SBMA) microgels (a), 1 M NaCl + 0.1 g/L P(SBMA) microgels (b) and 0.5 M NaCl (c).....	45
Figure 3.9. Photos of PES membranes taken after HA filtrations (top) and cleanings (bottom).....	46
Figure 3.10. Normalized flux graphs of yeast serial filtrations with 0.5 M NaCl + 0.1 g/L P(SBMA) microgels (a) and 0.5 M NaCl + 0.2 g/L P(SBMA) microgels at 150 rpm (Cleaning via ultra-pure water).....	49
Figure 3.11. Resistance graphs of yeast serial filtrations with 0.5 M NaCl + 0.1 g/L P(SBMA) microgels (a) and 0.5 M NaCl + 0.2 g/L P(SBMA) microgels at 150 rpm (Cleaning via ultra-pure water) .....	50
Figure 3.12. Normalized flux graphs of yeast serial filtrations in the presence of 0.1 M NaCl without microgel (a) and with 0.1 g/L P(SBMA) microgels (b) (Cleaning via 0.5 M NaCl) .....	51
Figure 3.13. Resistance graphs of yeast serial filtrations in the presence of 0.1 M NaCl without microgel (a) and with 0.1 g/L P(SBMA) microgels (b) (Cleaning via 0.5 M NaCl).....	53
Figure 3.14. Normalized flux (a) and resistance (b) graphs of yeast filtrations with 0.2 g/L P(SBMA) microgel and 0.1 M NaCl (cleaning via 0.5 M NaCl).....	55
Figure 3.15. Normalized flux (a) and resistance (b) graphs of yeast filtrations with 0.1 g/L P(SBMA) microgel and 0.1 M NaCl (cleaning via 0.5 M NaCl for 20 min).....	56
Figure 3.16. Normalized flux graphs of yeast serial filtrations in the presence of 0.1 M NaCl without microgel (a) and with 0.1 g/L P(SBMA) microgels (b) (Cleaning via 0.5 M NaCl and permeate volume: 20 mL) .....	58

Figure 3.17. Resistance graphs of yeast serial filtrations in the presence of 0.1 M NaCl without microgel (a) and with 0.1 g/L P(SBMA) microgels (b) (Cleaning via 0.5 M NaCl and permeate volume: 20 mL) .....	59
Figure 3.18. Normalized graphs of yeast serial filtrations on neat PES20 membrane (a) and on PES20 membrane with P(SBMA) deposited (b) (Cleaning via 0.5 M NaCl) .....	61
Figure 3.19. Resistance graphs of yeast serial filtrations on neat PES20 membrane (a) and on PES20 membrane with P(SBMA) deposited (b) (Cleaning via 0.5 M NaCl)	62
Figure 3.20. Schematic view of magnetic microgel recovery from retentate stream of the membrane process.....	67
Figure 3.21. Magnetic P(SBMA) particles .....	68
Figure C.1. BSA calibration line at 280 nm in UV/Visible Spectroscopy .....	88
Figure C.2. HA calibration line at 254 nm in UV/Visible Spectroscopy .....	89
Figure C.3. Yeast calibration line at 600 nm in UV/Visible Spectroscopy.....	90
Figure D.1. C1s XPS spectra of P(SBMA) microgels.....	91

## LIST OF ABBREVIATIONS

### ABBREVIATIONS

AIBN	2, 2'-Azobis(2-methylpropionitrile)
BA	N, N'-Methylenebis(acrylamide)
BSA	Bovine Serum Albumin
DLS	Dynamic Light Scattering
DMSO	Dimethyl Sulfoxide
EDX	Energy-dispersive X-Ray
HA	Humic Acid
LCST	Lower Critical Solution Temperature
MF	Microfiltration
MW	Molecular Weight
NF	Nanofiltration
PEG400	Polyethylene glycol 400
PES	Polyether sulfone
PMMA	Poly (methyl methacrylate)
PNIPAM	Poly(N-isopropylacrylamide)
P(NIPAM-co-Am)	Poly(N-isopropylacrylamide-co-acrylamide)
P(SBMA)	Poly (sulfobetaine methacrylate)
PSVBP	Poly(4-(2-sulfoethyl)-1-(4-vinylbenzyl) pyridiniumbetaine)
PVDF	Polyvinylidene fluoride
PWP	Pure Water Permeance

RO	Reverse Osmosis
SBMA	Sulfobetaine methacrylate
SEM	Scanning Electron Microscopy
THF	Tetrahydrofuran
TMP	Transmembrane Pressure
TRP	Thermo-Responsive Polymer
UF	Ultrafiltration
V-70	2, 2' Azobis(4-methoxy-2, 4-dimethylvaleronitrile)
XPS	X-Ray Photoelectron Spectroscopy

## LIST OF SYMBOLS

### SYMBOLS

A	Membrane area, cm <sup>2</sup> or m <sup>2</sup>
C <sub>f</sub>	Concentration of feed solution, g/L
C <sub>p</sub>	Permeate concentration, g/L
J	Permeate flux, L/h.m <sup>2</sup> .bar
R	Resistance, m <sup>-1</sup>
R <sub>fouling</sub>	Total fouling resistance, m <sup>-1</sup>
R <sub>irr</sub>	Irreversible fouling resistance, m <sup>-1</sup>
T	Temperature, °C
t	Time, s or h
V	Permeate volume, mL or L
η	Permeate Viscosity, Pa.s or bar.h
R	Retention or rejection, %



## CHAPTER 1

### INTRODUCTION

A membrane is a selectively permeable barrier between two phases which controls the rate of permeation of species through (Baker, 2012). In the membrane processes, separation depends on both physical and chemical properties of the membrane such as pore size, hydrophilicity, distribution of pores and charge. Membranes find a wide range of applications in the biotechnology, environmental, food and pharmaceutical industries. In membrane applications, the purpose is to allow the passage of some components in a solution while rejecting others.

Regarding industrial processes, membrane technology has advantages since there is low energy consumption and chemical usage for membrane separation processes. Also, separation at low temperatures is possible by this technology.

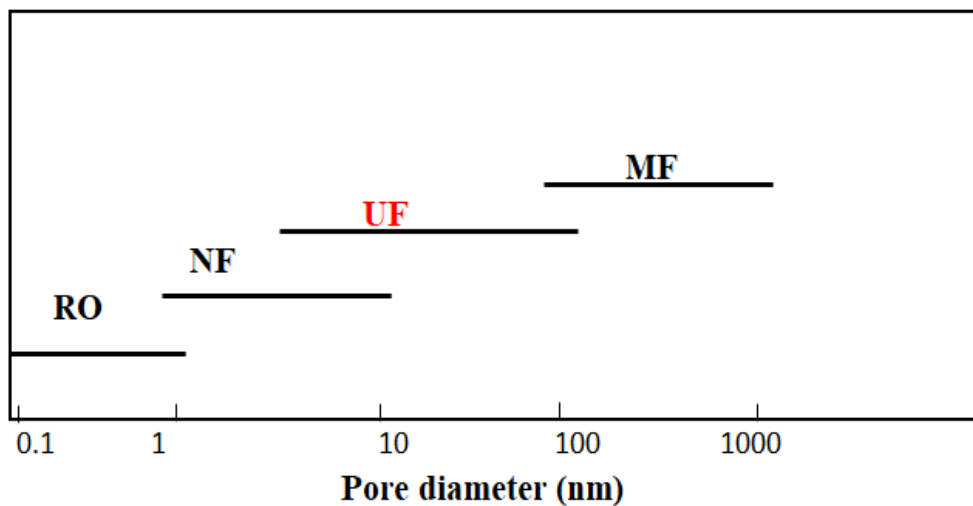


Figure 1.1. Nominal pore size of membranes (Greenlee et al., 2009)

As given in Figure 1.1 according to membrane pore size, pressure-driven membrane separation processes are classified as reverse osmosis (RO), nanofiltration (NF), ultrafiltration (UF) and microfiltration (MF) which are well developed industrial membrane applications (Baker, 2012). In porous membranes like UF and MF, separation is controlled according to pore size and shape (pore-flow model) while solution-diffusion model controls the separation in non-porous(dense) membranes.

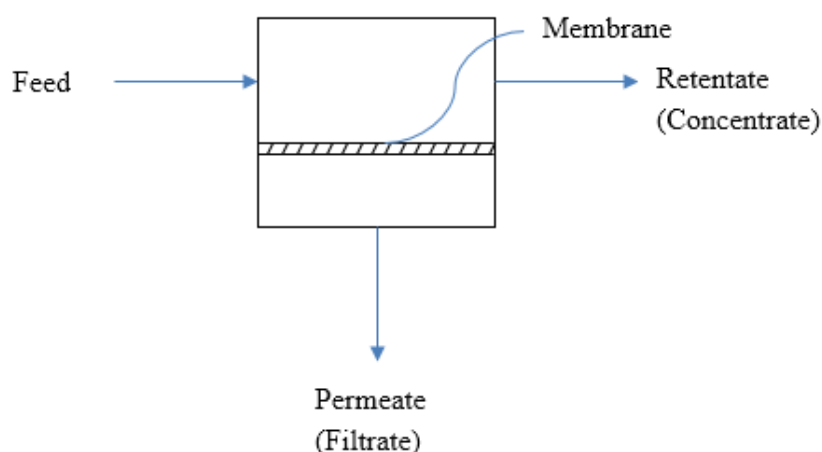


Figure 1.2. Schematic view of the basic membrane module

A basic membrane module consists of three streams; feed stream fed to the system, retentate or concentrate stream containing retained molecules and permeate stream passing through the membrane, respectively, as it is seen in Figure 1.2. The membrane transport is driven by one or more driving force(s) such as pressure, electrical potential, partial pressure, and concentration differences.

Membranes are used in several separation and purification processes such as water treatment, food industry, bio-separations, medical applications, and pharmaceutical industry. Especially in the recent years, the demand to fresh water access exceeds available water sources due to an increase of water waste and population growth; therefore, water purification becomes a worldwide concern (Greenlee et al., 2009). Membrane technology has an essential role to solve this because wastewater

treatment, drinking water production, and cooling water reuse are main applications of it (Fritzmann et al., 2007). Another area where membrane processes are widely used is medical applications such as blood purification, drug release, blood oxygenation, and hemodialysis.

### 1.1. Ultrafiltration Membranes

UF membranes, whose average pore diameter is in the 1-100 nm, are used in order to separate microsolute and water from colloids and macromolecules. Industrial applications of UF started to exist in the 1960s. Over the recent 30 years, this sector has gradually grown.

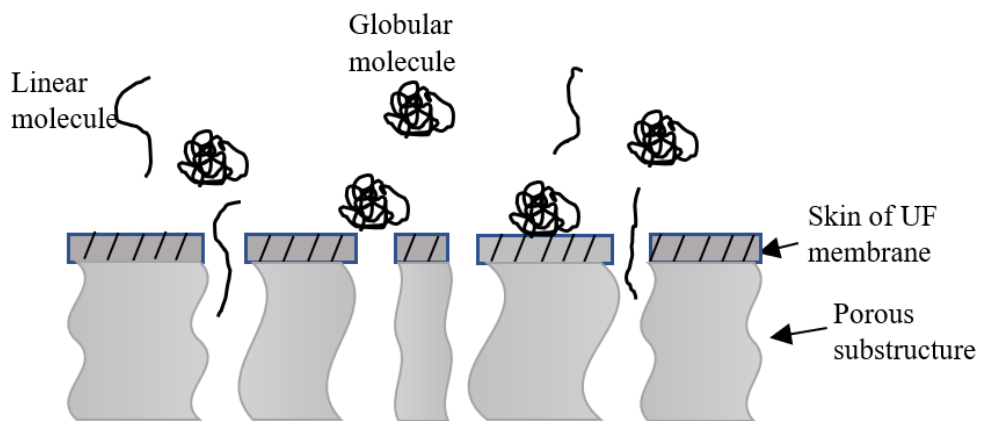


*Figure 1.3.* Schematic view of UF separation mechanism according to shape of molecule

The structures of UF membranes are usually asymmetric which means surface layer (skin of the membranes) performing the separation are finely porous while substructure of the membranes has much more open micropores that provides good mechanical property. The membranes are mostly characterized by solute molecular weight cut-off. However, it is not mere factor affecting permeation. Besides that, shape of solute molecules to be rejected is another main factor. In Figure 1.3, linear

polymer molecules which are water soluble can pass through the membranes whereas globular protein molecules are not able to deform to cross the membrane even though they have same molecular weight (Baker, 2012).

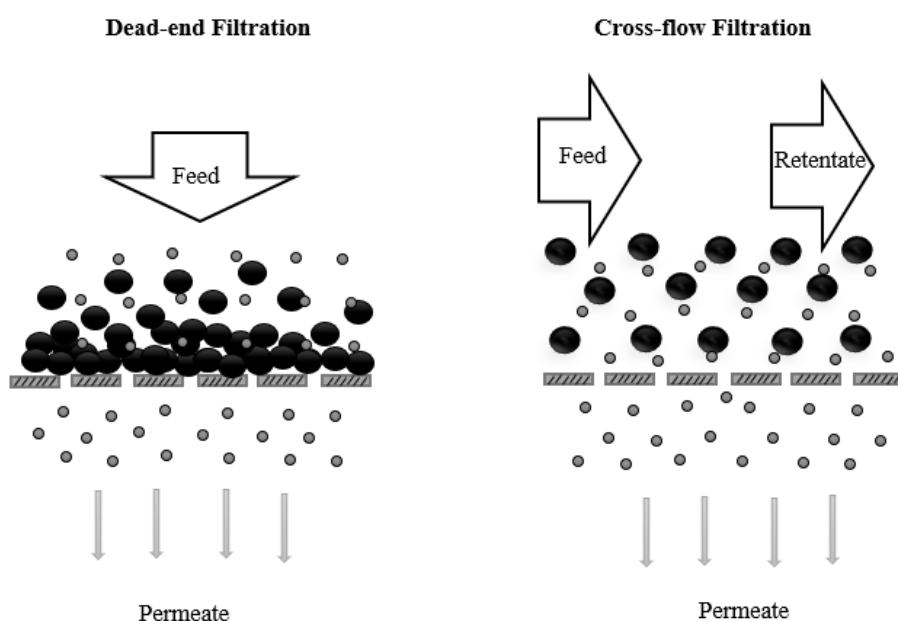


Figure 1.4. Dead-end and cross-flow filtrations

UF processes can be operated in either dead-end or cross-flow modes (Figure 1.4). While dead-end mode is preferred for small scale applications and feeds with small amount of material to be rejected, cross-flow systems are usually used for continuous work. In dead-end systems, there is no separate retentate stream and retained substances on the membrane surface during the filtration. In cross-flow systems, the feed flows tangential to the membrane which creates turbulence at the surface required for fouling control (Fröhlich et al., 2012).

In this study, polyether sulfone (PES) based UF membranes were used in dead-end mode as rejected molecules in dead-end filtration easily form as a cake layer on the

membrane surface, which made the analysis of fouling reversibility easier and more comparable among different experiments.

## 1.2. Concentration Polarization and Membrane Fouling

In UF membrane processes, flux through the membrane declines over time due to the phenomena of concentration polarization and fouling, which affects membrane performance and lifetime. The former results from selectively permeable nature of a membrane. This causes rejected species to accumulate in a mass transfer boundary layer adjacent to the membrane surface (Bacchin et al., 2006). While solvent molecules pass through the membrane via driving force, the transmembrane pressure (TMP), larger solute molecules are retained at the membrane surface. These larger solute molecules slowly diffuse back to the bulk solution, which leads to a concentration gradient near the membrane wall (Jonsson & Johansen, 1991). In other words, concentration of rejected species above the membrane surface steadily increases over time (Figure 1.5), which reduces permeate flow through the membrane.

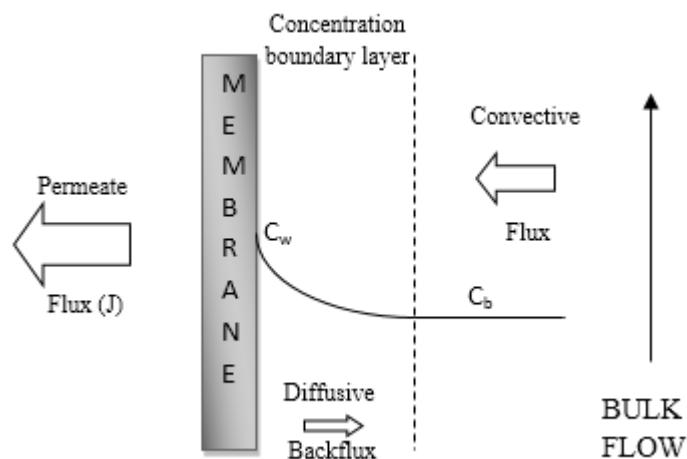


Figure 1.5. A schematic representation of concentration polarization

The latter, membrane fouling, can form in different types; plugging the pores, adsorptive fouling and cake (gel) layer formation as illustrated in Figure 1.6.

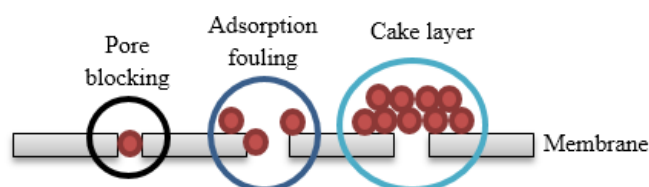


Figure 1.6. Types of membrane fouling

Pore blockage can occur when rejected molecules build-up in the pore structure partially or totally. This causes flux decline during the filtration. Specific membrane-solute interactions can lead to adsorption, one of the common membrane fouling type. Adsorptive fouling sometimes occurs even though there is no permeation flux, which results in an additional fouling resistance. In the case that degree of adsorption depends on the concentration of the solute, adsorption amount increases due to concentration polarization. Cake or gel layer formations occur owing to accumulation of the rejected species on the membrane surface causing a significant additional resistance.

Unlike the reversibility of concentration polarization, membrane fouling might lead to irreversible resistance causing a reduction in the membrane permeability. Indeed, reversibility based on resistance to cleaning is used to define characteristic of fouling: reversible fouling which can be cleaned by physical cleaning and irreversible fouling which cannot be possible to clean via physical methods (Kimura et al., 2004). Likewise, if there still is left over after chemical cleaning, it can be called as chemically irreversible fouling (Shi et al., 2014).

The effect of fouling on the membrane flux can be calculated by Darcy's Law (Equation 1) which is a model equation used to express the pressure-driven convective

flow in porous media (Baker, 2004). According to Darcy's law, resistance depends on the viscosity of permeate ( $\eta$ ), permeate flux ( $J$ ) and TMP.

$$R = \frac{TMP}{\eta J} \quad (1)$$

Permeate flux (Equation 2) depends on volumetric flowrate of permeate ( $V/t$ ) and membrane area of active side ( $A$ ).

$$J = \frac{V}{At} \quad (2)$$

Resistance is the property of a membrane; however, if  $\eta$  changes, pure water permeance (PWP) changes.

In this study, following correlation (Equation 3) depending on temperature ( $T$ ) was used to calculate the viscosity of permeate as it is almost pure water (van de Ven, 2008).

$$\eta = 0.497[T(^{\circ}\text{C}) + 42.5]^{-1.5} \quad (3)$$

Fouling resistances can be calculated by a series resistance model (Equation 4) in which the filtration flux at constant pressure is characterized with the total resistance ( $R_{total}$ ). As shown in Equation 5, fouling resistance ( $R_{fouling}$ ) is the sum of reversible ( $R_{reversible\ fouling}$ ) and irreversible ( $R_{irreversible\ fouling}$ ) fouling resistances. Membrane resistance ( $R_{membrane}$ ) can be determined using Darcy's law by measuring pure water flux at several pressures (TMP) which gives PWP. When  $R_{membrane}$  obtained from PWP measurement is subtracted from  $R_{total}$ , the resistance resulting from fouling on the membrane surface ( $R_{fouling}$ ) can be found. Resistance value calculated using PWP after physical cleaning is the sum of  $R_{membrane}$  and  $R_{irreversible\ fouling}$ . As a result, the fouling and cleaning effects on the membrane flux can be expressed with numerical values.

$$R_{total} = R_{membrane} + R_{fouling} \quad (4)$$

$$R_{fouling} = R_{reversible\ fouling} + R_{irreversible\ fouling} \quad (5)$$

Retention ( $\mathbb{R}$ ) of foulants is evaluated by the following equation:

$$\mathbb{R} (\%) = 100 \times \left(1 - \frac{C_p}{C_f}\right) \quad (6)$$

Here,  $C_p$  and  $C_f$  are concentration of foulants in the permeate and feed solutions, respectively.

### 1.3. Membrane Cleaning

Concentration polarization and membrane fouling cannot be avoided which has narrowed down the applications of UF membranes since they cause to shorten membrane lifetime, deteriorate the performance of a membrane, and rise operating cost (Potts et al., 1981). Many researchers have dedicated to modification of membrane surface to enhance anti-fouling performance of it. Although modified membranes were usually fouled less compared to neat ones, fouling is most of time inevitable which means membrane cleaning is necessary. There are several methods to clean a membrane which is fouled. These are usually classified into two groups which are physical and chemical cleaning methods. Sometimes, these two cleaning ways are applied together to obtain higher cleaning efficiency.

In the physical cleaning, foulants are forced to remove from the membrane surface by altering hydrodynamics or creating turbulence in the system. Mechanical and hydraulic forces are utilized separately or together for physical membrane cleaning. They lead to changing the shear forces on the surface of membrane to remove the deposits. There are many ways to apply them; reversing TMP called backwashing, rotating disks to create turbulence or air sparging. In the cross-flow systems, reversible fouling layer on the membrane system can be removed with a turbulence created via hydraulic flushing across the surface of membrane facing the retentate side (Shorrock et al., 1998). The flushing flow can be in the direction of the feed stream -forward flush- or in the reverse direction which is from permeate to the feed side -backwash. Backwashing dislodges the deposited materials from the membrane surface and pores

on the external side by a reversed flow (Gao et al., 2011). This method should be done carefully in order not to damage the membrane seeing that required flux for backwashing is usually two or more than two times higher than the filtration flux, so it is usually preferred to use the cleaning of ceramic or hollow fiber membranes which can endure a reversed flow from the permeate side (Baker, 2004).

If chemicals are used in the cleaning procedure, it is called as a chemical cleaning. Chemical agents modify the chemistry of solution medium to alter foulant-membrane and foulant-foulant interactions or react with rejected materials in order to decompose them. This method is usually applied to clean irreversible foulants. It is possible to divide chemical agents used for chemical cleaning into three categories; acid solution is effective for cleaning of inorganic foulants, alkali solution is responsible for removal of organic fouling, and biocide solution is used for the reduction of bio-fouling (Gao et al., 2011).

Despite the fact that chemical cleaning can provide total recovery of initial flux in many such cases, it has several drawbacks. Chemical agents may damage membranes, alter membrane properties or shorten the membrane lifespan since oxidants, acids, bases, detergents and enzymes commonly used for membrane cleaning can be highly hazardous and/or active substances (Baker, 2004). Hence, chemical cleaning ways are neither environmentally friendly nor cost effective compared to physical cleaning methods.

#### **1.4. Stimuli-responsive Polymeric Surfaces**

It is known that properties of a membrane surface such as hydrophilicity, charge properties, roughness, and chemical structure intensely affect non-fouling features of a membrane (Vrijenhoek et al., 2001). Recently, the use of stimuli-responsive polymers has attracted great attention since they have intrinsic properties. They change their size from swollen to shrunk or vice versa in the presence of a stimulus

which can be physical stimuli like pH, light, temperature, pressure, ionic strength, magnetic and electric field etc (Gorey & Escobar, 2011).

Yu et al. (2011) modified the surface of thin-film composite polyamide RO membranes via deposition of poly(N-isopropylacrylamide-co-acrylamide) (P(NIPAM-co-Am)), a thermo-responsive polymer, on the membrane surface. By this method, they achieved modified membranes indicating easy cleaning ability and enhanced antifouling features. They carried experiments in the cross-flow system using a model foulant, bovine serum albumin (BSA), via modified and virgin membranes. They found that deposition of P(NIPAM-co-Am) on the membrane surface increased the hydrophilicity and also thermo-responsive polymer facilitated the cleaning of fouling layer on the membrane surface by the phase transition above and below the lower critical solution temperature (LCST), which is a certain temperature that the polymer changes its size.

Another study related to modification of thin-film composite RO membrane was done by Meng and coworkers (2014). They grafted poly(4-(2-sulfoethyl)-1-(4-vinylbenzyl)pyridiniumbetaine) (PSVBP) - a zwitterionic polymer- onto the commercial membrane using redox initiated graft polymerization. Grafting of PSVBP enhanced the hydrophilicity of the membrane surface and negatively charged the membrane which provided to increase retention of NaCl from 98.0% to 99.7%. Moreover, PSVBP shrinks at pure water or low salt concentration while its chains swell and form a hydration layer around them at high salt concentrations. Thanks to salt responsive property of PSVBP, fouling layer could be easily released from the membrane surface by tuning salinity conditions during the cleaning.

You et al. (2016) claimed that cleaning by regulating temperature needs more energy than cleaning by regulating salt concentration. They prepared both PNIPAM grafted RO membranes, thermo-responsive, and PSVBP grafted membranes, ionic strength responsive, so as to evaluate cleaning performance and anti-fouling properties of stimuli-responsive RO membranes. They reported that antifouling properties of

modified membranes with PNIPAM and PSVBP were improved when using calcium carbonate as the model foulant; however, PSVBP grafted membrane exhibited higher cleaning performance and superior antifouling feature because of its hydrophilicity, negative charged surface and low roughness of the membrane surface.

Bera and coworkers (2015) prepared temperature or pH or both temperature and pH responsive UF membranes which have high flux and foul less by blending polyvinylidene fluoride (PVDF) and amphiphilic copolymer via phase inversion method. In this research, since poly (methyl methacrylate) (PMMA) is compatible with PVDF, different amphiphilic copolymers (PMMA-co-X) were synthesized to prepare these stimuli responsive blended UF membranes. Compared to neat PVDF membranes, all PVDF-copolymer blend membranes displayed non-fouling property and higher flux owing to enhanced hydrogen bonding capacity with water and higher porosity of them.

Ngang et al. (2017) found that the thermo-responsive PVDF/ silica-poly (N-isopropylacrylamide) ( $\text{SiO}_2$ -P(NIPAm)) composite membrane tended to adsorb less oil in ultra-pure water than virgin PVDF membrane because P(NIPAm) addition increased hydrophilicity of the PVDF membrane. They proved that the actuation force by alternating thermal cycle which provided swelling and shrinking of the P(NIPAm) located on the membrane surface removed approximately 20% of adsorptive fouling layer from the surface of the composite membrane.

Kaner and co-workers (2017) developed photo-responsive membranes that are able to clean fouling layer themselves via changing surface morphology under visible or UV light. Porous support membranes were coated with comb-shaped graft copolymers having photo-reactive side chains in order to prepare light responsive thin film composite membranes. While the membranes alter their surface conformation, they can maintain stable pure water permeance and pore size.

Yu et al. (2012) investigated the effect of thermo-responsive polymer (TRP) on bovine serum albumin (BSA) fouling removal from the surface of RO membranes. After the

filtration, fouled membranes were soaked by TRP aqueous solution at temperature below lower critical solution temperature (LCST), which is the temperature that polymer chains change their configuration. In this stage, they claimed that TRP diffused into the cake layer over time. After that, TRP solution was heated above LCST to make TRP insoluble. Finally, cleaning procedure was done with rinsing the membrane with pure water at room temperature. As a result, they observed that compared to cleaning via only pure water, cleaning efficiency significantly increased by phase transition of TRP. In addition, Aksoy (2018) studied humic acid gel fouling removal using PNIPAm (thermo-responsive) and poly(n-isopropylacrylamide-co-sulfobetainemethacrylate) (P(NIPAm-co-SBMA), both ionic strength and thermos-responsive) microgels. These microgels were deposited into fouling layer during the filtration at different temperatures and salt concentrations and membrane cleaning was performed by thermal cycle. She indicated that addition of P(NIPAm-co-SBMA) microgels into the feed solution provided lower flux decline during the humic acid filtrations and increased the cleaning efficiency. Apart from these two studies, there is no study in the literature related to cake layer removal by using stimuli-responsive polymers.

Besides enhancing antifouling properties and cleaning efficiency of the membranes, stimuli-responsive polymeric microgels are utilized to produce composite membranes with multifunctionalities such as responsive flow regulation, dynamic pore sizing and size screening (Adiga et al., 2009).

Shi et al. (2008) studied salt responsive polyether sulfone (PES) UF membranes to improve anti-fouling properties of PES membranes. After casting polymer solution, membranes were coagulated in pure water and salt solution baths. The flux of the membranes depended on ionic strength because of their zwitterionic nature. Permeate flux can be considerably adjustable by altering salt concentration of the coagulation bath. Zhai et al. (2003) also produced ionic strength responsive PVDF MF membranes by phase inversion in the coagulation bath containing different salt concentration at different temperatures.

Huang et al. (2009) produced biocompatible salt responsive UF membranes using poly-N-vinyl lactam microgels to change pore size of membranes for control of protein transmission. Polymer shrinks at low NaCl concentration while it swells at concentrated NaCl solution. Hence, the pores of membranes close at low salt concentrations and fully open at high salt concentration so that protein transmission can be adjusted through the membranes.

Chen et al. (2013) tried to achieve quadri-stimuli-sensitive grafted membranes which are able to change their size with changing pH, temperature, anion species and salt concentration. They aimed that grafted membrane pores can fully open or partially close according to environmental conditions. Similarly, Tamada et al. (1995) fabricated hydrolyzed pH-responsive membranes to control pore diameter of membranes. Some researchers, also, improved light sensitive thin film composite membranes by grafting photo-responsive polymers on the membrane surfaces or adsorbing azobenzene to the pores of the membranes to alter permeate flux of the membranes (Trushinski et al., 1993, Chung et al, 1994, Park et al, 1998 & Weh et al, 2002).

### 1.5. Poly (sulfobetaine methacrylate) (P(SBMA)) Microgel: an Ionic Strength Polymeric Microgel

Zwitterions are molecules having functional groups with equal number of positive and negative charges. In the recent years, researchers have focused on zwitterionic polymers which are perfect materials used for control of membrane fouling due to their superior hydrophilic nature (You et al., 2016, Kaner et al., 2017, Chiang et al. 2012 & Zhao et al., 2011).

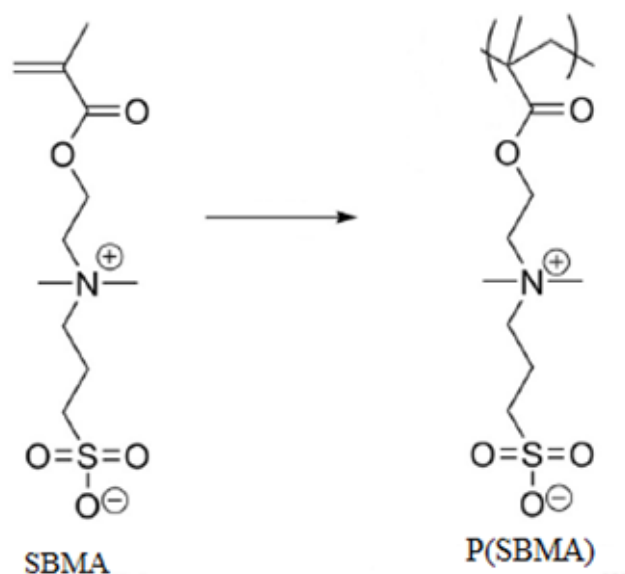


Figure 1.7. Chemical Structure of SBMA and P(SBMA)

In this study, poly (sulfobetaine methacrylate) (P(SBMA)), a typical zwitterionic polymeric microgel, was synthesized by inverse emulsion free radical polymerization and utilized in the performance tests as it has been commonly used to modify membranes in the literature (Lalani et al., 2011, Li et al., 2012, You et al., 2016, & Bengani-Lutz et al., 2017). Figure 1.7 represents the structure of this zwitterionic polymer.

P(SBMA) microgels can collect water around themselves thanks to their strong hydrogen bonding capacity (Choi et al., 2015). In addition to this, they interact with water molecules electrostatically, which leads to the formation of a strong hydration layer on the microgels. The main reason of these electrostatic interactions between water molecules and microgels is the coexistence of positively and negatively charged groups in the monomer, sulfobetaine methacrylate (SBMA) (Lalani et al., 2011).

Jhan and coworkers (2014) reported that P(SBMA) shows ‘anti-polyelectrolyte’ behavior which means it can alter its polymer conformation in salt solutions. If solution contains salt ions, zwitterions of P(SBMA) microgels attract salt ions and this renders them to remarkably change their hydrated states. In other words, the presence of salt ions in the solution improve the solubility of P(SBMA) microgels since polymer chains of P(SBMA) expand with electrostatic interactions among salt ions, water molecules and zwitterions (You et al., 2016). Moreover, P(SBMA), a salt-responsive or ionic strength responsive polymer, is able to release foulants via changing polymer conformation by regulating ion concentration.

Looking at the literature, it is known that there are several ionic strength responsive polymers not only as membrane materials but also for other purposes such as using as a biomaterial. For example, phosphobetaine and carboxybetaine, widely used pendant groups for zwitterionic polymeric microgels like sulfobetaine in the literature, have been gaining great attention as antifouling and biocompatible materials (Li et al., 2012).

In this study, P(SBMA) crosslinked in the form of microgels was used for fouling removal.

## 1.6. Foulants

Three modal foulants widely used in the literature, humic acid (HA) in the presence of calcium chloride ( $\text{CaCl}_2$ ), bovine serum albumin (BSA), and yeast cells, were selected to test cleaning performance of the microgels in the filtrations. All foulants are organic foulants; HA is a main foulant during UF applications of surface water treatment (Yuan et al., 2000) and the others are potential foulants and main components of fouling in the food and bioprocessing with membranes as well as membrane bioreactors (MBRs) (Mores et al., 2003 & Hashino et al., 2011).

Soils involve HA due to a degradation of proteins, lignin and carbohydrates so surface water generally contains HA whose amount changes seasonally. This substance alters the color of water from yellowish to brownish due to its natural color. In addition to this, it is the main source of fouling problems in the UF of natural water sources. HA is able to bind some metal ions such as copper and cadmium at a certain pH levels (Nyström, 1996). Besides that, HA forms gel with calcium ions which act a binding agent of carboxyl functional groups of HA (Srisurichan et al., 2005). For this reason, deposition of HA gel increases with increasing calcium ions which results in flux decline. HA fouling is a set of phenomena consisting of concentration polarization, adsorption and cake layer formation.

BSA, a water-soluble natural polymer in blood plasma of mammals, contains approximately 30-50 amino groups (Du et al., 2013). Its main duty is to carry drugs, cholesterol, fatty acid, metals and bile pigments. Furthermore, it plays an important role of osmotic pressure regulation between compartments (Roche et al., 2008). Due to its intrinsic binding ability to other substances, BSA causes different types of fouling on the membrane surface such adsorptive fouling and gel layer formation. Hashino (2011) stated that degree of BSA adsorptive fouling is related to hydrophilicity of membrane surface. Amount of BSA adsorption is high on hydrophobic membrane surfaces compared to hydrophilic ones.

Many researchers have been studying on living yeast cells as a modal foulant for biofouling since they not only cause deposition and adsorption on the membrane surface but also interact with proteins and some metal ions (Li et al., 2018). Ye and Chen (2005) reported that living yeast cells aggregate with proteins leading to an increase of cake layer on the membrane surface during the filtration.

### **1.7. Aim of the Study**

In this study, ionic strength responsive P(SBMA) microgels were utilized for cleaning the fouling layer in the membrane filtration by adding them into feed solution so that they can co-deposit in the cake layer on the membrane surface during the filtration. After that, fouling layer removal was performed via changing the size of the microgels due to alteration of the ionic strength in the solution. By this way, it was aimed to clean the fouling owing to the size change of the ionic strength responsive microgels by ‘breaking’ the gel layer. This proposed approach can be more practical than blending them with membrane solutions or grafting them on the membrane surfaces since it might be possible to apply this technique in any process independent of membrane and module types in the systems. Large amount of cake or gel layer formation is quite prevalent in the wastewater treatment and MBR systems and downstream processes in biotechnology. Some cleaning procedures such as forward flush and backwash are usually preferred to overcome this. However, after a certain amount of fouling has occurred, they are less efficient. Proposed cleaning technique is an alternative method or supplement to these kind of physical cleaning operations.

## CHAPTER 2

### EXPERIMENTAL METHOD

#### 2.1. Materials

Polyethersulfone (PES, Ultrason E6020P) which was used as a membrane material in this study was supplied by BASF. 99.5% pure dimethyl sulfoxide (DMSO), the solvent of PES, and polyethylene glycol 400 (PEG400, MW = 400 Da), a pore-forming agent, were purchased from Sigma Aldrich and Merck. Reverse-osmosis (RO) water was used as non-solvent for coagulation bath during the membrane production.

Hexane ( $\geq 95\%$ ), N, N'-Methylenebis(acrylamide) (Bis- acrylamide (BA), 99%), 2-(Methacryloyloxy)ethyl]dimethyl-(3-sulfopropyl)ammonium hydroxide (sulfobetaine methacrylate (SBMA), 97%), 2, 2'-Azobis(2-methylpropionitrile) (AIBN), surfactants (Tween 80 and Span 80) were bought from Sigma Aldrich. 2,2'-Azobis(4-methoxy-2,4-dimethylvaleronitrile) (V-70) and tetrahydrofuran (THF) were purchased from Wako Chemicals USA and VWR (West Chester, PA), respectively.

Two foulants, humic acid sodium salt and bovine serum albumin (BSA, MW = 66 kDa), calcium chloride dihydrate ( $\geq 99\%$ ), sodium hydroxide and hydrochloric acid (37%) were supplied by Sigma Aldrich, as well. Sodium chloride, Iron(III) chloride hexahydrate ( $\geq 99\%$ ), and Iron(II) chloride tetrahydrate ( $\geq 99\%$ ) were purchased from Merck. Dr. Oetker brand instant dried yeast was bought from supermarket.

Technical ethanol (99.5%) was supplied from Sigma Aldrich or Gurup Deltalar. Ultra-pure (UP) water was used in performance tests to prepare feed solutions and in physical cleaning.

## 2.2. Membrane Production

PES (Figure 2.1) was used as a membrane polymer. According to PES concentration, two different polymer solutions were prepared. The first consisted of 20% PEG400, 20% PES and 60% DMSO while the second consisted of 20% PEG400, 25% PES and 55% DMSO. Membranes were called as PES20 and PES25, respectively.

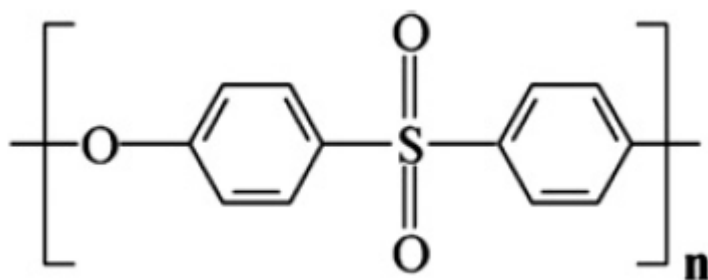


Figure 2.1. Chemical structure of Polyether Sulfone (PES)

After these polymer solutions were prepared, they were mixed for approximately a week in the roller mixer to dissolve them completely. When they totally dissolved, they were cast via casting bar whose thickness is 250  $\mu\text{m}$  and then, coagulated into coagulation bath containing pure water (phase inversion method) for 10 minutes as shown in Figure 2.2. Next, to remove their solvents, they were kept for 1 hour into a beaker containing RO water and then water in the beaker was refreshed to keep them in it for 24 hours. Finally, they were stored at 20% ethanol- 80% water solution to protect them from microorganisms.

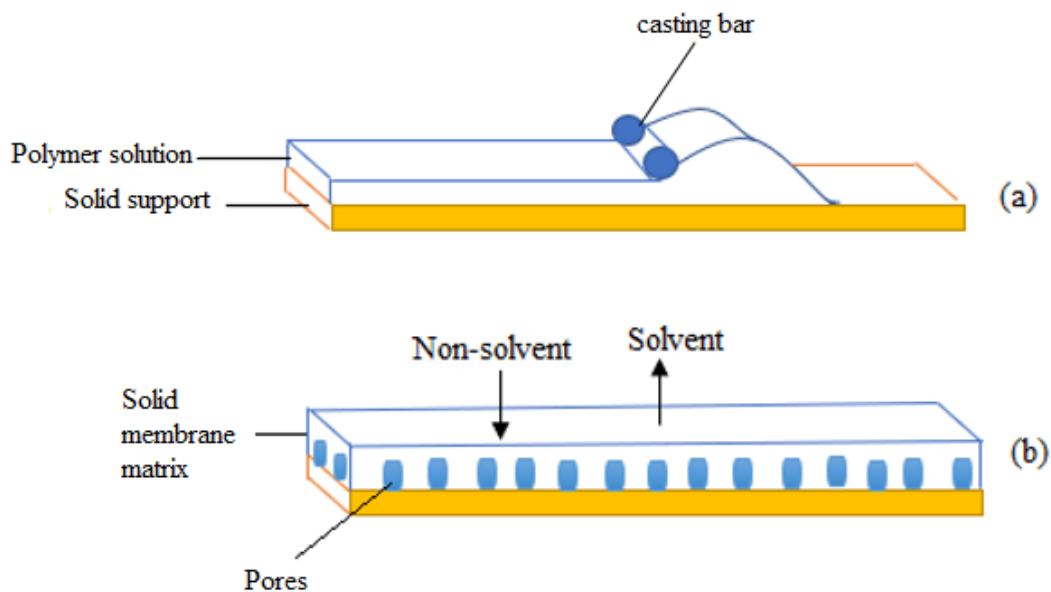


Figure 2.2. Scheme representation of polymer solution casting (a) and phase inversion (b)

### 2.3. P(SBMA) Microgel Synthesis

P(SBMA) microgels were synthesized by inverse emulsion free-radical polymerization that is a process based upon polymerizing water soluble monomers dispersed in an oil phase. Water-in-oil type emulsions where polymer chains are trapped in water droplets form in this process.

P(SBMA) microgel synthesis was done using two different initiators; V-70 and AIBN.

#### *P(SBMA) Microgel Synthesis with V-70*

Monomer solution consisting of 0.916 g SBMA (monomer), 0.0184 g BA (cross-linker) and 2 mL UP water was prepared in the round bottom flask (500 mL) and stirred at 200 rpm until SBMA were completely dissolved. At the same time, continuous phase solution composed of 160 mL hexane (solvent), 0.032 g V-70 (initiator), 5.6 g Tween 80 (surfactant) and 6.4 g Span 80 (surfactant) was mixed in

the ice bath so that V-70, a low temperature free-radical initiator, cannot activate before adding the monomer solution. After that, these two solutions were combined in the ice bath. Then, they were well-mixed under the nitrogen for 30 minutes and the round bottom flask containing combining solution was placed into the oil bath at 40°C the way that all liquid was submerged. Next, polymerization reaction was allowed to take place for 4 hours at 320 rpm. After 4 hours, polymer precipitate was washed by acetone or THF overnight three times by stirring at 240 rpm to get rid of solvent, initiator, surfactants, leftover monomer and cross-linker. After each washing, solution was left to settle for a night and then the supernatant solution was poured away. Finally, obtained P(SBMA) microgels were dried under the vacuum below the reaction temperature.

#### *P(SBMA) Microgel Synthesis with AIBN*

In this synthesis, continuous phase solution composed of 160 mL dodecane (solvent), 0.0085 g AIBN (initiator), 5.6 g Tween 80 (surfactant) and 6.4 g Span 80 (surfactant) different from the synthesis with V-70. Activation temperature of AIBN is around 70°C; therefore, reaction took place at that temperature. During the reaction, polymer precipitation could not be observed at the end of 4 hours. For this reason, reaction time was increased from 4 to 15 hours in order to increase the yield. All other conditions of the synthesis were kept same with P(SBMA) microgel synthesis done by V-70.

#### **2.4. Scanning Electron Microscopy (SEM)**

Membrane morphologies were analyzed by SEM. While membrane surfaces were analyzed by SEM (QUANTA 400F Field Emission SEM) in METU Central Laboratory, their cross-sections were observed by Phenom Pure Desktop SEM in Tufts University. Samples for cross-section analysis were frozen with liquid nitrogen and then they were broken. All samples were kept under vacuum overnight before they were sputter-coated with Au/Pd.

## **2.5. Dynamic Light Scattering (DLS)**

DLS analysis was done at room temperature (20-25°C) at Tufts University, USA (Malvern Zetasizer Nano) to measure hydrodynamic diameters of P(SBMA) microgels. DLS solutions were prepared in different salt concentrations to measure their size according to ionic strength of the solution.

### *DLS Solution Preparation*

250 mL of 0.01 g/L P(SBMA) microgel solution were stirred at 300 rpm at least 8 hours. After that, the solution was filtered via 0.45 µm syringe filter to remove dust and aggregated P(SBMA) particles. Then, 0, 0.1168 g, 0.5840 g and 1.164 g NaCl were added into 2 mL sample bottles separately. Next, microgel solution was added up to 2 mL line to obtain microgels in 0 M, 0.1 M, 0.5 M and 1 M NaCl solutions and then, samples were mixed using vortex on highest setting for 5-10 second to dissolve salt in the solutions. Finally, samples were sonicated at least 10 minutes just before the DLS measurement.

## **2.6. High Resolution X-Ray Photoelectron Spectroscopy (XPS)**

P(SBMA) powder particles were analyzed by high resolution XPS spectra (PHI) in METU Central Laboratory. Chemical analysis of P(SBMA) particles was done to understand their surface chemistry. Before analyzing them, they were dried under vacuum for 3 hours.

## **2.7. Performance Tests**

50 mL Amicon stirred cell was used at room temperature and 2 bar TMP in dead end mode without stirring for BSA and HA gel filtrations and with stirring at 150 rpm for yeast filtrations for all performance tests. Schematic view of experimental set-up is given in Figure 2.3. Active surface area of the membrane was 13.4 cm<sup>2</sup>. In the filtration

tests, 40 mL feed solutions were prepared, and 10 mL permeates were usually collected at each time so that foulants can accumulate in the same amount on the surface of membrane during the filtration. Foulant concentrations were 1 g/L BSA, 1 g/L HA with 2 mM CaCl<sub>2</sub>, and 1 g/L yeast suspension while 0.01 g/L, 0.1 g/L or 0.2 g/L P(SBMA) microgels were used in the feed solutions. The aim of using P(SBMA) microgels in various concentrations is to observe the effect of P(SBMA) microgel concentration on the fouling removal. Cleaning was done by three ways; changing size of the microgels from swollen to shrunk (Figure 2.4-a), from swollen to more swollen (Figure 2.4-b), from shrunk to swollen (Figure 2.5).

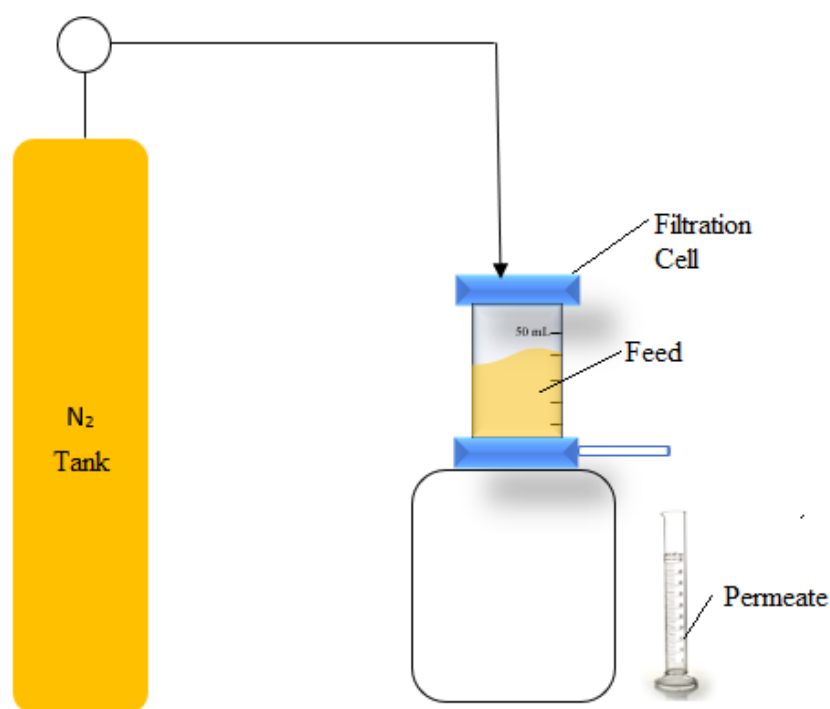
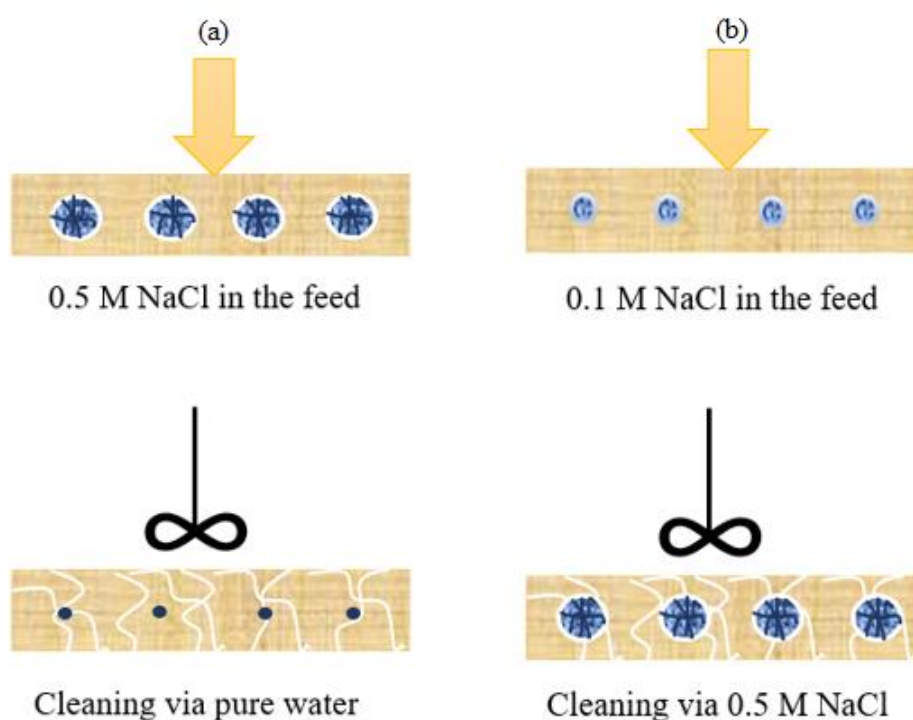


Figure 2.3. Experimental set-up for performance tests

To begin with, pure water permeance (PWP) of fresh membranes was measured at room temperature using UP water before the filtrations. After that, following filtration and cleaning procedures were applied.

### *Filtration and cleaning procedure 1*

- Filtration was performed in the absence/presence of 0.5 M NaCl in which microgels had maximum swelling ratio.
- After the filtration, retentate solution was replaced with 60 mL UP water where microgels were shrunk.
- Cleaning was done via stirring at 400 rpm for 5 minutes.



*Figure 2.4.* Schematic representation of microgel sizes during the filtration (top) and cleaning (bottom)

### *Filtration and cleaning procedure 2*

- Filtration was performed in the presence of 0.1 M NaCl in which microgels were slightly swollen.

- After the filtration, retentate solution was replaced with 0.5 M NaCl solution in which microgels had maximum swelling ratio.
- Cleaning was done via stirring at 500 rpm for 5 minutes.

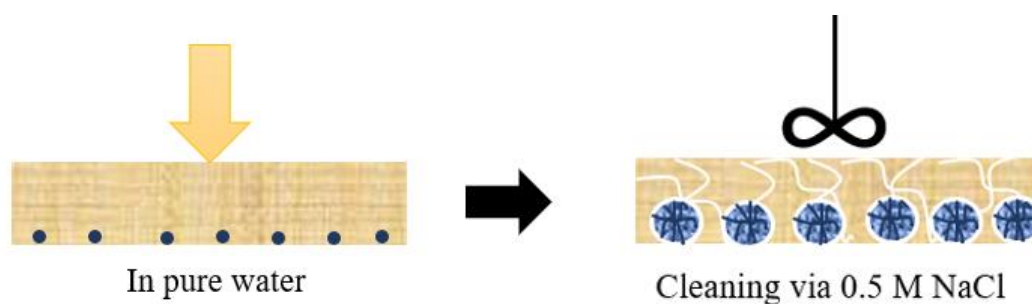


Figure 2.5. Schematic representation of microgel sizes during the filtration and cleaning on P(SBMA) microgel deposited membrane

*Filtration and cleaning procedure 3 (Figure 2.5)*

- 10 ml of 0.1 g/L P(SBMA) microgels in 0.5 M NaCl solution in which microgels had maximum swelling ratio were deposited on the membrane surface at room temperature and 2 bar.
- After the deposition, UP water was filtered until ionic conductivity reached 2.4  $\mu\text{m}/\text{cm}$  (ionic conductivity of pure water) in order to remove salt and precipitate microgels on the membrane surface.
- Filtration was performed in the absence of NaCl.
- After the filtration, retentate solution was replaced with 0.5 M NaCl solution in which microgels had maximum swelling ratio.
- Cleaning was done via stirring at 500 rpm for 5 minutes.

Finally, PWP of membranes was measured again after cleaning was performed to find irreversible fouling resistance.

Foulants concentrations of permeate solutions collected during the filtrations were measured by UV/Visible Spectroscopy (Schimadzu UV-1601) to find rejection values of foulants. Analyses were performed at 280, 254 and 600 nm wavelengths for BSA, HA gel and yeast solution, respectively. Rejections were calculated by using equation 6. Calibration lines for BSA, HA gel and yeast were shown in Appendix C.

Percentage of fouling irreversibility was calculated by dividing irreversible fouling resistance into total fouling resistance (Equation 7).

$$\text{Irreversibility (\%)} = \frac{R_{\text{irreversible fouling}}}{R_{\text{fouling}}} \times 100 \% \quad (7)$$

Also, flux recovery was evaluated using the following equation (Equation 8) to understand what percentage of initial flux has been recovered.

$$\text{Flux recovery (\%)} = \frac{\text{PWP after the cleaning}}{\text{PWP before the filtration}} \times 100 \% \quad (8)$$

Filtration experiments were performed on the same membrane at least three times. These filtration sets were repeated two times to see reproducibility of the experiments. Error bars were reported under same conditions in the resistance bar charts.

## 2.8. Adsorption Tests

Adsorption tests were done to assess the extent of foulant adsorption on the membranes. Two types of adsorption tests were performed;

### *Static adsorption test*

Microgel deposited and virgin membrane pieces with known areas were put into BSA, HA and yeast solutions for a day. At the beginning and after a day, foulant concentrations of the solutions were measured via UV/Visible Spectroscopy (Schimadzu UV-1601) at 280, 254 and 600 nm wavelengths for BSA, HA gel and yeast solution, respectively.

Differences between initial and final concentrations were divided into the membrane area to find adsorbed amount ( $\mu\text{g}$ ) per  $\text{cm}^2$ .

#### *Adsorption resistance test*

Before and after the adsorption tests, PWP values were measured to see the effect of the adsorptive fouling on the PWP. After that, flux decline was calculated by the following equation:

$$\text{Flux Decline (\%)} = \left(1 - \frac{\text{PWP after the adsorption test}}{\text{PWP of the membrane}}\right) \times 100 \% \quad (9)$$

## **2.9. Iron Oxide Decoration of P(SBMA) Microgels**

Iron oxide particles were incorporated with P(SBMA) microgels in order to recover them from retentate using magnetic field for reusing them into the system.

#### *Standard procedure*

First of all, 1 g NaOH was dissolved in 250 mL UP water to obtain 0.1 M aqueous NaOH solution (solution 1). And then, 0.1 g of P(SBMA) microgels were dispersed in 50 mL of solution 1. 0.865 g HCl was dissolved in 250 mL UP water to get 0.1 M HCl solution (solution 2).  $\text{FeCl}_2 \cdot 4\text{H}_2\text{O}$  and  $\text{FeCl}_3 \cdot 6\text{H}_2\text{O}$ , whose amounts are given in Table 2.1 were dissolved in 50 mL of solution 2. After that, solution 2 containing iron salts was added dropwise to the solution 1 under continuous stirring. In this step, microgel dispersion turned to reddish color. After synthesis was completed, combined solution was left to settle for several hours. After pouring away the supernatant solution, magnetic microgels were washed with UP water. Finally, wet particles were dried overnight in the fume hood.

Table 2.1. Concentrations of iron salts and P(SBMA) used in the syntheses of the iron decorated microgels (Rubio-Retama et al., 2010)

Synthesis Number	FeCl <sub>2</sub> .4H <sub>2</sub> O (g)	FeCl <sub>3</sub> .6H <sub>2</sub> O (g)	PSBMA (mg)
1	0.01789	0.04866	100
2	0.03579	0.09731	100

*Alternative procedure 1*

P(SBMA) microgels, and FeCl<sub>2</sub>.4H<sub>2</sub>O, FeCl<sub>3</sub>.6H<sub>2</sub>O, whose amounts are given in Table 2.1 were added in 50 mL of solution 2. Then, solution 2 containing iron salts and microgels was added dropwise to 50 mL of solution 1 under continuous stirring. Washing and drying procedures given in standard procedure part were applied.

*Alternative procedure 2*

2.92 g NaCl was added in in 50 mL of solution 2 and P(SBMA) microgels were dispersed with FeCl<sub>2</sub>.4H<sub>2</sub>O and FeCl<sub>3</sub>.6H<sub>2</sub>O, whose amounts are given in Table 2.1 in this solution. Then, solution 2 containing NaCl, iron salts and microgels was added dropwise to 50 mL of solution 1 under continuous stirring. Washing and drying procedures given in standard procedure part were applied.



## CHAPTER 3

### RESULTS AND DISCUSSION

#### 3.1. PES Based UF Membranes

In the performance tests, PES, widely used as a membrane material in separation fields, was selected since it is easily fouled due to its hydrophobic character. Hydrophobicity has a direct relationship with membrane fouling (Van der Bruggen, 2009 & Khulbe et al., 2010). PEG 400 was added in the membrane solution as a pore-forming agent and is known to leach out of the membrane forming solution during coagulation (Wang et al., 2006).

Morphology of the membranes used in the filtrations is shown in Figure 3.1. While PES20 membranes were selected to use in BSA and yeast filtrations because of its 100% rejection of BSA and yeast, HA gel filtrations were performed via PES25 membranes which are tighter to get higher retention since low rejection was obtained when PES20 membranes were used in HA gel filtrations.

When SEM images are examined, it is obviously clear that both PES20 and PES25 membranes are asymmetric with a microporous thin selective layer that provides higher permeance and good mechanical properties. Additionally, thickness of the apparent skin layer increases with increasing polymer concentration as it is seen from cross-sectional views in Figure 3.1. Selective layer of PES25 membranes is thicker than PES20 membranes.

PWP value of PES20 membranes was measured as  $100 \pm 35$  L/h.m<sup>2</sup>.bar while the ones PES25 membranes were approximately  $45 \pm 12$  L/h.m<sup>2</sup>.bar. A decrease of PES concentration in the membrane solution renders larger pores and higher water flux.

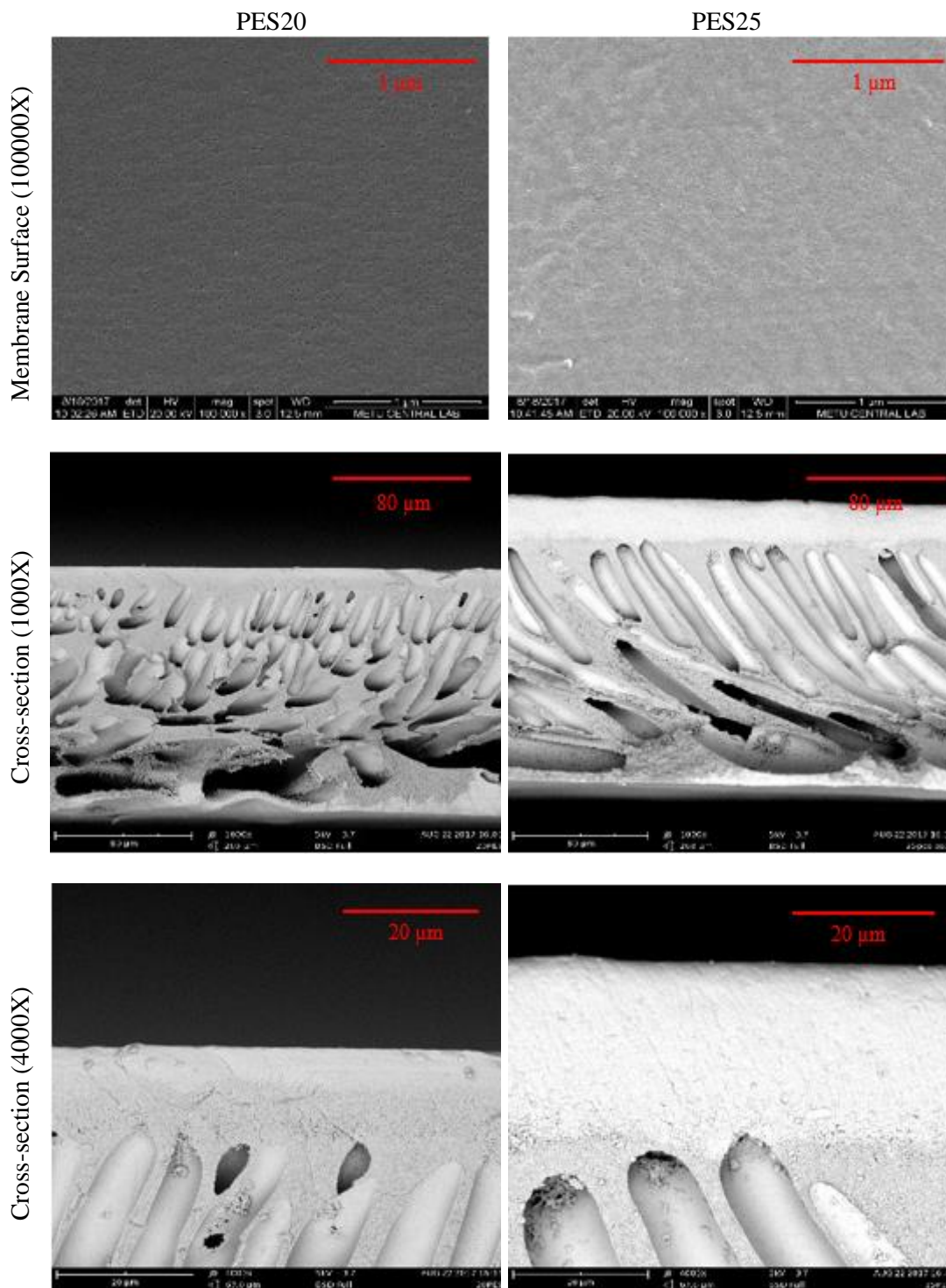


Figure 3.1. SEM Images of PES based UF membranes

From SEM images (Figure 3.1), pore diameters on the surface of PES20 and PES25 membranes were calculated as  $23\pm 7$  and  $10\pm 3$  nm by ImageJ program, respectively. PES20 membrane with thinner apparent skin layer and larger pore size has higher water permeance than PES25.

### **3.2. P(SBMA) Microgels**

Zwitterionic P(SBMA) microgels were synthesized using two different initiators by inverse emulsion free-radical polymerization (Cheng et al., 2010). In this polymerization technique, water soluble SBMA monomers were emulsified in a continuous oil phase, which is called a water-in-oil type emulsion. Tween 80 and Span 80 were cosurfactants to provide an optimal hydro lipidic balance emulsifying system. Decomposition of oil soluble initiator formed primary free radicals and then, these radicals grew by adding monomer units. In addition, polymer structures were adapted using crosslinkers to obtain polymeric microgels.

The first synthesis was accomplished with V-70 (initiator). After the synthesis, these zwitterionic microgels used in the filtration tests were characterized from the viewpoint of particle size in different salt concentrations by DLS.

Hydrodynamic diameter of P(SBMA) is significantly changed as its zwitterionic groups attract salt ions with the addition of salt in the system. The hydrodynamic diameter of zwitterionic P(SBMA) microgels was analyzed using DLS in ultra-pure water and different salt concentrations at room temperature to find swelling ratio of microgels in various salt concentration.

From Figure 3.2, it is clear that swelling ratio of P(SBMA) microgels increased with increasing salt concentration until 0.5 M in which the zwitterionic microgels had maximum swelling ratio. Salt ions could enter P(SBMA) chains crosslinked in the form of microgels and interact with zwitterions within the chains. This can decrease ionic interactions among and within cross-linked P(SBMA) chains which results in

expanding the chains (Lalani & Liu, 2011). Namely, P(SBMA) microgels could transfer to hydrated state. However, the microgels started to shrink after 0.5 M NaCl. It can be explained that when the solution contains a large amount of salt, the excess salt causes an osmotic pressure gradient between the solution and the microgels, causing the microgels to shrink (Jhan et al., 2014).

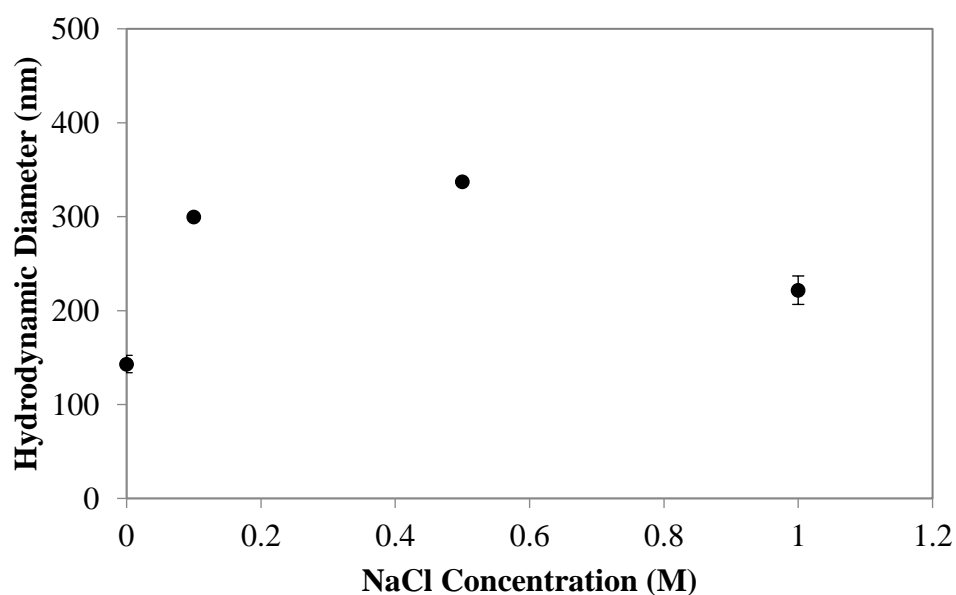


Figure 3.2. Hydrodynamic diameter of zwitterionic P(SBMA) microgels synthesized with V-70 in different NaCl concentration

Secondly, since V-70 is not commercially available in Turkey, P(SBMA) microgels were synthesized using AIBN. V-70 can be activated at low temperature whereas AIBN activation temperature is around 70 °C; therefore, dodecane was used as a solvent rather than hexane because hexane is too volatile. Inverse emulsion free-radical polymerization method was used in this adaptation of P(SBMA) microgel synthesis as well.

P(SBMA) microgel syntheses done by V-70 and AIBN are compared in Table 3.1. During the synthesis, polymer precipitation (white product) can be easily observed by naked eyes. While a great amount of P(SBMA) precipitation has been observed for 4 hours in the synthesis with V-70, white product formation could not be seen at the end of the 4 hours during the synthesis with AIBN. Hence, its polymerization reaction was allowed to take place approximately 15 hours. In other words, reaction with AIBN was quite slow in comparison to one with V-70. Looking at their yields, roughly 60% yield was obtained in the adaptation of the synthesis while it was more than 90% in the standard synthesis procedure. There was no change in the product colors.

Table 3.1. Comparison of P(SBMA) microgel syntheses according to initiators

	<b>Standard Procedure</b>	<b>Adaptation Procedure</b>
<b>Initiator</b>	<b>V-70</b>	<b>AIBN</b>
<b>Solvent</b>	Hexane	Dodecane
<b>Reaction Temperature</b>	40 °C	70 °C
<b>Reaction Rate</b>	fast	relatively slow
<b>Reaction Time</b>	4 hrs	nearly 15 hrs
<b>Initiator amount</b>	Same amount (mole)	
<b>Surfactant</b>	Tween80, Span80 (Same amount)	
<b>Washing</b>	Acetone or THF	Acetone or THF
<b>Color</b>	White	
<b>Yield</b>	85 – 90%	60 – 65%

The hydrodynamic diameter of zwitterionic microgels synthesized by AIBN was characterized in various salt concentrations by DLS. When we look at the graph in Figure 3.3, these microgels maximally swell in 0.5 NaCl solution like the ones prepared using V-70.

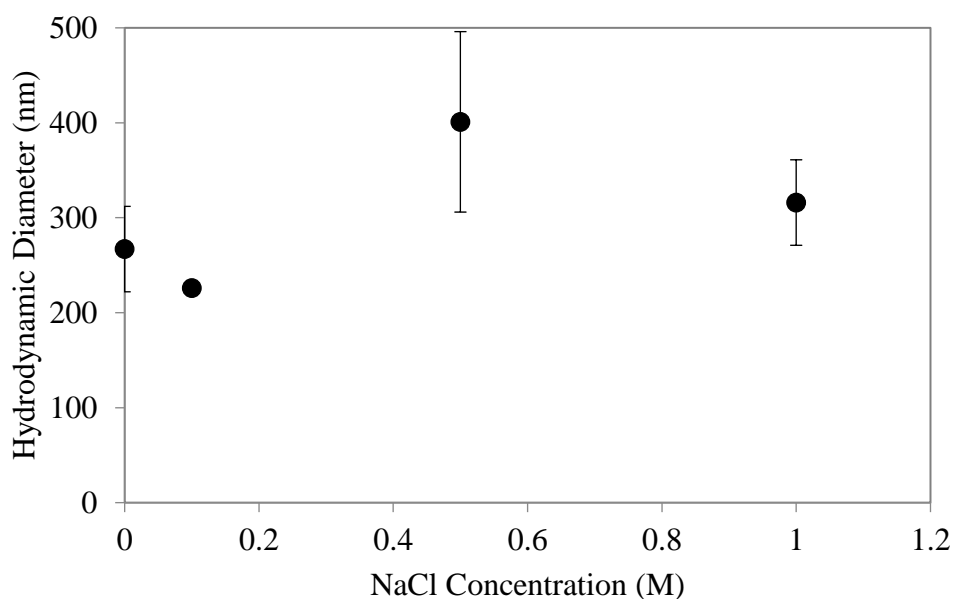


Figure 3.3. Hydrodynamic diameter of P(SBMA) microgels synthesized with AIBN in different NaCl concentration

As a result, ionic strength responsive P(SBMA) microgels were obtained and utilized in the performance tests for fouling removal.

### 3.3. Performance Tests

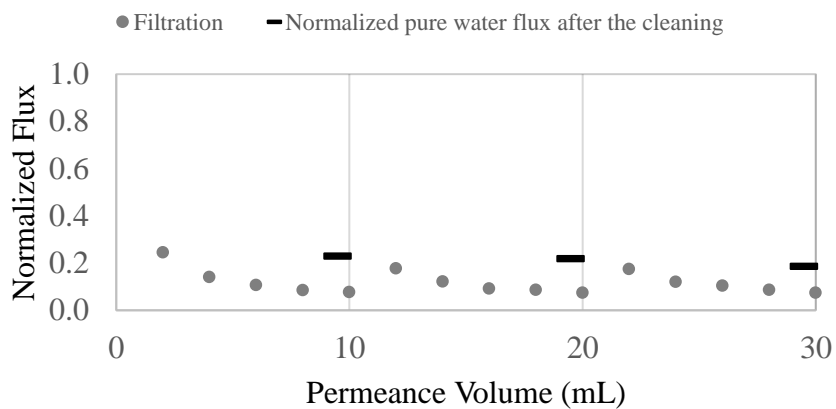
Filtration tests were performed by using different foulants, membranes and microgels. In addition to these, different filtration and cleaning procedures were applied to find the best conditions for proposed approach. PES20 and PES25 membranes were preferred, BSA, humic acid and yeast were foulants and finally, P(SBMA) was the ionic strength responsive polymeric microgel.

### **3.3.1. The Use of P(SBMA) Microgels with PES20 Membrane for BSA Fouling Removal**

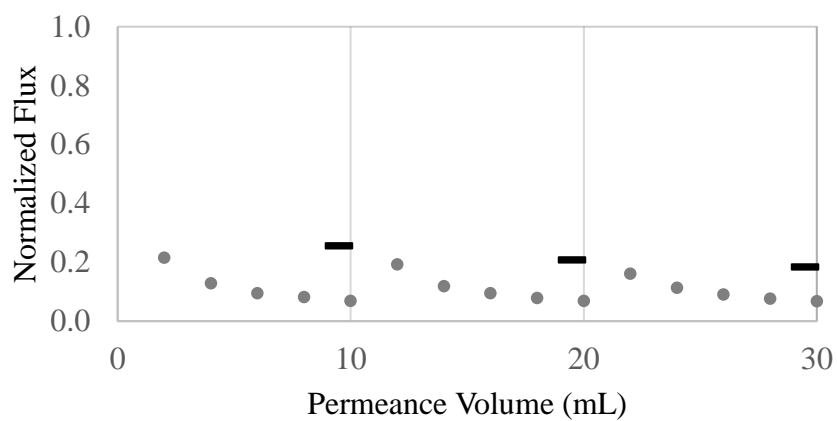
BSA filtrations via PES20 membranes were done with different P(SBMA) microgel concentrations and without microgel. In general, feed solutions were prepared by adding 0.5 M NaCl into them so that microgels can completely dissolve into the feed solution. To get maximum volume change, cleaning was always performed via pure water. Thanks to this, microgels changed their size from swollen to shrunk during the cleaning. Retention values of all BSA filtrations were calculated as %100.

In Figure 3.4, BSA filtrations performed at room temperature and 2 bar TMP without microgel, with 0.01 g/L and 0.1 g/L P(SBMA), respectively were compared. Apart from microgel concentration, all experimental conditions were same in the BSA performance tests. These experiment sets were done in series as three times by using the same membrane for each set. Before second and third filtrations, retentate solution was poured out and 60 mL ultrapure water was added to clean the membrane surface. Then, at room temperature cleaning was performed by stirring at 400 rpm for 5 minutes.

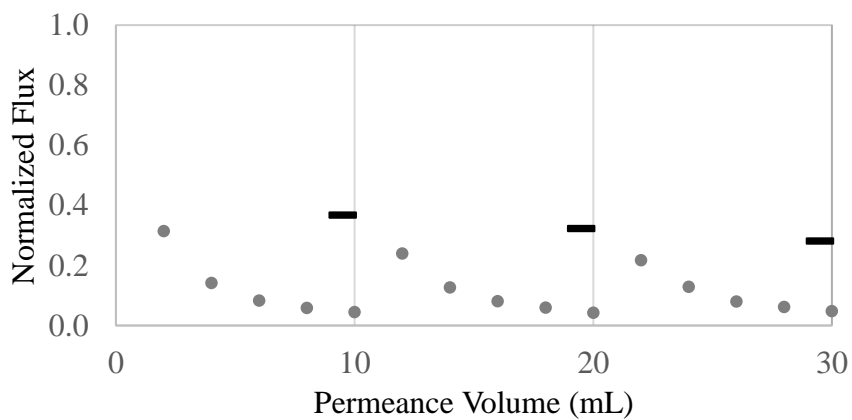
Looking at the plots in Figure 3.4, it is noticeable that filtration fluxes fell to below 30% of the initial pure water permeance (PWP) at the beginning of both microgel-free and microgel-added BSA filtrations. At the end of each filtration, these values went moderately down to around %10 of the initial membrane flux. To explain that, it can be said that BSA can quickly adsorb onto the membrane surface. In addition to this, both BSA and PES membrane have hydrophobic domains which resulted in an increase of PES-BSA adhesion forces (Miao et al., 2016). When these come together, hydration forces created by P(SBMA) microgels could not prevent its adsorptive fouling.



a)



(b)



(c)

Figure 3.4. Normalized flux graphs of three serial BSA + 0.5 M NaCl (a), BSA+ 0.5 M NaCl +0.01 g/L P(SBMA) microgels (b) and BSA+ 0.5 M NaCl +0.1 g/L P(SBMA) microgels (c) filtrations on PES20 membrane and PWP values after the cleaning.

At the end of the third filtration with 0.1 g/L P(SBMA) microgels, flux relatively increased approximately from 5% to 30% of the initial pure water flux while this value barely rose to around 20% of the initial flux with less microgel concentration and in the absence of the microgel.

The bar charts given in Figure 3.5 indicate total fouling resistance (sum of reversible and irreversible fouling resistance) and irreversible resistance of BSA filtrations as  $R_{\text{fouling}}$  and  $R_{\text{irr}}$ , respectively. When they are compared, especially in the first filtrations there is a marked difference among them. While  $R_{\text{fouling}}/R_{\text{irr}}$  is around 8% in the presence of 0.1 g/L P(SBMA) microgels into the feed solution, this ratio is more than three times for the filtrations both with less microgel and without microgel. If we look at the other filtrations, irreversible fouling resistances are quite low expect the third filtration without microgel. It can be said that adsorptive fouling could not be completely removed in the first filtrations with or without microgels. After the first ones, cake layer over the adsorptive fouling was almost cleaned in the presence of 0.1 g/L P(SBMA) microgels.

Whole picture of BSA filtrations with PES20 membranes shows that utilizing from P(SBMA) microgels does not get efficient fouling removal performance since adsorptive fouling rapidly developed at the beginning of the first filtrations due to hydrophobic domains of BSA. For this reason, flux recovery could be merely obtained till where filtration flux suddenly declined at the first permeate drops via P(SBMA) microgels. Hence, after the adsorption of BSA on the PES20 membrane, it was not possible to remove adsorptive fouling of BSA from the PES20 membranes by size change of P(SBMA) microgels.

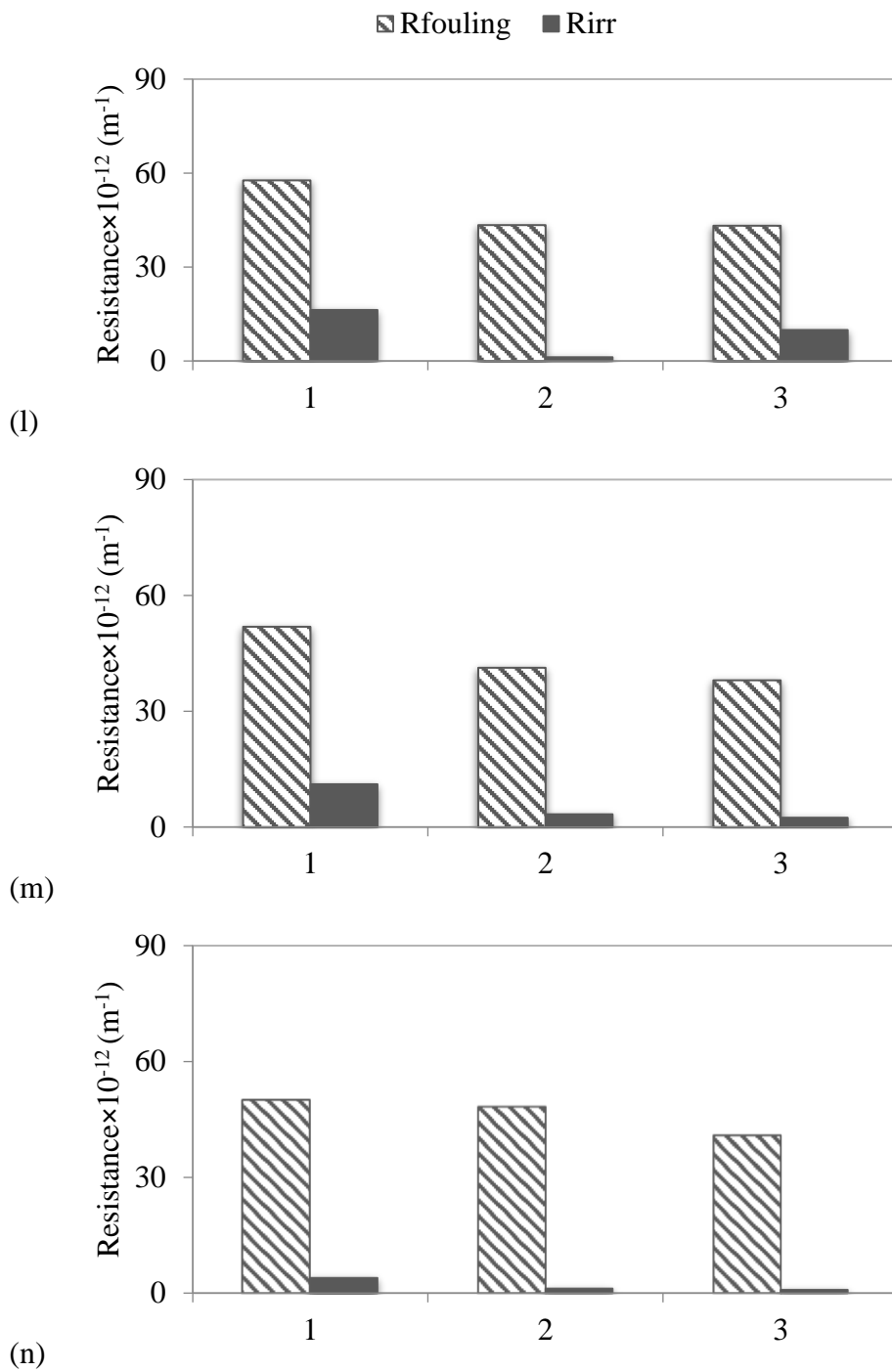


Figure 3.5. Resistance graphs of three serial BSA + 0.5 M NaCl (a), BSA+ 0.5 M NaCl +0.01 g/L P(SBMA) microgels (b) and BSA+ 0.5 M NaCl +0.1 g/L P(SBMA) microgels (c) filtrations on PES20 membrane

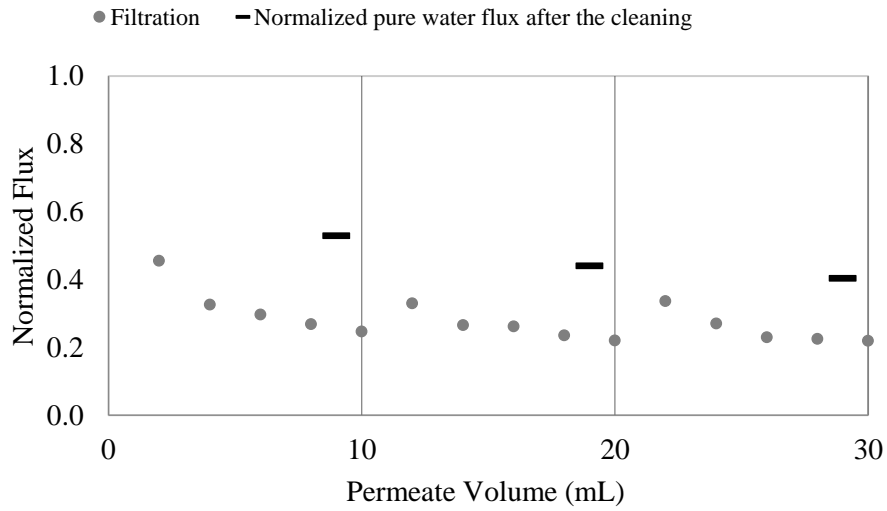
### **3.3.2. The Use of P(SBMA) Microgels with PES25 Membrane for HA Gel Fouling Removal**

Membranes were fouled with HA in the presence of  $\text{CaCl}_2$  since  $\text{Ca}^{+2}$  ions are known to form a gel of HA. After fouling, the feed was replaced with pure water to shrink microgels for investigating the influence of P(SBMA) microgels on HA gel fouling removal. After this cleaning step, the pure water permeance was measured again to assess the degree of reversibility of fouling.

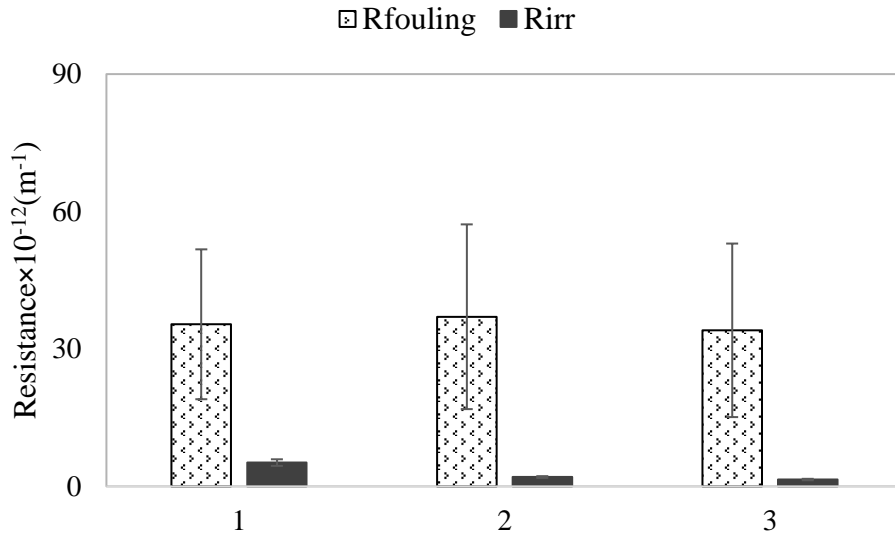
HA gel filtrations were performed with PES25 membranes. Microgel-added HA filtrations were done by making 0.1 g/L g/L P(SBMA) addition into the feed solutions. HA retentions were calculated as  $84\pm 5\%$  for all HA filtrations.

Unlike BSA, from HA normalized flux graphs it is easily seen that fluxes of HA gel filtrations with and without microgel moderately declined during the filtrations. In other words, HA adsorption onto the PES membrane surface is less dominant fouling factor than BSA adsorption.

To begin with, the experiment set was performed with HA gel solution without microgel and salt ions. In Figure 3.6-(b), it is noticeable that irreversible fouling resistance is 31% of the total fouling resistance in the first filtration while this value is quite small in the other HA experiment sets. When both salt and microgel were removed from the feed solution, flux was just recovered till 53% of the initial flux in the first filtration and it gradually declined to 40% at the end of the third filtration.



a)



b)

Figure 3.6. Normalized flux (a) and resistance (b) graphs of three serial HA gel filtrations without microgel and salt

P(SBMA) microgel-added HA gel filtrations were performed via salt addition into the feed solution in different concentrations which are 0.5 M NaCl where microgels have maximum swelling ratio and 1 M NaCl, higher concentration. The purpose of this is to see how salt concentration affects the microgel performance. When we look at normalized flux graphs in Figure 3.7-(a) and (b), similar tendency is observed in the

flux decline and cleaning performance for both microgel-added HA filtrations with 0.5 M NaCl and 1 M NaCl. Accordingly, in both filtration sets, irreversible fouling resistances were calculated around 15% of the total fouling resistances after the cleaning at the end of the first filtrations (Figure 3.8-(a) and (b)).

After the filtrations done by P(SBMA) microgels in different salt concentrations, microgels were removed from the feed solution and all other filtration and cleaning conditions were kept same in order to see the effect of the microgels on HA gel layer removal.

Looking at the normalized flux graph of HA gel filtrations with 0.5 M NaCl (Figure 3.7-(c)), it is clear that cleaning performances are again quite similar with microgel-added HA gel filtrations; roughly 70% flux recovery at the end of the third filtrations and less irreversible fouling resistance ratio.

In addition, fouling resistances of both salt and microgel-free filtrations were most irreversible compared to resistances of salt-added filtration sets with or without microgels. In the literature, severity of HA fouling increases with increasing ionic strength since HA molecules tend to change their configuration and create a denser layer at a higher salt concentration (Sutzkover-Gutman et al., 2010 & Taheri et al., 2015). However, if we compare fouling resistance values of HA filtrations with 0.5 M NaCl (Figure 3.8-(c)) to resistances of HA filtrations without microgel and salt shown in Figure 3.6-(b) , it can be said that there is no significant difference between them. The possible reason of that can be  $Ca^{+}$  has already increased severity of HA fouling layer as maximum.

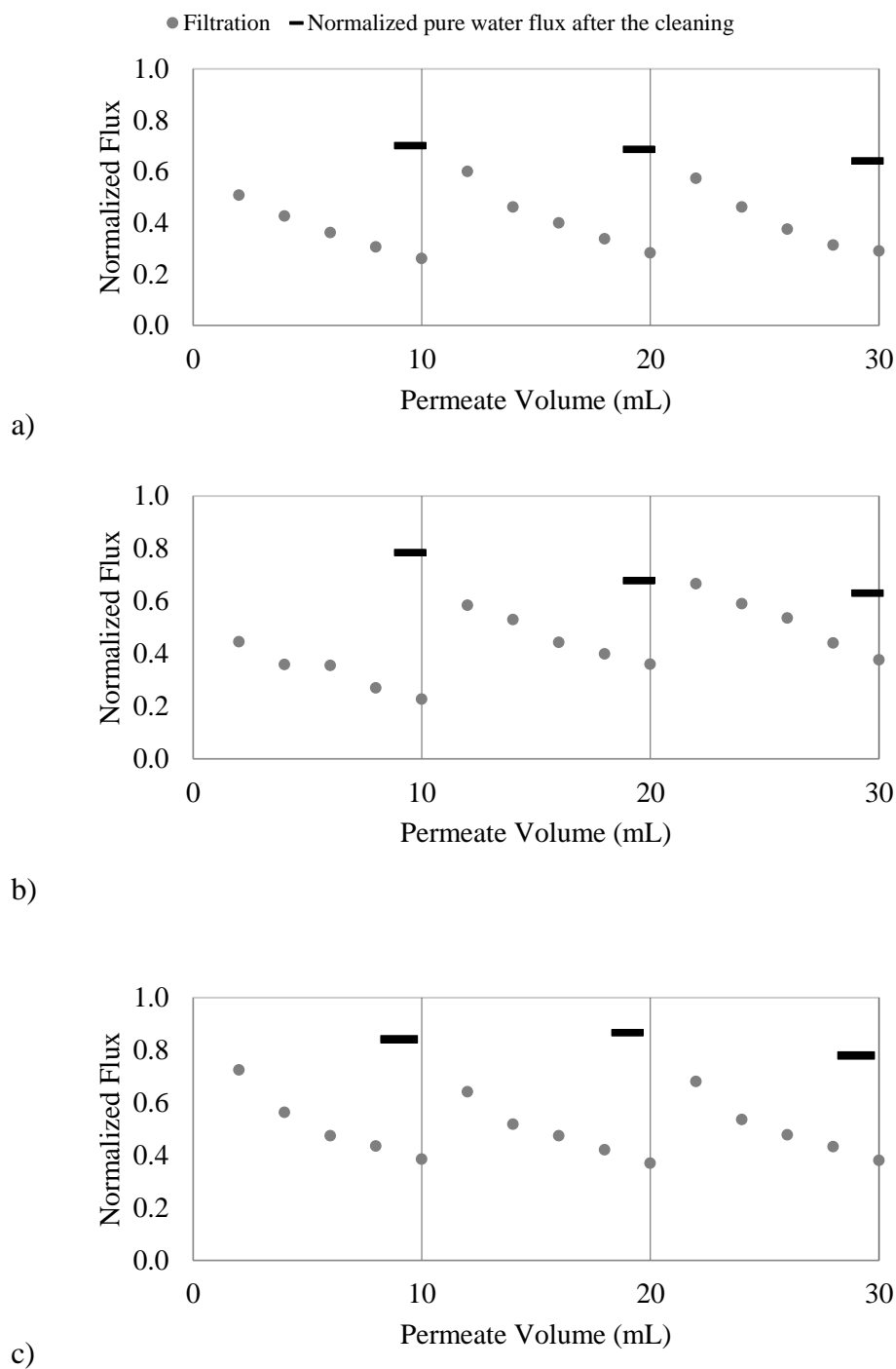


Figure 3.7. Normalized flux graphs of three serial HA gel filtrations with 0.5 M NaCl + 0.1 g/L P(SBMA) microgels (a), 1 M NaCl + 0.1 g/L P(SBMA) microgels (b) and 0.5 M NaCl (c)

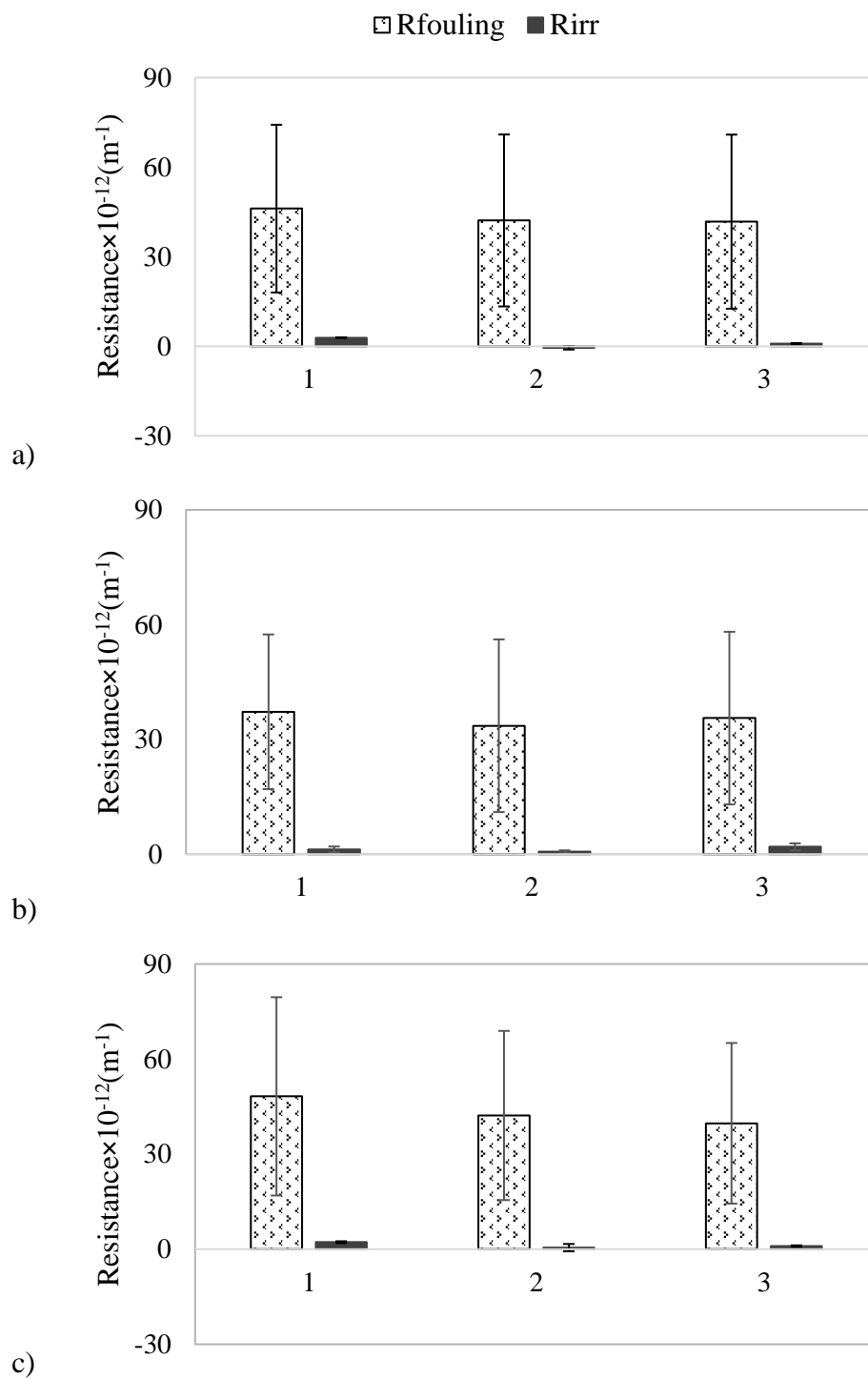


Figure 3.8. Resistance graphs of three serial HA gel filtrations with 0.5 M NaCl + 0.1 g/L P(SBMA) microgels (a), 1 M NaCl + 0.1 g/L P(SBMA) microgels (b) and 0.5 M NaCl (c)

When the effect of salt ions on the cleaning performance of PES membrane is considered, cleaning is more efficient in the presence of salt ions. It is known that  $\text{Ca}^{+2}$  acts like a binding agent of two negatively charged carboxyl functional groups in HA structure so HA gel is formed in the presence of  $\text{Ca}^{+2}$ . It is also known that HA molecules form spherical binary complexes with increasing ionic strength in the solution medium since negatively charged carboxyl functional groups in HA electrostatically interact with  $\text{Na}^{+}$  ions (Hong et al, 1997 & Srisurichan et al., 2004). When  $\text{Na}^{+}$  ions were present in HA solution medium with  $\text{Ca}^{+2}$  ions, these  $\text{Na}^{+}$  could be counterions of some carboxyl groups. Thus, it is possible that interactions between HA and  $\text{Ca}^{+2}$  ions decreased, and less gel formation occurred. As a result, it can be said that  $\text{Na}^{+}$  ions provided a looser cake layer formation, which made HA gel easily cleanable.

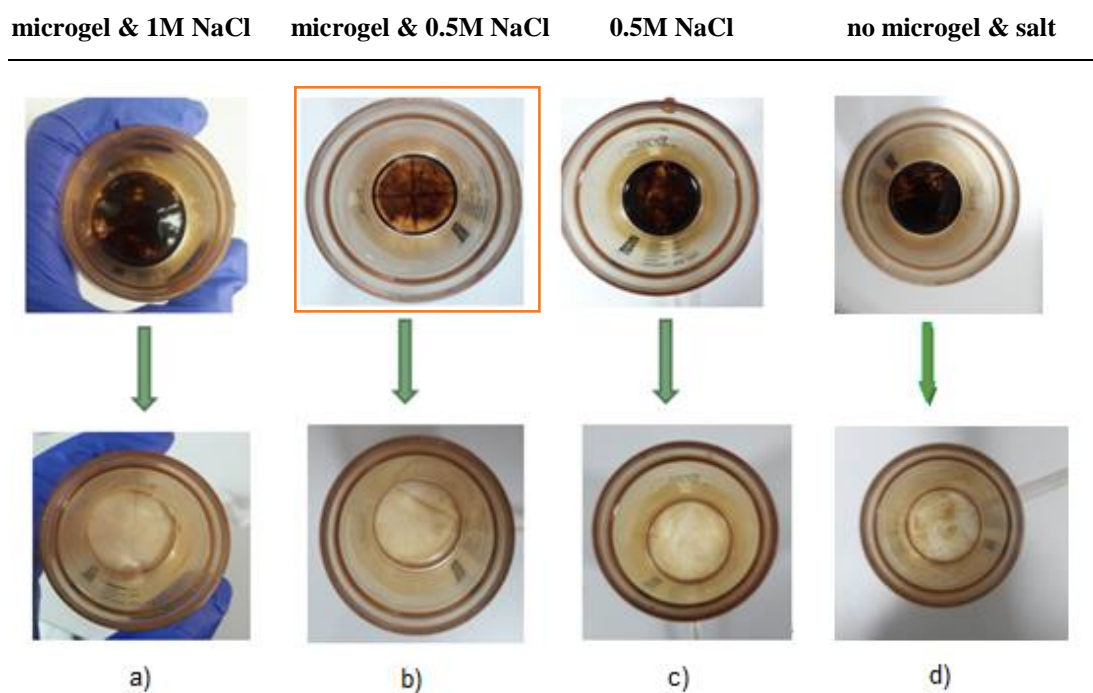


Figure 3.9. Photos of PES membranes taken after HA filtrations (top) and cleanings (bottom)

The PES membranes were photographed after each filtration with HA to observe cake layer formation and after each cleaning (Figure 3.9). When the photographs are examined, it is evident that cake layer formations are quite similar after the filtrations shown in Figure 3.9 (a), (c) and (d). On the other hand, when microgels were added into HA gel solution in 0.5 M NaCl presence (Figure 3.9-b), looser but probably thicker cake layer formation was observed. Its possible reason can be the microgel size during the filtration. In the presence of 0.5 M NaCl, microgels are most hydrated and swollen, which can create more porous cake layer due to water layer around the microgels.

Considering the results of all HA gel filtrations, we can say that HA fouling in the absence of NaCl was the most irreversible while when NaCl was in the feed, reversibility was similar with or without microgel. This possibly implies that a cake layer can be easily removable in NaCl presence. When microgels were swollen form in the presence of 0.5 M NaCl, a looser cake layer formed during the filtration.

### 3.3.3. The Use of P(SBMA) Microgels with PES20 Membrane for Yeast Fouling Removal

0.1 wt% suspension of yeast cells in brine solutions (0.5 M or 0.1 M NaCl) was used with 20% PES membranes to investigate the effect of P(SBMA) microgels on the yeast fouling removal. Yeast rejections were found 100% for all performance tests.

First of all, yeast filtration sets were done at room temperature in the absence and presence of the P(SBMA) microgels without stirring during the filtration. Since yeast cells are quite large ( $\sim 5 \mu\text{m}$  in diameter), they precipitated over time during the filtration without stirring. In order to prevent this, yeast filtrations were redone by stirring at 150 rpm during the filtration, unlike performance tests done via other foulants.

In Figure 3.10 & Figure 3.11-(a) and (b), yeast filtration sets were done at 150 rpm, 2 bar in the presence of 0.5 M NaCl by adding into the feed solution 0.1 g/L and 0.2 g/L P(SBMA) microgels, respectively. Cleaning was performed via pure water (*procedure 1*) for both sets after each filtration to shrink microgels. In the former, the flux fell below 20% of the initial PWP (Figure 3.10-(a)) and the irreversible fouling resistance was quite high especially in the first filtration (Figure 3.11-(b)). Based on these results, the concentration of microgels was doubled and then the experiment set was repeated. As shown in Figure 3.10-(b) & Figure 3.11-(b), when the amount of microgel was increased, the result was not changed, and the desired cleaning was not achieved.

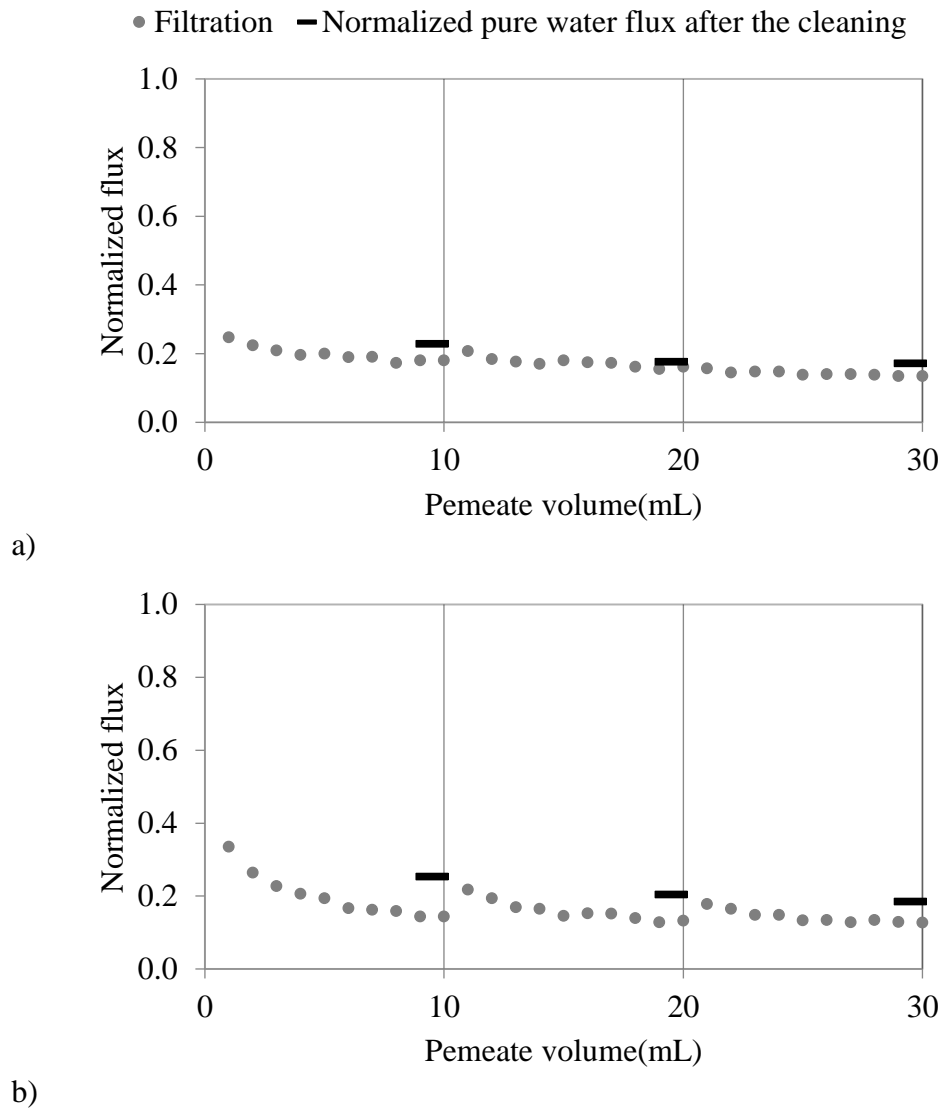


Figure 3.10. Normalized flux graphs of yeast serial filtrations with 0.5 M NaCl + 0.1 g/L P(SBMA) microgels (a) and 0.5 M NaCl + 0.2 g/L P(SBMA) microgels at 150 rpm (Cleaning via ultra-pure water)

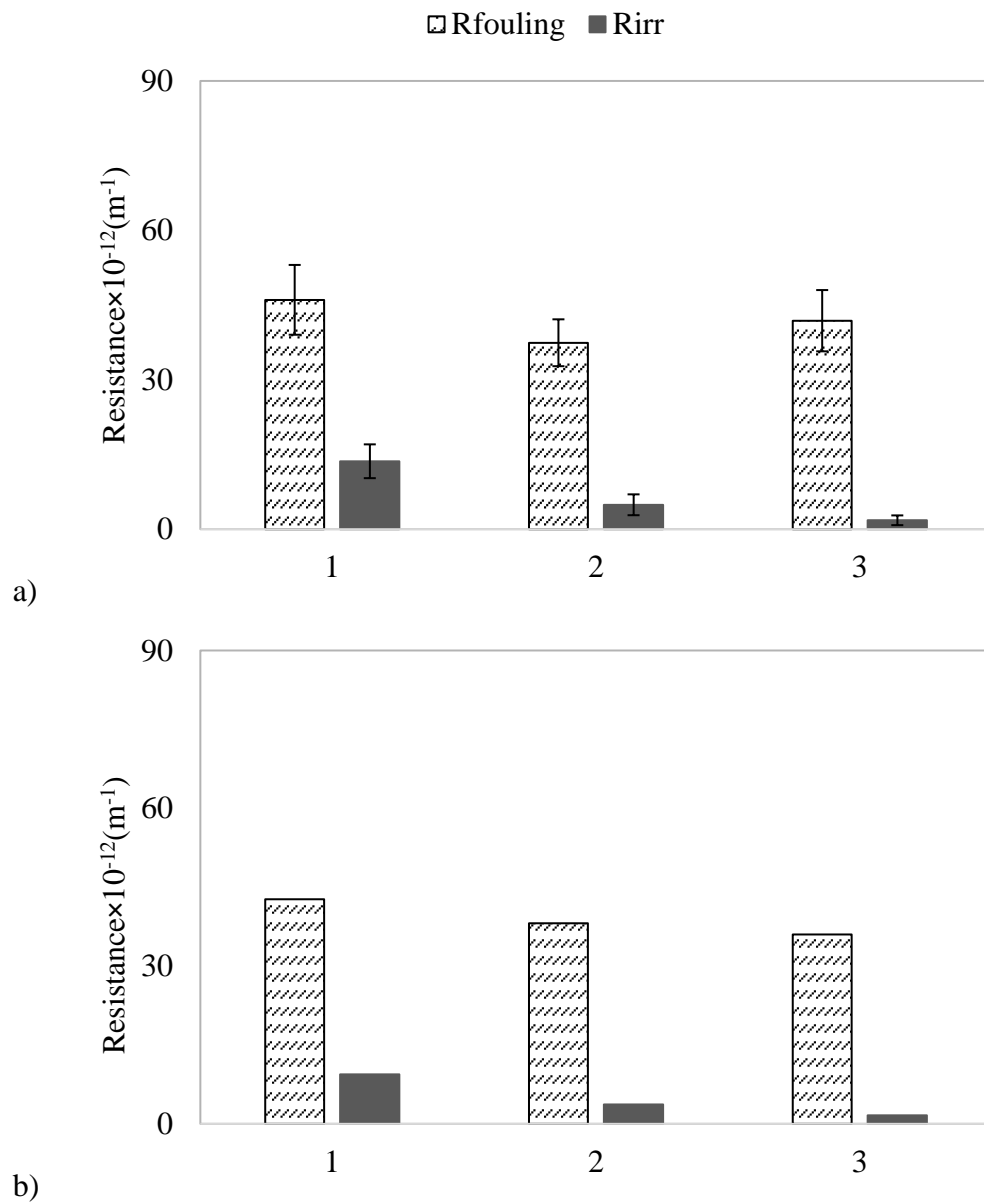


Figure 3.11. Resistance graphs of yeast serial filtrations with 0.5 M NaCl + 0.1 g/L P(SBMA) microgels (a) and 0.5 M NaCl + 0.2 g/L P(SBMA) microgels at 150 rpm (Cleaning via ultra-pure water)

From plots in Figure 3.10, it can be easily seen that filtration fluxes sharply decreased to around 30% of the initial PWP at the beginning of the first filtration which implies that adsorptive fouling immediately formed.

The cleaning via pure water to shrink microgels having maximum swelling ratio during the filtration could not remove the cake layer of yeast cells. Hence, following performance tests were done by changing cleaning and filtration procedures (*procedure 2*).

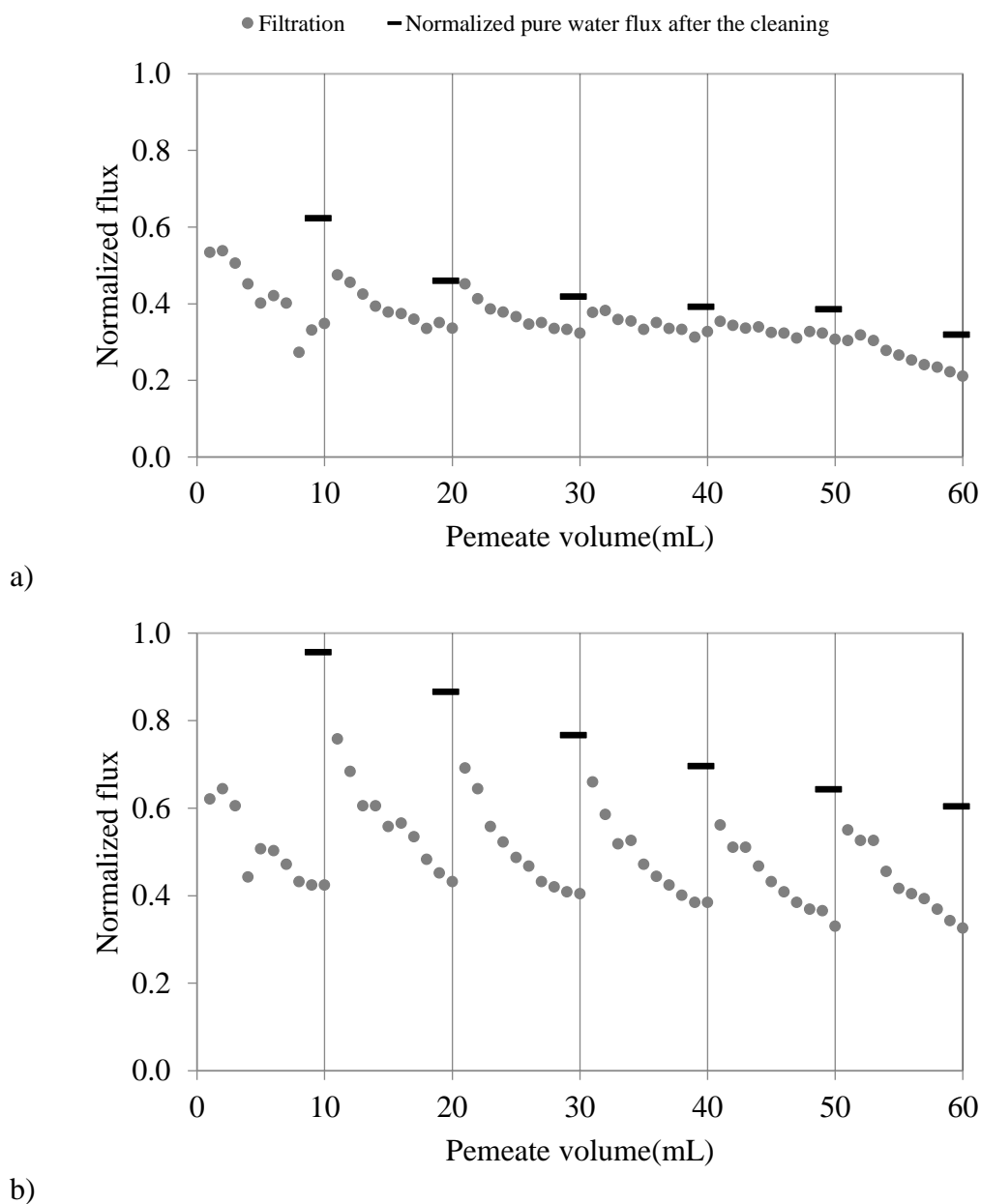


Figure 3.12. Normalized flux graphs of yeast serial filtrations in the presence of 0.1 M NaCl without microgel (a) and with 0.1 g/L P(SBMA) microgels (b) (Cleaning via 0.5 M NaCl)

Zwitterionic materials are strongly hydrated in the ionic solutions which is the key of their antifouling properties (Chen et al., 2008). To put it another way, P(SBMA) microgels, zwitterionic, can prevent fouling by the water layer formed around them. Since zwitterionic P(SBMA) microgels are non-fouling in the medium containing salt ions, it was proposed that microgels in 0.1 M NaCl, which are slightly swollen during filtration, will be swollen during the cleaning via 0.5 M NaCl and the cake layer will be better cleaned.

Yeast filtration set shown in Figure 3.12 and Figure 3.13 was performed in the presence of 0.1 M NaCl without microgel and with 0.1 g/L P(SBMA) microgels. After each filtration, retentate was replaced with 60 mL 0.5 M NaCl and cleaning was done at 500 rpm for 5 minutes. Thus, the microgels, which were slightly swollen during the filtration, became maximally swollen.

Looking at the plot in Figure 3.12-(a), it is evident that especially after the third filtration, pure water fluxes after the cleanings were quite close the point where filtration fluxes declined, which means cleaning was almost never achieved in the microgel-free yeast filtrations.

In detail, if the results of first filtrations are compared, flux recovery was 96% of the initial flux in the presence of P(SBMA) microgel (Figure 3.12-(a)) while this value in the experiments without microgel was around 60% (Figure 3.12-(b)). When the results in Figure 3.12 are examined, this method provided nearly more than 60% flux recovery compared to initial PWP at the end of the sixth filtration. On the other hand, flux recovery in the microgel-free yeast filtrations was only around 30% of initial PWP at the end of the sixth filtration. Likewise, if the ratio of irreversible fouling resistance to total one in the first filtration where the most fouling occurred is considered, the addition of the microgel to the feed increases the cleaning efficiency. When microgel was added to the feed, this ratio was only 6% but it increased to 11% in the filtration in the absence of the P(SBMA) microgels as given in Figure 3.13-(b) and (a), respectively.

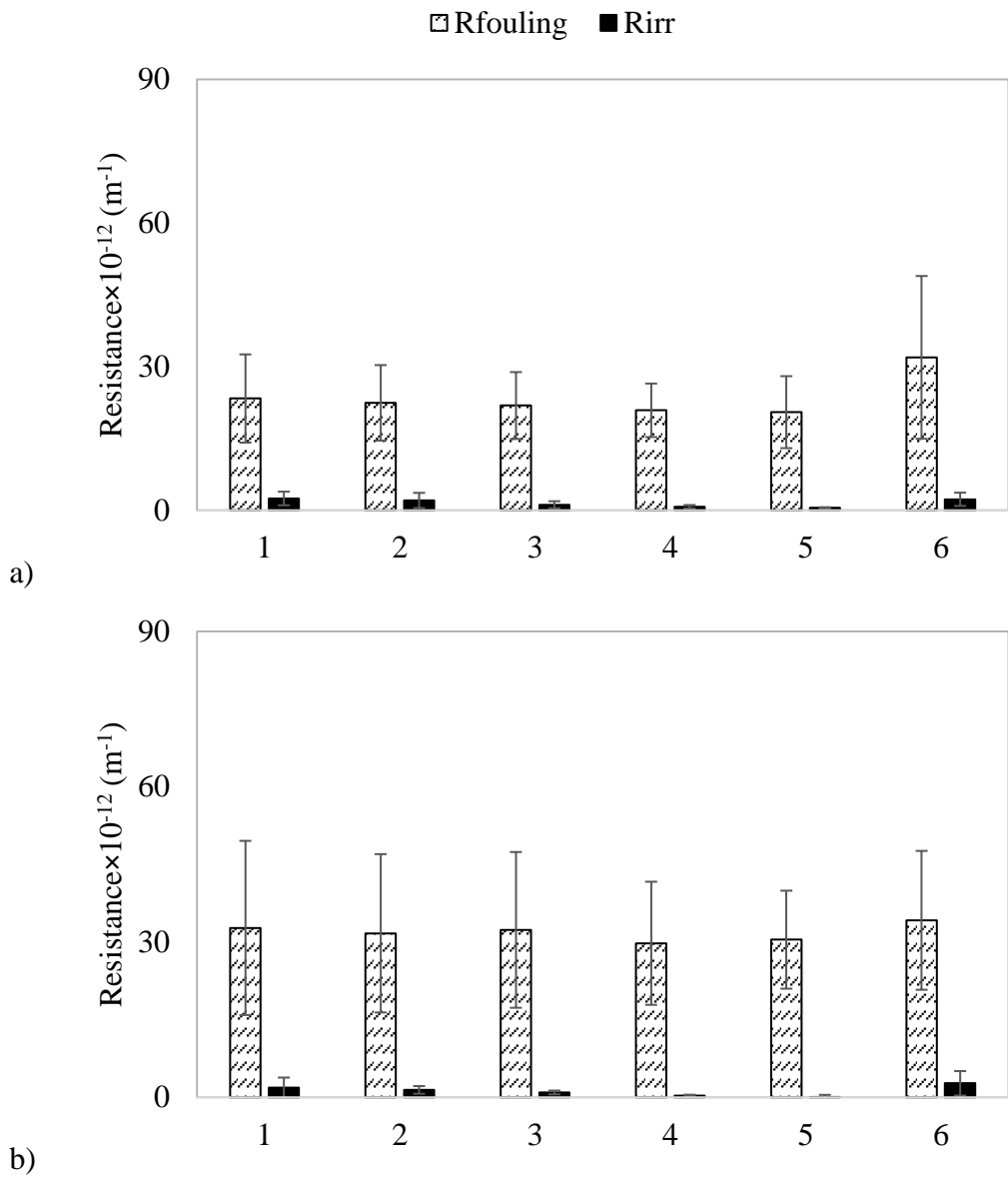
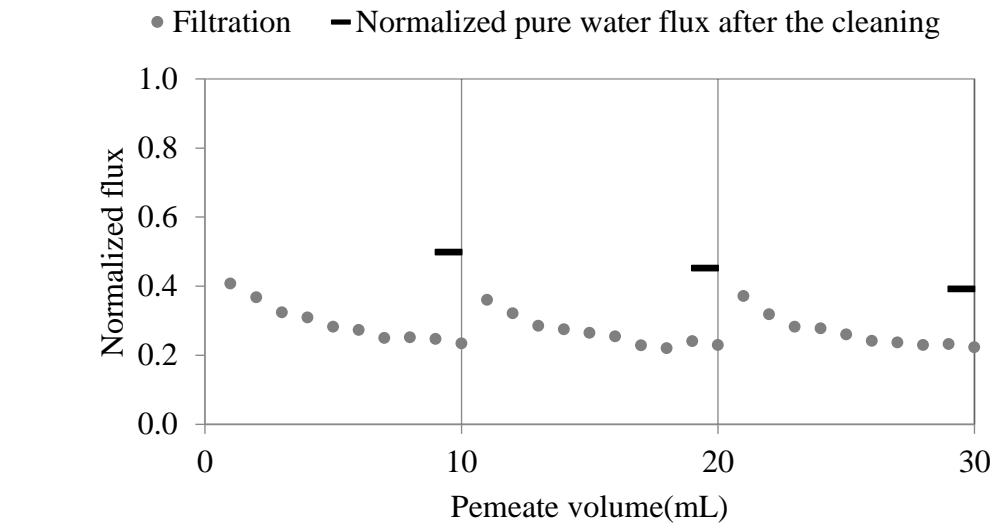


Figure 3.13. Resistance graphs of yeast serial filtrations in the presence of 0.1 M NaCl without microgel (a) and with 0.1 g/L P(SBMA) microgels (b) (Cleaning via 0.5 M NaCl)

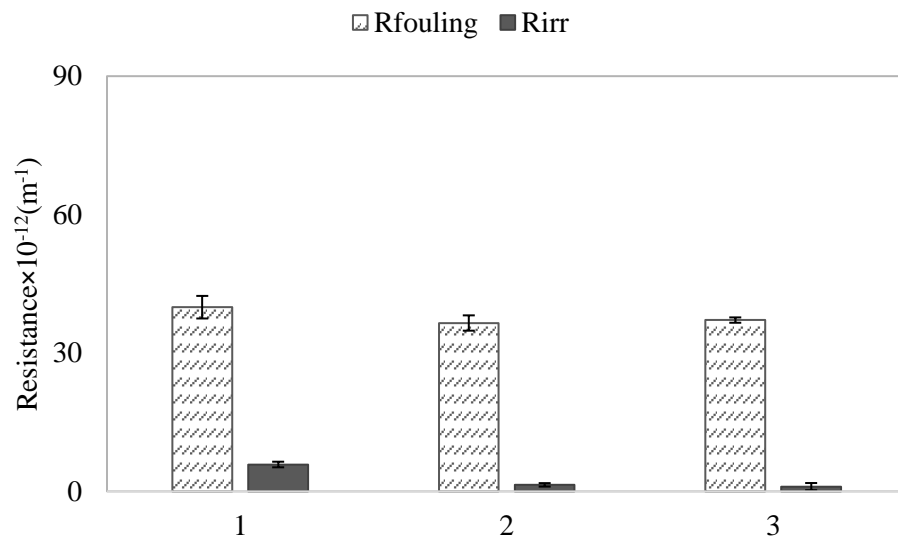
When 0.1 g/L P(SBMA) microgel-added filtrations done by applying *procedure 1* and *procedure 2* were compared, irreversible fouling resistance was 32% of total fouling resistance in the first filtration (Figure 3.11-(a)) when cleaning was performed by size

change of microgels from swollen to shrunk state; however, this ratio was only 6% (Figure 3.13-(b)) when microgels passed from slightly swollen to more swollen state during the cleaning. Namely, cleaning via 0.5 M NaCl shows higher efficiency than cleaning via pure water in the presence of microgels. In addition to this, it is clearly understood that more yeast adsorptive fouling was observed in the presence of 0.5 M NaCl.

With cleaning *procedure 2*, P(SBMA) microgel concentration was doubled and the performance test was repeated. According to results shown in Figure 3.14, 40% flux recovery was obtained with the increase of the amount of microgels at the end of the third filtration while this ratio was more than 60% in the filtrations in the presence of 0.1 g/L P(SBMA) microgels. In the first filtration where most fouling was usually observed, irreversibility of fouling was more than twice compared to filtration set with 0.1 g/L P(SBMA) microgel addition. Looking at plot in Figure 3.14-(a), at the beginning of the first filtration, filtration permeance went down to around 40% of initial PWP while this value was around 70% in the presence of 0.1 g/L P(SBMA) microgels (Figure 3.12-(b)). This can be explained that yeast adsorbed less via addition of 0.1 g/L P(SBMA) in the feed than addition of 0.2 g/L P(SBMA) microgels. Moreover, while flux recovery with 0.2 g/L P(SBMA) addition into the feed could be only obtained until filtration flux of first permeate drops, 0.1 g/L microgel in the feed provided higher cleaning efficiency. As a result, it can be said that relatively better cleaning performance was obtained by adding 0.1 g / L P(SBMA) microgels into the feed solution. In the yeast filtrations, irreversibility slightly increases with increasing P(SBMA) microgel concentration.

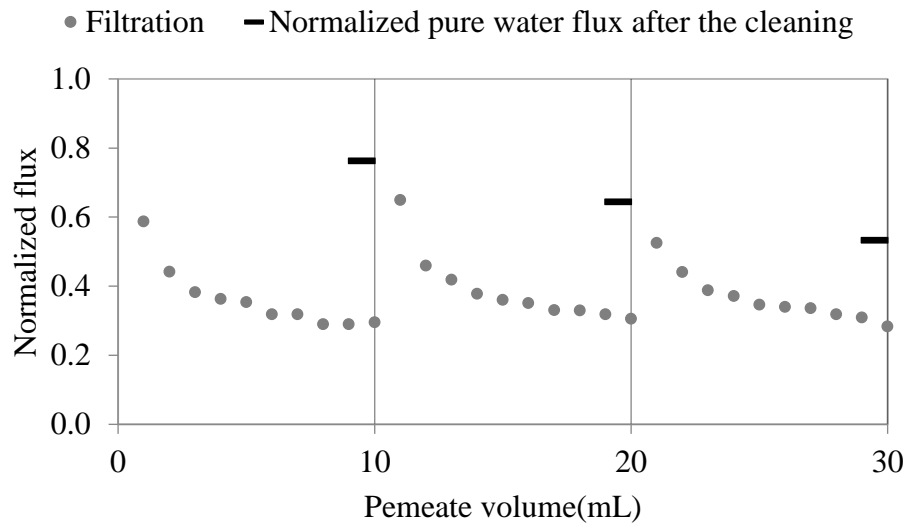


a)

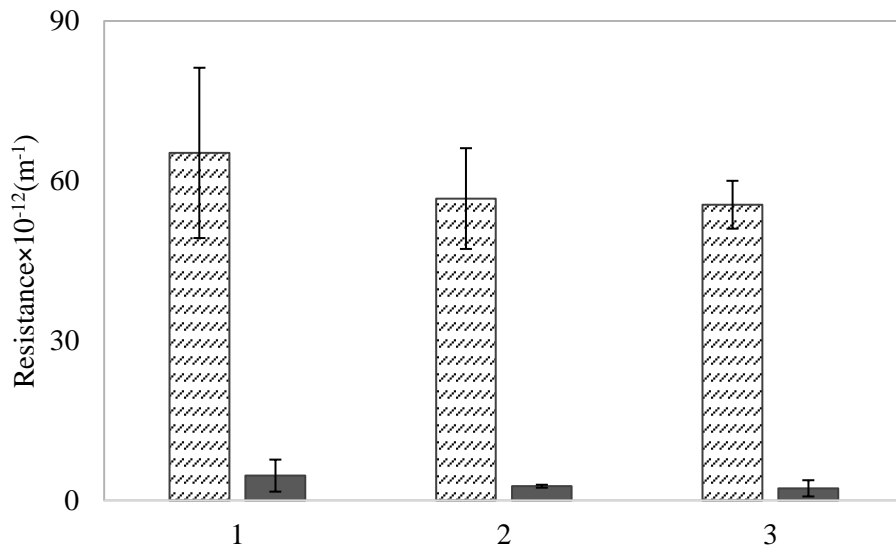


b)

Figure 3.14. Normalized flux (a) and resistance (b) graphs of yeast filtrations with 0.2 g/L P(SBMA) microgel and 0.1 M NaCl (cleaning via 0.5 M NaCl)



a)



b)

Figure 3.15. Normalized flux (a) and resistance (b) graphs of yeast filtrations with 0.1 g/L P(SBMA) microgel and 0.1 M NaCl (cleaning via 0.5 M NaCl for 20 min)

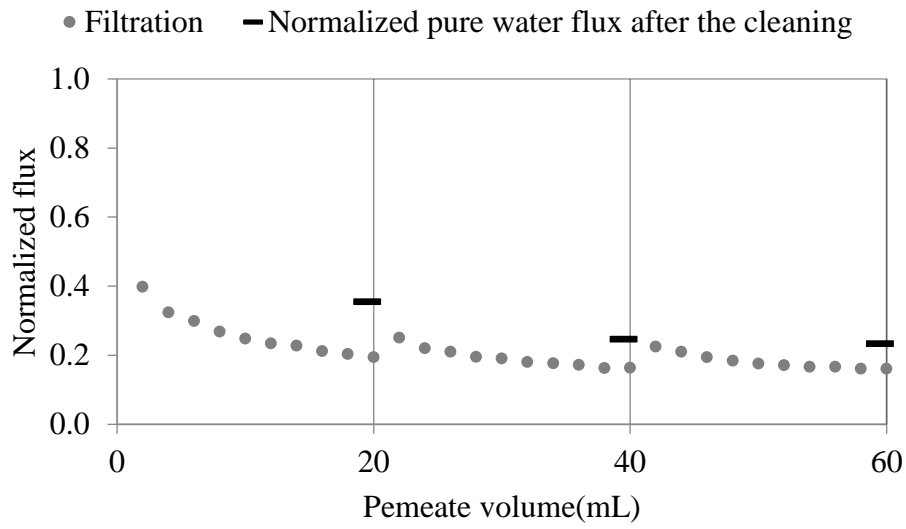
In Figure 3.15, yeast filtrations were done by applying *filtration and cleaning procedure 2*, and then cleaning time was increased from 5 minutes to 20 minutes to investigate how cleaning time affects the removal of the yeast fouling layer. Apart from cleaning time, all other experimental conditions remained unchanged.

Compared to plots illustrated in Figure 3.12-(b) and Figure 3.15-(a), flux ratios in the first filtrations are around 90% and 80% of the initial PWP, respectively. When we look at in Figure 3.13-(b) and Figure 3.15-(b) , irreversible fouling resistances are quite small (around 7-9% of the total resistance) for each filtration. As a result, cleaning for 5 minutes is adequate for microgels to change their size.

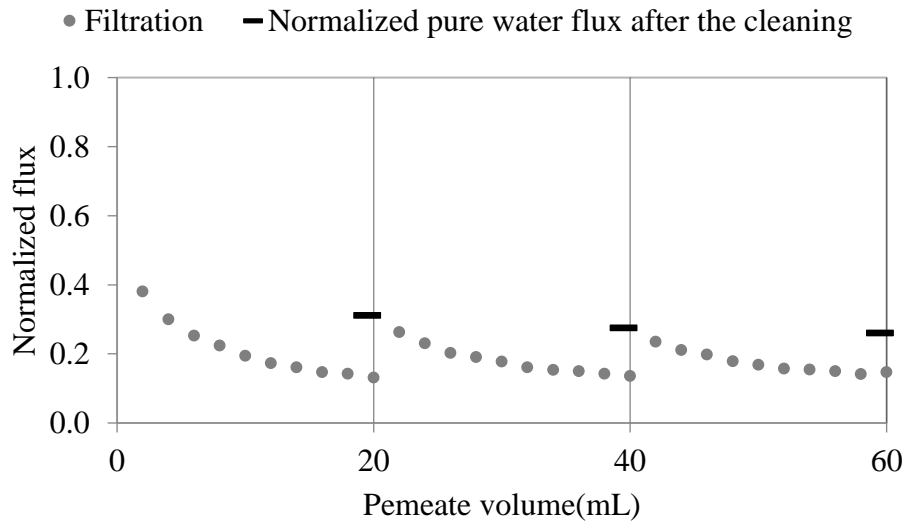
Microgel-added and microgel-free yeast experiment sets were done by taking 20 mL permeate for each serial filtration whose results are given in Figure 3.16 and Figure 3.17. With these performance tests, it was desired to observe the cleaning performance of P(SBMA) microgels when the thickness of the cake layer increases.

When we look at Figure 3.13 and Figure 3.17, it is seen that total fouling resistances were usually between  $30$  and  $40 \times 10^{12} \text{ m}^{-1}$ . The likely reason of that can be explained that permeate volume could not change the total fouling resistance since yeast filtrations were carried out by stirring at 150 rpm. Despite the fact that  $R_{\text{irr}}/R_{\text{fouling}}$  was quite low in the experiment set performed by taking 20 ml permeate, the total flux recovery at the end of the third filtration reduced to 25% of the initial PWP while it was approximately 70% in the filtration set by taking 10 ml permeate.

Looking at the normalized flux versus permeate volume plot of yeast filtrations (Figure 3.16), cleaning performance without microgel was quite similar with microgel-added one. This means addition of P(SBMA) microgels into the feed solution did not have a significant effect on the fouling removal while increasing permeate volume. It can be said that the force created by the size change of microgels was insufficient to remove cake fouling layer from the membrane surface.



a)



b)

Figure 3.16. Normalized flux graphs of yeast serial filtrations in the presence of 0.1 M NaCl without microgel (a) and with 0.1 g/L P(SBMA) microgels (b) (Cleaning via 0.5 M NaCl and permeate volume: 20 mL)

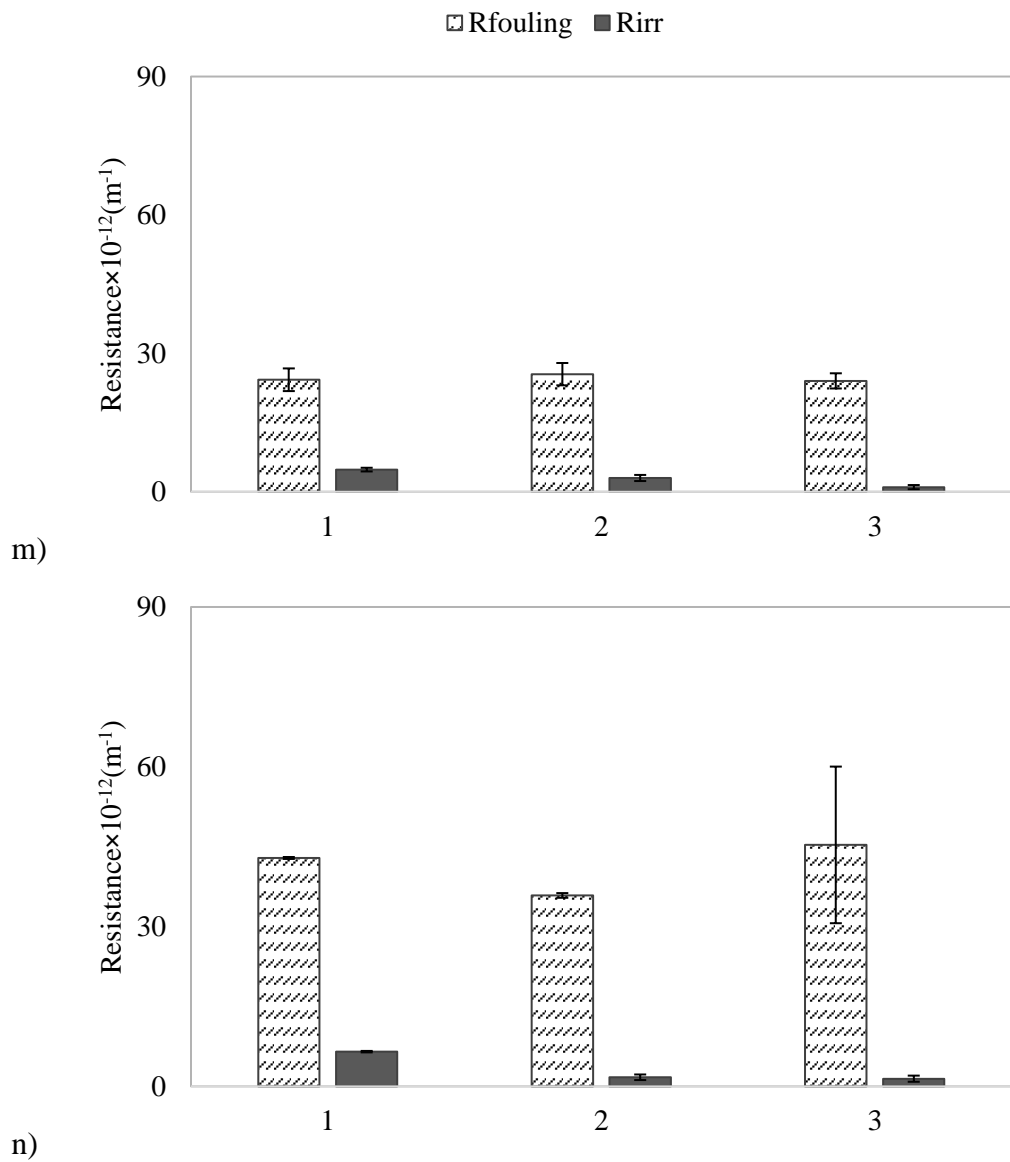


Figure 3.17. Resistance graphs of yeast serial filtrations in the presence of 0.1 M NaCl without microgel (a) and with 0.1 g/L P(SBMA) microgels (b) (Cleaning via 0.5 M NaCl and permeate volume: 20 mL)

Consequently, yeast fouling was the most reversible via addition of 0.1 g/L P(SBMA) to the feed in the presence of 0.1 M NaCl compared to 0.5 M NaCl. In other words, when microgels changed their size swollen to more swollen, cleaning efficiency of

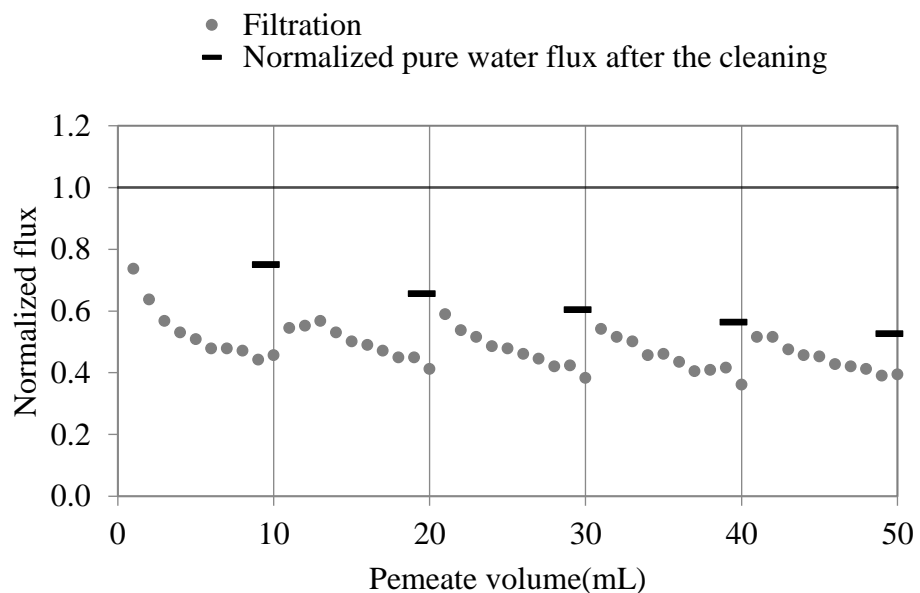
yeast fouling was higher. Moreover, less adsorptive fouling formed in the presence of 0.1 M NaCl where microgels are slightly swollen.

#### **3.3.4. P(SBMA) Microgel Deposition on PES20 Membrane for Yeast Fouling Removal**

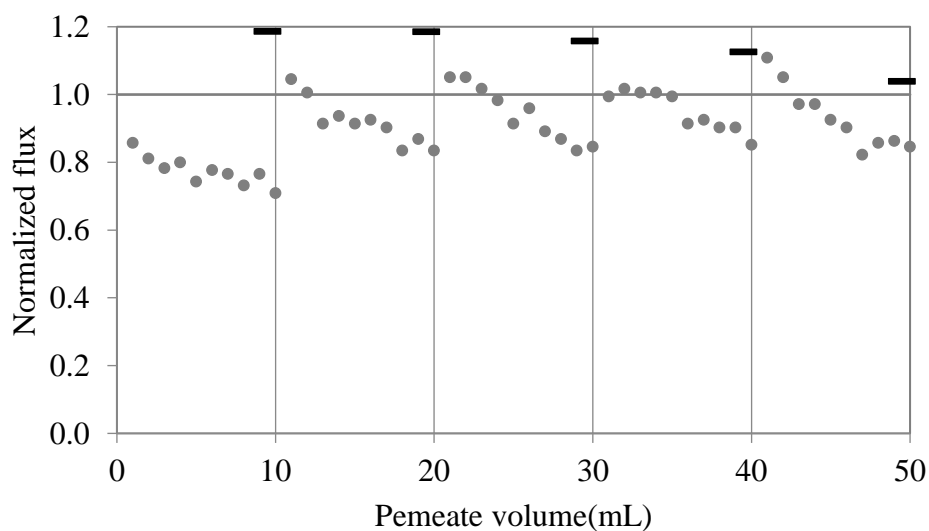
Since zwitterionic P(SBMA) microgels are insoluble in pure water, adding them into the feed in the absence of salt is not a convenient way to clean the membranes. For this reason, a different approach was used in this part, unlike performance tests given so far. Before filtration tests, membrane surface was covered with zwitterionic P(SBMA) microgels instead of co-depositing them with fouling layer. Accordingly, in these performance tests, zwitterionic P(SBMA) microgels were deposited on the surface of PES20 membrane in the presence of 0.5 M NaCl and then microgel deposited membrane was washed by UP water until salt was completely removed so that P(SBMA) microgels can shrink on the membrane surface. And then, filtrations were performed with 1 g/L yeast suspension in the absence of salt. Finally, fouled membranes were cleaned via 0.5 M NaCl after each filtration. These performance tests aimed to investigate cleaning efficiency of P(SBMA) microgels deposited on the membrane surface when they changed their size from shrunk to swollen. Similar tests, also, were performed without microgel deposition to compare the results.

Looking at Figure 3.18, P(SBMA) microgel deposition enabled higher cleaning performance compared to neat one. In the first filtration done on the neat PES20 membrane (Figure 3.18-a), filtration flux decreased more, 40% of the initial flux and then, these trends went on in the others. It, however, declined to around 70% of initial flux at the end of first cycle while in the other cycles, filtration fluxes have never declined to below 80% of initial flux when we look at the filtrations on P(SBMA) deposited one (Figure 3.18-b). Without microgel deposition, PWP went down roughly 50% of initial PWP at the end of the fifth filtration. On the other hand, in the filtrations done on the membrane with P(SBMA) deposition, it can be easily seen that, PWP values after the cleaning were usually more than the initial PWP. It can be explained

that P(SBMA) microgels slightly washed away after each cleaning as microgels transformed swollen phase during the cleaning, which may result in elution of them.



a)



b)

Figure 3.18. Normalized graphs of yeast serial filtrations on neat PES20 membrane (a) and on PES20 membrane with P(SBMA) deposited (b) (Cleaning via 0.5 M NaCl)

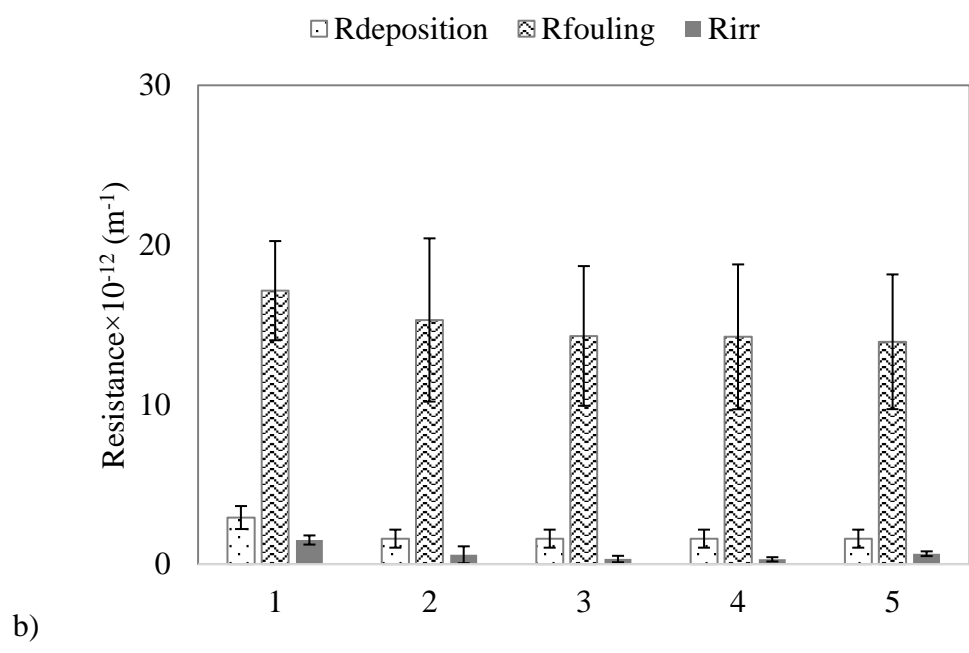
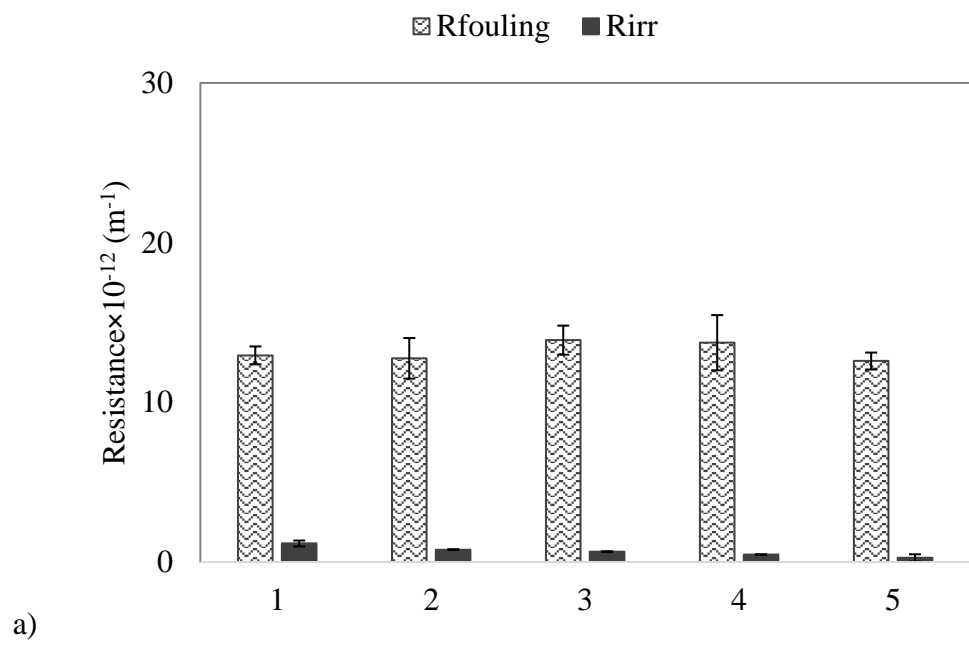


Figure 3.19. Resistance graphs of yeast serial filtrations on neat PES20 membrane (a) and on PES20 membrane with P(SBMA) deposited (b) (Cleaning via 0.5 M NaCl)

From Figure 3.19, total fouling resistances in the filtrations on the membrane with P(SBMA) deposition were higher than neat one due to effect of  $R_{\text{deposition}}$  which shows resistance of P(SBMA) microgel deposition.  $R_{\text{deposition}}$  was getting smaller after each cleaning because of elution of microgels during the cleaning. Accordingly, irreversible fouling resistances were less than the deposition resistance which explains why PWP values after the cleaning were higher than initial one (Figure 3.19-b).

Hence, efficient cleaning is possible by depositing zwitterionic P(SBMA) microgels on PES20 membrane before yeast filtration. This approach can still be applicable to existing membrane systems.

### 3.4. Adsorption Tests

As it was mentioned in the previous parts, PES based membranes are prone to adsorption of foulants due to their hydrophobic character. From normalized flux graphs, it was obviously seen that adsorptive fouling occurred at the beginning of the filtrations. As a result, static adsorption and adsorption resistance tests were done to understand the effect of adsorption on the membrane fouling.

In the BSA filtrations, the effect of adsorptive fouling was clearly understood since flux immediately declined to below 30% of the initial PWP. From Table 3.2, it is evident that PES20 membrane adsorbed BSA to quite a high extent ( $204 \pm 14 \mu\text{g}/\text{cm}^2$ ) which also explains why fluxes sharply go down during BSA filtration. When, surface of the membrane was covered with P(SBMA) microgels, BSA adsorption on it was relatively lower than naked one ( $160 \pm 18 \mu\text{g}/\text{cm}^2$ ). It can be said that zwitterionic microgels slightly decreased adsorption of BSA on the membrane surface thanks to hydration layer on the microgels.

Looking at the literature, similarly, Orooji et al. (2017) soaked PES membranes in 0.5 mg/mL BSA solution in the absence of NaCl at 6 h at room temperature and they found BSA adsorbed amount on PES is  $41 \mu\text{g}/\text{cm}^2$ . It can be said that salt addition in the system or/and adsorption test time increase BSA adhesion on PES membrane surface. Wang et al. (2017) stated that BSA adsorption on PES membrane was calculated as roughly  $15 \mu\text{g}/\text{cm}^2$  when PES membranes were soaked in 1 mg/ml BSA solution at 37 °C for 1 h. Moreover, Wu and coworkers (2018) performed BSA adsorption tests on PES membranes at about 1.5 h, 3 h and 4 h. They demonstrated that PES-BSA had a high adsorption capacity (192.38 mg/g) and a short adsorption equilibrium time (1.5 h).

Table 3.2. *BSA adsorption on PES20 membrane in the presence of NaCl and/or P(SBMA)*

<b>BSA adsorption on</b>	<b><math>\mu\text{g}/\text{cm}^2</math></b>
PES20 membrane in the presence of NaCl	204±14
PES20 membrane with P(SBMA) microgels deposited in the presence of NaCl	160±18

From Table 3.3, adsorption amount of HA with  $\text{CaCl}_2$  on the surface of PES25 membrane remained roughly same in the absence ( $132\pm 16 \mu\text{g}/\text{cm}^2$ ) and presence ( $118\pm 8 \mu\text{g}/\text{cm}^2$ ) of NaCl. Likewise, the membrane surface covered by P(SBMA) microgels in the presence and absence of salt adsorbed HA gel as  $135\pm 10 \mu\text{g}/\text{cm}^2$  and  $137\pm 3 \mu\text{g}/\text{cm}^2$ , respectively. It can be said that HA adsorptive fouling remains unchanged independently from addition of salt and P(SBMA) microgels into the system.

Table 3.3. *HA gel adsorption on PES25 membrane in the absence and presence of NaCl and/or P(SBMA)*

<b>HA gel adsorption on</b>	<b><math>\mu\text{g}/\text{cm}^2</math></b>
PES25 membrane in the presence of NaCl	132±16
PES25 membrane	118±8
PES25 membrane with P(SBMA) microgels deposited in the presence of NaCl	135±10
PES25 membrane with P(SBMA) microgels deposited	137±3

Finally, it was observed that PES20 membrane adsorbs yeast cells as a considerable amount ( $151\pm 71 \mu\text{g}/\text{cm}^2$ ), as well.

Table 3.4. *Yeast adsorption on PES20 membrane in the presence of NaCl*

<b>Yeast adsorption on</b>	<b><math>\mu\text{g}/\text{cm}^2</math></b>
PES20 membrane in the presence of NaCl	151±71

Additionally, adsorption resistance tests were performed for all foulants by measuring pure water permeance before and after the static adsorption experiments to find how much adsorptive fouling of BSA decreases the flux. As shown in Table 3.5, the results were compared with total fouling resistances and irreversible fouling resistances obtained from filtration tests. According to BSA adsorption resistance tests, flux decreased by  $24\pm 4\%$  of initial flux which brought  $9\pm 4\times 10^{12} \text{ m}^{-1}$  resistance due to adsorption. From HA gel adsorption resistance tests, it is found that HA gel caused  $12\pm 2\times 10^{12} \text{ m}^{-1}$  adsorptive fouling resistance which resulted in  $46\pm 1\%$  flux decline. Finally, from yeast adsorption resistance tests, flux decline was found as  $77\pm 9\%$ , which is quite high. This, also, led to  $15\pm 7\times 10^{12} \text{ m}^{-1}$  yeast adsorptive fouling resistance.

In details, while irreversible fouling resistances of both HA gel and Yeast are less than their adsorptive fouling resistances ( $R_{\text{adsorption}}$ ), irreversible fouling resistance of BSA is nearly as much as its adsorptive fouling resistance. It can be explained that BSA adsorption tendency is higher than HA gel and Yeast. In other words, BSA can immediately adsorb on the membrane surface compared to others since in the performance tests, filtration times varied between 15 minutes and 1 hour to collect 10 mL permeate while adsorption tests time was at least 24 hours to be sure that solution concentration reaches the equilibrium.

Table 3.5. Adsorption resistance test results compared with fouling resistances in the filtrations

<b>Foulant</b>	<b><math>R_{\text{fouling}}\times 10^{-12} \text{ (m}^{-1}\text{)}</math></b>	<b><math>R_{\text{irreversible fouling}}\times 10^{-12} \text{ (m}^{-1}\text{)}</math></b>	<b><math>R_{\text{adsorption}}\times 10^{-12} \text{ (m}^{-1}\text{)}</math></b>
BSA	$48\pm 7$	$9\pm 6$	$9\pm 4$
HA gel	$43\pm 28$	$1\pm 1$	$12\pm 2$
Yeast	$23\pm 9$	$2\pm 1$	$15\pm 7$

To sum up, adsorption tests provide consistent results with the filtration experiments. BSA is the most adsorptive foulant compared to HA and yeast cells.

### 3.5. Modification of PSBMA Microgels for Recovery

In the final part of this study, it was aimed to incorporate of magnetic particles into the P(SBMA) microgels to recover them from retentate stream by utilizing magnetic field and reuse them in the filtration system. Figure 3.20 schematically represents the recovery of iron decorated microgels from the retentate stream.

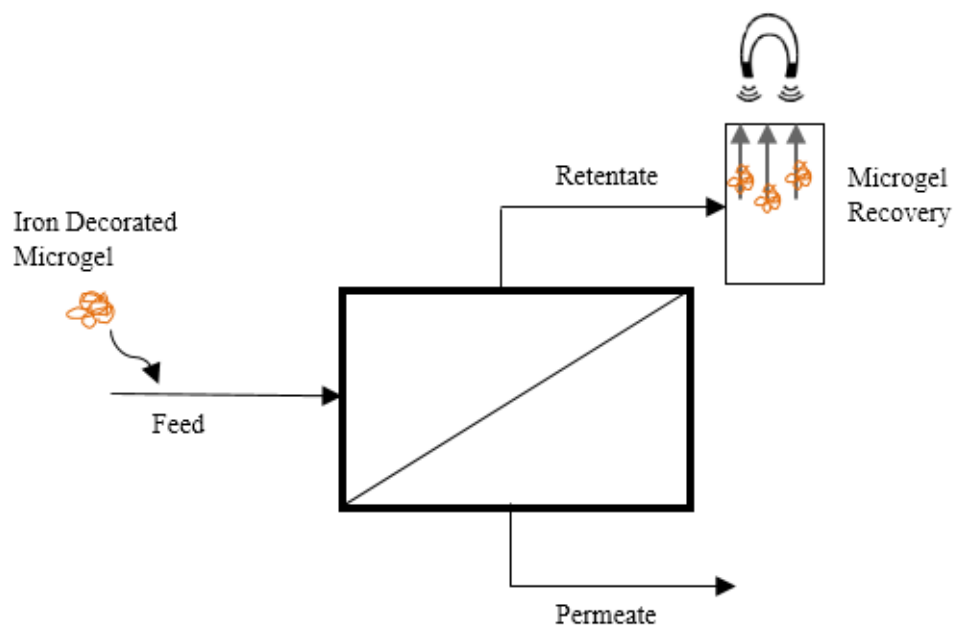
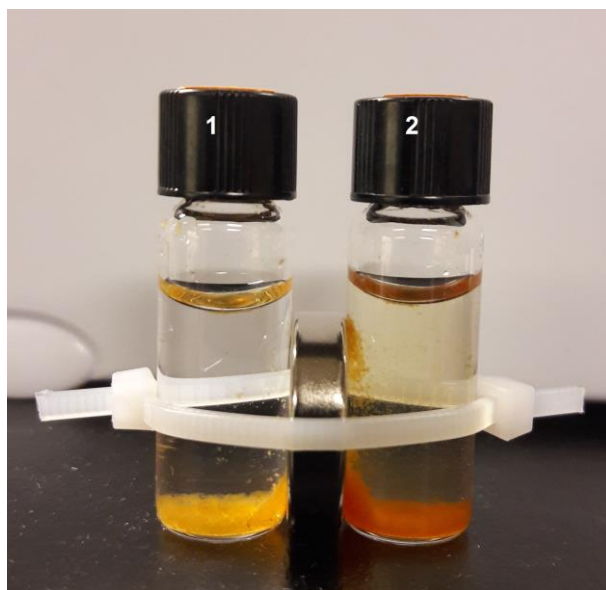


Figure 3.20. Schematic view of magnetic microgel recovery from retentate stream of the membrane process

To achieve this goal,  $\text{Fe}_2\text{O}_3$  nanoparticles produced by precipitation of an  $\text{Fe}^{+2}/\text{Fe}^{+3}$  solution were incorporated into zwitterionic P(SBMA) microgels obtained by inverse emulsion free-radical polymerization. Iron decorated microgel syntheses were done with two different concentrations of  $\text{Fe}^{+2}/\text{Fe}^{+3}$  in the solution to get different iron content in the zwitterionic microgels. Iron salt amounts used in the syntheses are given in Table 2.1 and Figure 3.21 shows modified P(SBMA) microgels with magnetic particles.



*Figure 3.21. Magnetic P(SBMA) particles*

The color of the magnetic microgels in Figure 3.21-1 which have less amount of iron oxide are orange while the other ones in Figure 3.21-2 have dark orange color because of higher amount of iron oxide. The magnetic properties of the microgels have been tested by placing magnets with strong pulling force between the magnetic microgels and it has been observed that a small portion of the microgels could be attracted by magnets. In this step, the magnetic features of these orange particles are not strongly enough.

In addition to this problem, particle size of iron decorated microgels which can be easily seen by naked eye is another obstacle. Large precipitates, which are not soluble in both pure water and brine solutions, were formed during the iron oxide decoration process. When they were filtered by a syringe filter (1  $\mu\text{m}$ ) for DLS measurement, all orange particles were hold by the filter. It can be said that large iron oxide particles form in the solution medium or cover the microgels instead of incorporation in the microgels.

In *standard procedure*, iron decoration was done via dispersing P(SBMA) in NaOH solution and microgels and dissolving iron salts in HCl solution. To solve these problems, magnetic particles were synthesized again by applying *alternative procedure 1* and *alternative procedure 2*. In the first one, both iron salts and zwitterionic microgels were dissolved together in HCl solution to create complex before producing magnetic particles. In the second one, in addition to *alternative procedure 1*, NaCl was added since P(SBMA) solubility increases via salt addition. By this way, it was considered that magnetic particles will easily incorporate with zwitterionic P(SBMA) microgels.

Table 3.6. *Elemental analysis of magnetic P(SBMA) particle by Energy-dispersive X-Ray (EDX) spectroscopy*

<b>Atomic Wt%</b>	<i>Standard Procedure</i>	<i>Alternative Procedure 1</i>	<i>Alternative Procedure 2</i>
	1000x	1000x	1000x
<b>C</b>	73.9	75.4	61.9
<b>O</b>	20.4	8.0	22.0
<b>N</b>	0.0	0.0	4.8
<b>S</b>	2.3	0.4	4.3
<b>Fe</b>	2.8	8.4	3.0
<b>Na</b>	0.2	0.3	1.7
<b>Cl</b>	0.4	8.4	2.3

Magnetic P(SBMA) particles containing iron salt amount given in Table 2.1-2 were synthesized by these three methods, separately. And then, EDX analysis of all was done to find how much iron incorporated into the zwitterionic microgels. As it is seen from Table 3.6, magnetic particles synthesized by *alternative procedure 1* have 8.4% iron while the other two have around 3%. Although particles with 8.4% iron have more iron compared to others, their magnetic property is still not sufficient to recover them from the system by the magnetic field. Accordingly, size of these new magnetic particles, which are quite big, is not appropriate for filtrations as well.

It is suggested that this modification procedure can be tried by adding iron particles in P(SBMA) microgel synthesis medium to get microgel-iron complexes during the synthesis.

## CHAPTER 4

### CONCLUSION

Proposed methods in this study aimed membrane fouling removal by adding zwitterionic P(SBMA) microgels in the feed during UF processes or deposition of them on the membrane surface before filtrations. Firstly, when P(SBMA) microgels were added into the feed in the presence of NaCl, they were co-deposited with cake layer in swollen phase during the filtration. After the filtration, membrane cleaning was performed via altering ionic strength in the solution medium, such as replacing retentate solution with pure water or more concentrated NaCl solution, in order to change microgel size from swollen to shrunk or swollen to more swollen. Secondly, before the filtration, P(SBMA) microgels were deposited on the membrane surface in the presence of 0.5 M NaCl where microgels maximally swell and washed with pure water for salt removal to shrink the microgels. After that, cake layer was formed on shrunk microgels during the filtration. Cleaning was performed via 0.5 M NaCl solution to alter microgels from shrunk to swollen. In these two methods, it was proposed that mechanical effects created by swelling and shrinking actions of ionic strength responsive P(SBMA) microgels break the fouling layer during the cleaning. Recently, fouling removal by utilizing stimuli responsive polymer has been studied in the literature via grafting these polymers on the membrane surface or blending them with other membrane materials to obtain stimuli responsive surfaces. Many researchers stated that these polymers improve non-fouling features and/or fouling release properties of membranes. Besides that, stimuli responsive surfaces have often been used to control permeate flow or pore size by changing stimulus intensity. However, there are very few studies related to cake layer removal from membrane surface by the size change of stimuli responsive polymeric microgels. In this study, it was proposed that addition of P(SBMA) microgels in the feed or deposition of them

on the membrane surface to clean the membranes easily can be applied to existing membrane processes since these zwitterionic microgels are freely found in the feed. By these methods, size change of P(SBMA) microgels could break or weaken cake layer formed during the filtration and accordingly improve the cleaning performance.

Zwitterionic P(SBMA) microgels can swell approximately 2.5 times of its own size in the presence of 0.5 M NaCl. The microgels could not provide an effective BSA fouling removal because of high amount of adsorptive fouling. HA gel fouling in the absence of NaCl was the most irreversible; however, when NaCl was in the feed, reversibility was similar with or without microgel which possibly means a looser cake layer formation in the presence of NaCl. Actuation force came from the size change of microgels could make yeast fouling more reversible compared to fouling with yeast in pure water or in 0.5 M NaCl. Additionally, P(SBMA) microgel deposition on the membrane surface before the filtration provided efficient yeast fouling removal.

Consequently, this study showed the effect of P(SBMA) microgel addition in the feed solution on fouling removal from PES UF membranes. In this purpose, BSA was chosen as a representative foulant for proteins, HA was selected as a model foulant for humic substances and finally, yeast was used as a representative bio-foulant. Use of zwitterionic P(SBMA) microgels into feed solutions could bring higher flux recovery and cleaning efficiency than microgel-free filtrations for all foulants. Especially, both addition of these microgels into the feed and depositing them on the membrane surface made yeast fouling easily cleanable. These novel physical cleaning methods can be applied to existing membrane processes to remove yeast-like foulants. Also, it is expected that these methods can provide a decrease of operating cost and increase membrane lifetime since a membrane can be used again and again by these methods.

## REFERENCES

- Adiga, S. P., Jin, C., Curtiss, L. A., Monteiro-Riviere, N. A., & Narayan, R. J. Nanoporous membranes for medical and biological applications. (2009). *Wiley Interdisciplinary Reviews: Nanomedicine and Nanobiotechnology*, 1(5), 568-581.
- Aksoy, C. (2018). *Responsive Polymer Particles for Fouling Removal During Membrane Filtrations*. METU Thesis.
- Bacchin, P., Aimar, P., & Field, R. . Critical and sustainable fluxes: Theory, experiments and applications. (2006). *Journal of Membrane Science*, 281(1-2), 42-69.
- Baker. (2004). *Membranes and Modules. Membrane Technology and Applications (2nd ed.)*. Chichester: J. Wiley.
- Baker, R. W. (2012). *Membrane Technology and Applications*. Hoboken: NJ: John Wiley & Sons.
- Bera, A., Kumar, C. U., Parui, P., & Jewrajka, S. K. Stimuli responsive and low fouling ultrafiltration membranes from blends of polyvinylidene fluoride and designed library of amphiphilic poly(methyl methacrylate) containing copolymers. (2015). *Journal of Membrane Science*, 137-147.
- Chen, S., & Jiang, S. An New Avenue to Nonfouling Materials. (2008). *Advanced Materials*, 20(2), 335-338.
- Cheng, G., Mi, L., Cao, Z., Xue, H., Yu, Q., Carr, L., & Jiang, S. Functionalizable and Ultrastable Zwitterionic Nanogels. . (2010). *Langmuir*, 26(10), 6883-6886.
- Chiang, Y., Chang, Y., Chuang, C., & Ruaan, R. A facile zwitterionization in the interfacial modification of low bio-fouling nanofiltration membranes. (2012). *Journal of Membrane Science*, 389, 76-82.

- Choi, H., Jung, Y., Han, S., Tak, T., & Kwon, Y. Surface modification of SWRO membranes using hydroxyl poly(oxyethylene) methacrylate and zwitterionic carboxylated polyethyleneimine. (2015). *Journal of Membrane Science* , 486, 97-105.
- Chung, D., Ito, Y., & Imanishi, Y. . (1994). Preparation of porous membranes grafted with poly(spiropyran-containing methacrylate) and photocontrol of permeability. . *Journal of Applied Polymer Science*, 51(12) , 2027-2033.
- Du, C., Deng, D., Shan, L., Wan, S., Cao, J., Tian, J., ... Gu, Y. A pH-sensitive doxorubicin prodrug based on folate-conjugated BSA for tumor-targeted drug delivery. (2013). *Biomaterials*, 34(12), 3087-3097.
- Fritzmann, C., Löwenberg, J., Wintgens, T., & Melin, T. State-of-the-art of reverse osmosis desalination. (2007). *Desalination*, 216(1-3), 1-76.
- Fröhlich, H., Villian, L., Melzner, D., & Strube, J. Membrane Technology in Bioprocess Science. (2012). *Chemie Ingenieur Technik*, n/a-n/a.
- Gao, W., Liang, H., Ma, J., Han, M., Chen, Z., Han, Z., & Li, G. Membrane fouling control in ultrafiltration technology for drinking water production: A review. (2011). *Desalination*, 272(1-3), 1-8.
- Gorey, C., & Escobar, I. C. N-isopropylacrylamide (NIPAAM) modified cellulose acetate ultrafiltration membranes. (2011). *Journal of Membrane Science*, 383(1-2), 272-279.
- Greenlee, L. F., Lawler, D. F., Freeman, B. D., Marrot, B., & Moulin, P. . (Water Research). Reverse osmosis desalination: Water sources, technology, and today's challenges. 2009, 43(9), 2317-2348.
- Hong, S., & Elimelech, M. Chemical and physical aspects of natural organic matter (NOM) fouling of nanofiltration membranes. (1997). *Journal of Membrane Science*, 132(2), 159-181.

- Huang, R., Kostanski, L., Filipe, C., & Ghosh, R. Environment-responsive hydrogel-based ultrafiltration membranes for protein bioseparation. (2009). *Journal of Membrane Science*, 336(1-2), 42-49.
- Jhan, Y., & Tsay, R. Salt effects on the hydration behavior of zwitterionic poly(sulfobetaine methacrylate) aqueous solutions. (2014). *Journal of the Taiwan Institute of Chemical Engineers*, 45(6), 3139-3145.
- Jonsson, G., & Johansen, P. Selectivity of ultrafiltration membranes influence of fouling and cleaning conditions. (1991). *Filtration & Separation*, 28(1), 23.
- Kaner, P., Hu, X., Thomas, S. W., & Asatekin, A. Self-Cleaning Membranes from Comb-Shaped Copolymers with Photoresponsive Side Groups. (2017). *ACS Applied Materials & Interfaces*, 9(15), 13619-13631.
- Kaner, P., Rubakh, E., Kim, D. H., & Asatekin, A. Zwitterion-containing polymer additives for fouling resistant ultrafiltration membranes. (2017). *Journal of Membrane Science*, 533, 141-159.
- Khulbe, K. C., Feng, C., & Matsuura, T. The art of surface modification of synthetic polymeric membranes. (2010). *Journal of Applied Polymer Science*, 115(2), 855-895.
- Kimura, K., Hane, Y., Watanabe, Y., Amy, G., & Ohkuma, N. Irreversible membrane fouling during ultrafiltration of surface water. (2004). *Water Research*, 38(14-15), 3431-3441.
- Lalani, R., & Liu, L. Synthesis, characterization, and electrospinning of zwitterionic poly(sulfobetaine methacrylate). (2011). *Polymer*, 52(23), 5344-5354.
- Li, J., Ma, G., Liu, H., & Liu, H. Yeast cells carrying metal nanoparticles. (2018). *Materials Chemistry and Physics*, 207, 373-379.
- Li, Q., Bi, Q., Zhou, B., & Wang, X. Zwitterionic sulfobetaine-grafted poly(vinylidene fluoride) membrane surface with stably anti-protein-fouling performance via

- a two-step surface polymerization. (2012). *Applied Surface Science*, 258(10), 4707-4717.
- Meng, J., Cao, Z., Ni, L., Zhang, Y., Wang, X., Zhang, X., & Liu, E. A novel salt-responsive TFC RO membrane having superior antifouling and easy-cleaning properties. (2014). *Journal of Membrane Science*, 461, 123-129.
- Miao, R., Wang, L., Zhu, M., Deng, D., Li, S., Wang, J., ... Lv, Y. Effect of Hydration Forces on Protein Fouling of Ultrafiltration Membranes: The Role of Protein Charge, Hydrated Ion Species, and Membrane Hydrophilicity. (2016). *Environmental Science & Technology*, 51(1), 167-174.
- Mores, W. D., & Davis, R. H. Yeast-Fouling Effects in Cross-Flow Microfiltration with Periodic Reverse Filtration. (2003). *Industrial & Engineering Chemistry Research*, 42(1), 130-139.
- Mulder, M. Membrane Processes. (1996). *Basic Principles of Membrane Technology*, 280-415.
- Ngang, H., Ahmad, A., Low, S., & Ooi, B. Adsorption-desorption study of oil emulsion towards thermo-responsive PVDF/SiO<sub>2</sub>-PNIPAM composite membrane. (2017). *Journal of Environmental Chemical Engineering*, 5(5), 4471-4482.
- Nyström. (1996). Humic acid as a fouling agent in filtration. *Desalination*, 106(1-3), 79-87.
- Park, Y. S., Ito, Y., & Imanishi, Y. (1998). Photocontrolled Gating by Polymer Brushes Grafted on Porous Glass Filter. *Macromolecules*, 31(8), 2606-2610.
- Potts, D., Ahlert, R., & Wang, S. A critical review of fouling of reverse osmosis membranes. (1981). *Desalination*, 36(3), 235-264.
- Roche, M., Rondeau, P., Singh, N. R., Tarnus, E., & Bourdon, E. The antioxidant properties of serum albumin. (2008). *FEBS Letters*, 582(13), 1783-1787.

- Rubio-Retama, J., Zafeiropoulos, N. E., Frick, B., Seydel, T., & López-Cabarcos, E. Investigation of the Relationship between Hydrogen Bonds and Macroscopic Properties in Hybrid Core–Shell  $\gamma$ -Fe<sub>2</sub>O<sub>3</sub>–P(NIPAM-AAS) Microgels. (2010). *Langmuir*, 26(10), 7101-71.
- Shi, Q., Su, Y., Zhao, W., Li, C., Hu, Y., Jiang, Z., & Zhu, S. Zwitterionic polyethersulfone ultrafiltration membrane with superior antifouling property. (2008). *Journal of Membrane Science*, 319(1-2), 271-278.
- Shi, X., Tal, G., Hankins, N. P., & Gitis, V. Fouling and cleaning of ultrafiltration membranes: A review. (2014 ). *Journal of Water Process Engineering*, 1, 121-138.
- Shorrock, C., & Bird, M. Membrane Cleaning: Chemically Enhanced Removal of Deposits Formed During Yeast Cell Harvesting. (1998). *Food and Bioproducts Processing*, 76(1), 30-38.
- Sigon, F., Servida, A., & Galashev, A. E. Molecular dynamic study of hydrophilicity of the NaCl molecule. (1996). *Journal of Structural Chemistry*, 37(2), 260-269.
- Srisurichan, S., Jiratananon, R., & Fane, A. Humic acid fouling in the membrane distillation process. (2005). *Desalination*, 174(1), 63-72.
- Sutzkover-Gutman, I., Hasson, D., & Semiat, R. Humic substances fouling in ultrafiltration processes. (2010). *Desalination*, 261(3), 218-231.
- Taheri, A., Sim, L., Chong, T., Krantz, W., & Fane, A. Prediction of reverse osmosis fouling using the feed fouling monitor and salt tracer response technique. (2015). *Journal of Membrane Science*, 475, 433-444.
- Tamada, M., Asano, M., Spohr, R., Vetter, J., Trautmann, C., Yoshida, M., ... Omichi, H. Preparation of hydrolyzed pH responsive ion track membrane. (1995). *Macromolecular Rapid Communications*, 16(1), 47-51.

- Trushinski, B. J., Dickson, J. M., Childs, R. F., & McCarry, B. E. . (1993). Photochemically modified thin-film composite membranes. I. Acid and ester membranes. *Journal of Applied Polymer Science*, 48(2), 187-198.
- van de Ven, W. J. (2008). *Towards optimal saving in membrane operation*. Enschede.
- Van der Bruggen, B. Chemical modification of polyethersulfone nanofiltration membranes: A review. (2009). *Journal of Applied Polymer Science*, 114(1), 630-642.
- Vrijenhoek, E. M., Hong, S., & Elimelech, M. Influence of membrane surface properties on initial rate of colloidal fouling of reverse osmosis and nanofiltration membranes. (2001). *Journal of Membrane Science*, 188(1), 115-128.
- Wang, Y., Wang, T., Su, Y., Peng, F., Wu, H., & Jiang, Z. Protein-adsorption-resistance and permeation property of polyethersulfone and soybean phosphatidylcholine blend ultrafiltration membranes. (2006). *Journal of Membrane Science*, 270(1-2), 108-114.
- Weh, K., Noack, M., Hoffmann, K., Schröder, K., & Caro, J. (2002). Change of gas permeation by photoinduced switching of zeolite-azobenzene membranes of type MFI and FAU. . *Microporous and Mesoporous Materials*, 54(1-2), 15-26.
- You, M., Wang, P., Xu, M., Yuan, T., & Meng, J. Fouling resistance and cleaning efficiency of stimuli-responsive reverse osmosis (RO) membranes. (2016). *Polymer*, 103, 457-467.
- Yu, S., Chen, Z., Liu, J., Yao, G., Liu, M., & Gao, C. Intensified cleaning of organic-fouled reverse osmosis membranes by thermo-responsive polymer (TRP). (2012). *Journal of Membrane Science*, 392-393, 181-191.
- Yu, S., Liu, X., Liu, J., Wu, D., Liu, M., & Gao, C. Surface modification of thin-film composite polyamide reverse osmosis membranes with thermo-responsive

- polymer (TRP) for improved fouling resistance and cleaning efficiency. (2011). *Separation and Purification Technology*, 76(3), 283-291.
- Yuan, W., & Zydney, A. L. Humic Acid Fouling during Ultrafiltration. (2000). *Environmental Science & Technology*, 34(23), 5043-5050.
- Zhai, G., Toh, S. C., Tan, W. L., Kang, E. T., Neoh, K. G., Huang, C. C., & Liaw, D. J. Poly(vinylidene fluoride) with Grafted Zwitterionic Polymer Side Chains for Electrolyte-Responsive Microfiltration Membranes. (2003). *Langmuir*, 19(17), 7030-7037.
- Zhao, J., Shi, Q., Luan, S., Song, L., Yang, H., Shi, H., ... Stagnaro, P. Improved biocompatibility and antifouling property of polypropylene non-woven fabric membrane by surface grafting zwitterionic polymer. (2011). *Journal of Membrane Science*, 369(1-2).



## APPENDICES

### A. Static Adsorption Tests

Membrane areas used in tests, solution volumes, solution absorbance and concentration measured before and after the tests are shown in the following tables for BSA, HA gel and yeast cells. Membranes deposited with P(SBMA) microgels or not with certain areas were kept into foulant solutions in the presence/absence of NaCl for at least a day. Then, adsorbed amounts by the membranes were calculated using concentration differences before and after the tests.

#### *BSA adsorption on neat PES20 membrane in the presence of NaCl*

Prepared solution concentration for the tests is 0.5 g/L BSA and 1 M NaCl whose value measured using UV spectrometry is 0.312 g/L BSA.

Table A.1. *BSA adsorption test results on neat PES20 membrane in the presence of NaCl*

<b>PES20 Membrane Area (cm<sup>2</sup>)</b>	<b>Solution Volume (mL)</b>	<b>Absorbance at 280 nm after a day</b>	<b>Concentration after a day(g/L)</b>	<b>Adsorbed amount (mg)</b>	<b>Adsorbed amount (µg/cm<sup>2</sup>)</b>
16	20	0.216	0.348	3.039	190
9	12	0.212	0.342	1.902	211
9	12	0.215	0.346	1.843	205
20	20	0.193	0.310	3.791	190
12	20	0.227	0.366	2.680	223
				<b>Average</b>	<b>204±14</b>

BSA adsorption on PES20 membrane with P(SBMA) microgel deposited in the presence of NaCl

Prepared solution concentration for the tests is 0.5 g/L BSA and 1 M NaCl whose value measured using UV spectrometry is 0.301 g/L BSA.

Table A.2. BSA adsorption test results on PES20 membrane with P(SBMA) microgel deposited in the presence of NaCl

<b>PES20 Membrane Area (cm<sup>2</sup>)</b>	<b>Solution Volume (mL)</b>	<b>Absorbance at 280 nm after a day</b>	<b>Concentration after a day(g/L)</b>	<b>Adsorbed amount (mg)</b>	<b>Adsorbed amount (µg/cm<sup>2</sup>)</b>
4.9	8	0.231	0.373	0.876	179
4.9	8	0.247	0.399	0.667	136
4.9	8	0.236	0.381	0.810	165
				<b>Average</b>	<b>160±18</b>

HA gel adsorption on neat PES25 membrane in the presence of NaCl

Prepared solution concentration for the tests is 0.5 g/L HA, 1 mM CaCl<sub>2</sub> and 1 M NaCl whose value measured using UV spectrometry is 0.320 g/L HA.

Table A.3. HA gel adsorption test results on neat PES25 membrane in the presence of NaCl

PES25 Membrane Area (cm <sup>2</sup> )	Solution Volume (mL)	Absorbance at 254 nm after a day	Concentration after a day(g/L)	Adsorbed amount (mg)	Adsorbed amount (µg/cm <sup>2</sup> )
9	12	0.295	0.219	1.222	136
8	10	0.289	0.214	1.063	133
9	15	0.345	0.256	0.972	108
6	10	0.309	0.229	0.915	152
				<b>Average</b>	<b>132±16</b>

HA gel adsorption on neat PES25 membrane

Prepared solution concentration for the tests is 0.5 g/L HA and 1 mM CaCl<sub>2</sub> whose value measured using UV spectrometry is 0.485 g/L HA.

Table A.4. HA gel adsorption test results on neat PES25 membrane

PES25 Membrane Area (cm <sup>2</sup> )	Solution Volume (mL)	Absorbance at 254 nm after a day	Concentration after a day(g/L)	Adsorbed amount (mg)	Adsorbed amount (µg/cm <sup>2</sup> )
6	8	0.538	0.399	0.693	116
6	8	0.543	0.402	0.664	111
6	9	0.539	0.399	0.773	129
				<b>Average</b>	<b>118±8</b>

HA gel adsorption on PES25 membrane with P(SBMA) microgel deposited in the presence of NaCl

Prepared solution concentration for the tests is 0.5 g/L HA, 1 mM CaCl<sub>2</sub> and 1 M NaCl whose value measured using UV spectrometry is 0.320 g/L HA.

Table A.5. HA gel adsorption test results on PES25 membrane with P(SBMA) microgel deposited in the presence of NaCl

PES25 Membrane Area (cm <sup>2</sup> )	Solution Volume (mL)	Absorbance at 254 nm after a day	Concentration after a day(g/L)	Adsorbed amount (mg)	Adsorbed amount (µg/cm <sup>2</sup> )
4.9	9	0.338	0.250	0.630	129
4.9	9	0.338	0.250	0.630	129
4.9	9	0.323	0.239	0.730	149
<b>Average</b>					<b>135±10</b>

HA gel adsorption on PES25 membrane with P(SBMA) microgel deposited

Prepared solution concentration for the tests is 0.5 g/L HA and 1 mM CaCl<sub>2</sub> whose value measured using UV spectrometry is 0.485 g/L HA.

Table A.6. HA gel adsorption test results on PES25 membrane with P(SBMA) microgel deposited

PES25 Membrane Area (cm <sup>2</sup> )	Solution Volume (mL)	Absorbance at 254 nm after a day	Concentration after a day(g/L)	Adsorbed amount (mg)	Adsorbed amount (µg/cm <sup>2</sup> )
4.9	8	0.542	0.401	0.670	137
4.9	8	0.539	0.399	0.687	140
4.9	8	0.545	0.404	0.652	133
<b>Average</b>					<b>137±3</b>

Yeast adsorption on neat PES20 membrane in the presence of NaCl

Prepared solution concentration for the tests is 0.5 g/L yeast and 0.5 M NaCl whose value measured using UV spectrometry is 0.562 g/L yeast.

Table A.7. *Yeast adsorption test results on neat PES20 membrane in the presence of NaCl*

<b>PES20 Membrane Area (cm<sup>2</sup>)</b>	<b>Solution Volume (mL)</b>	<b>Absorbance at 600 nm after a day</b>	<b>Concentration after a day(g/L)</b>	<b>Adsorbed amount (mg)</b>	<b>Adsorbed amount (µg/cm<sup>2</sup>)</b>
13.4	25	0.031	0.441	3.032	226
13.4	25	0.036	0.517	1.132	84
13.4	25	0.034	0.486	1.892	141
				<b>Average</b>	<b>151±71</b>

## B. Adsorption Resistance Tests

PWPs for each membrane were measured before tests and then, membranes were kept into 25 mL foulant solutions during at least a day. After that, PWPs of them were measured again. These values, flux decline, membrane and adsorption resistances were given in the following tables for each foulant.

### Adsorption Resistance Tests of BSA

Prepared solution concentration for the tests is 0.5 g/L BSA and 0.5 M NaCl.

Table B.1. *Adsorption resistance test results of BSA*

---

<b>PWP before the test</b>	<b>PWP after the test (1 day)</b>	<b>Flux Decline (%)</b>	<b>Membrane Resistance</b>	<b>Adsorption Resistance</b>
61	42	32	6	9
80	65	19	4	6
36	28	22	10	13
	<b>Average</b>	<b>24±4</b>		<b>9±4</b>

### Adsorption Resistance Tests of HA gel

Prepared solution concentration for the tests is 0.5 g/L HA, 1 mM CaCl<sub>2</sub> and 0.5 M NaCl.

Table B.2. Adsorption resistance test results of HA gel

---

<b>PWP before the test</b>	<b>PWP after the test (1 day)</b>	<b>Flux Decline (%)</b>	<b>Membrane Resistance</b>	<b>Adsorption Resistance</b>
50	27	46	7	14
72	40	45	5	9
54	28	49	6	13
	<b>Average</b>	<b>46±1</b>		<b>12±2</b>

### Adsorption Resistance Tests of Yeast

Prepared solution concentration for the tests is 0.5 g/L Yeast and 0.1 M NaCl.

Table B.3. Adsorption resistance test results of Yeast

---

<b>PWP before the test</b>	<b>PWP after the test (1 day)</b>	<b>Flux Decline (%)</b>	<b>Membrane Resistance</b>	<b>Adsorption Resistance</b>
88	31	65	4	8
182	37	80	2	10
109	16	86	3	24
	<b>Average</b>	<b>77±9</b>		<b>15±7</b>

### C. Calibration Lines

#### BSA Calibration Line

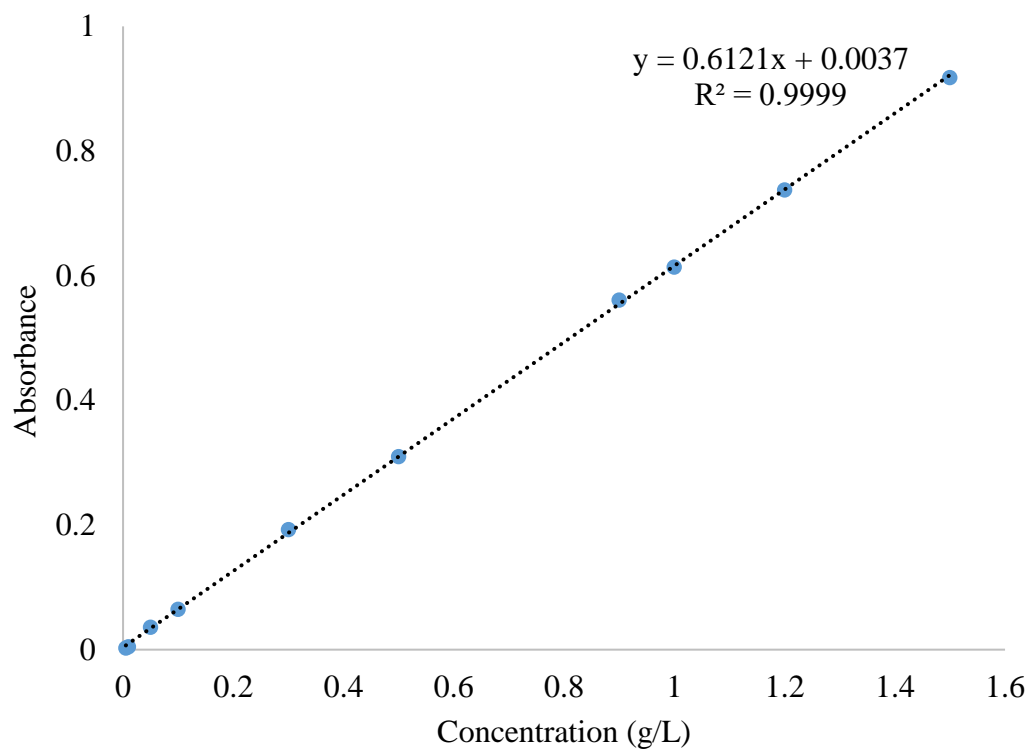


Figure C.1. BSA calibration line at 280 nm in UV/Visible Spectroscopy

HA Calibration Line

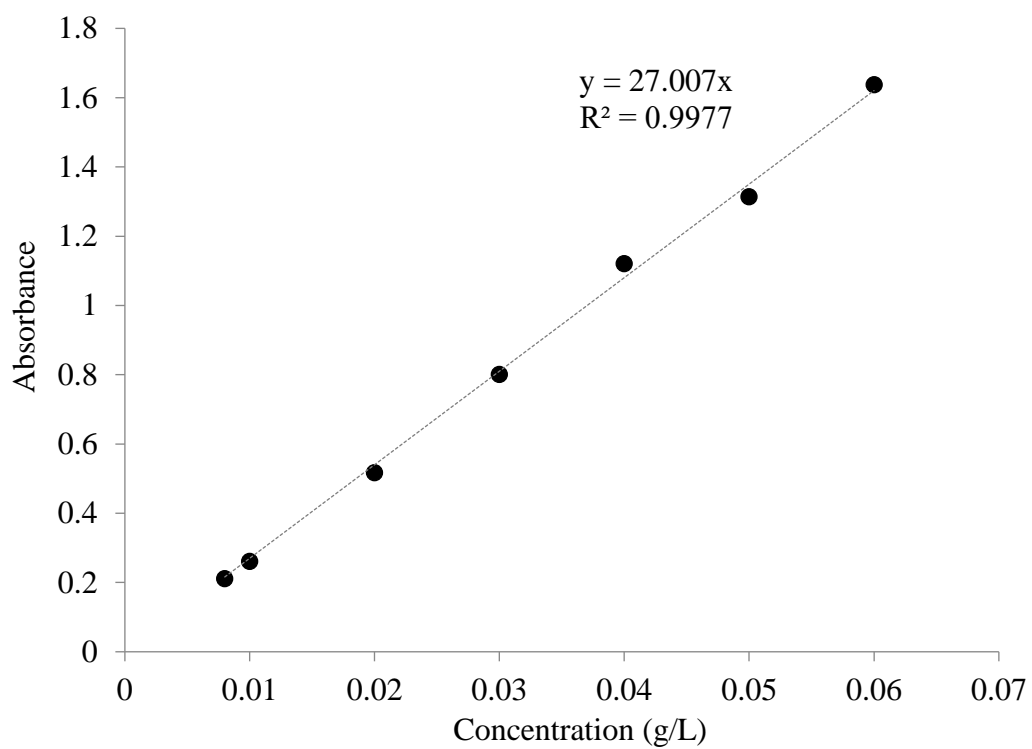


Figure C.2. HA calibration line at 254 nm in UV/Visible Spectroscopy

Yeast Calibration Line (Optical Density)

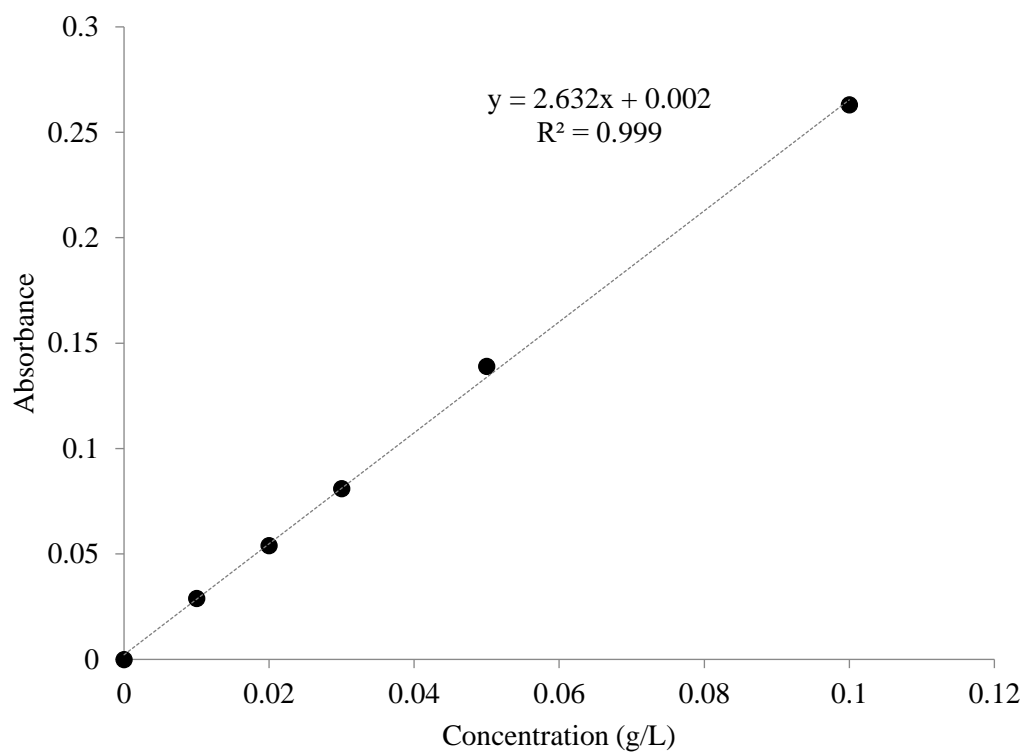


Figure C.3. Yeast calibration line at 600 nm in UV/Visible Spectroscopy

#### D. XPS Analysis of P(SBMA) Microgels

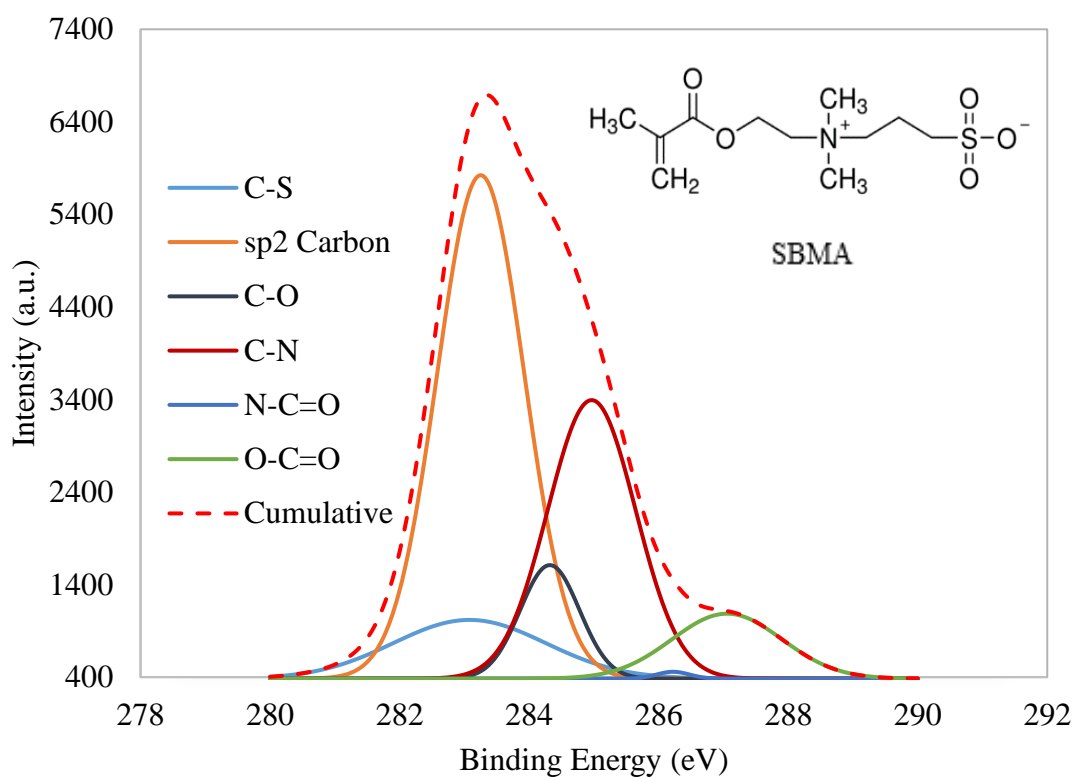


Figure D.1. C1s XPS spectra of P(SBMA) microgels

Zwitterionic P(SBMA) microparticles were analyzed by XPS analysis. Figure D.1 is C1s core-level spectra of P(SBMA) which was curve-fitted with six peak components: carbon-carbon single bonds (sp<sup>2</sup> carbon: 283 eV), carbon attached to sulfur (C-S: 283 eV), carbon adjacent to oxygen (C-O: 284 eV), carbon bonded to oxygen and nitrogen (N-C=O: 286 eV), carbon adjacent to nitrogen (C-N: 285 eV) and carbon attached to two oxygen atoms with single and double bonds (O-C=O: 287 eV). SBMA includes all bonds shown in Figure D.1, except carbon atoms attached to both oxygen and nitrogen (N-C=O) coming from BA which is a cross-linker.

## E. Filtration Data

### *BSA Filtrations*

All BSA filtrations were performed at room T and 2 bar TMP without stirring using PES20 membranes. 40 ml feed containing 1 g/L BSA was prepared in the presence of 0.5 M NaCl with or without P(SBMA) microgels and 10 ml permeate was collected for each filtration.

Table E.1. *BSA filtration data table*

<b>Filt. #</b>	<b>Feed</b>	<b>Cleaning</b>	<b>Initial PWP</b>	<b>Filtration Permeance</b>	<b>PWP after the cleaning</b>
1	BSA 0.5 M NaCl	Pure water	74	6	17
2			17	6	16
3			16	5	14
4	BSA 0.5 M NaCl 0.01 g/L PSBMA	Pure water	97	7	25
5			25	7	20
6			20	7	18
7	BSA 0.5 M NaCl 0.1 g/L PSBMA	Pure water	147	7	54
8			54	6	46
9			46	7	42

Table E.1. (Continued)

<b>Filt. #</b>	<b>R<sub>membrane</sub></b>	<b>R<sub>fouling</sub></b>	<b>R<sub>irr</sub></b>	<b>Irrevesibility %</b>	<b>Flux Recovery %</b>	<b>R%</b>
1	5	58	16	28	23	100
2	21	43	1	3	95	100
3	22	43	4	10	85	100
4	4	52	11	21	26	100
5	15	41	3	8	81	100
6	18	38	6	6	89	100
7	2	50	4	8	37	100
8	6	48	1	2	84	100
9	7	41	1	2	91	100

### HA Gel Filtrations

All HA gel filtrations were performed at room T and 2 bar TMP without stirring using PES25 membranes. 40 ml feed containing 1 g/L HA and 2 mM CaCl<sub>2</sub> was prepared in the absence/presence of 0.5 M NaCl with or without P(SBMA) microgels and 10 ml permeate was collected for each filtration.

Table E.2. HA gel filtration data table

<b>Filt. #</b>	<b>Feed</b>	<b>Cleaning</b>	<b>Initial PWP</b>	<b>Filtration Permeance</b>	<b>PWP after the cleaning</b>
10			55	14	29
11	HA gel	Pure water	29	12	24
12			24	12	22
13	HA gel	Pure water	67	17	47
14	0.5 M NaCl 0.1 g/L PSBMA		47	19	46
15			46	19	43
16	HA gel	Pure water	85	19	67
17	1 M NaCl 0.1 g/L PSBMA		67	24	58
18			58	22	54
19			34	13	28
20	HA gel 0.5 M NaCl	Pure water	28	13	30
21			30	13	27

Table E.2. (Continued)

<b>Filt. #</b>	<b>R<sub>membrane</sub></b>	<b>R<sub>fouling</sub></b>	<b>R<sub>irr</sub></b>	<b>Irrevesibility %</b>	<b>Flux Recovery %</b>	<b>R%</b>
10	8±1	35±16	5±0.7	15±4	53	
11	13±1	37±20	2±0.2	6±1	83	88±1
12	15±1	34±19	1±0.2	4±1	92	
13	10±3	46±28	3±0.1	6±0	70	
14	12±4	42±29	0±0.6	-1±2	98	84±1
15	12±3	42±29	1±0.1	2±0	93	
16	8±3	37±20	1±0.8	3±3	79	
17	9±3	34±23	1±0.3	2±1	87	80±6
18	9±2	36±23	2±0.9	5±4	93	
19	10±0	48±31	2±0.3	5±1	81	
20	12±0	42±27	0±1.2	1±4	107	82±2
21	13±1	40±25	1±0.2	2±1	90	

### *Yeast Filtrations*

All yeast filtrations were performed at room T and 2 bar TMP with stirring at 150 rpm using PES20 membranes. 40 ml feed containing 1 g/L yeast was prepared in the absence/presence of 0.5 M/0.1 M NaCl with or without P(SBMA) microgels and 10 ml permeate was usually collected for each filtration (Only in filt. #46-51, permeate volume was 20 ml).

Table E.3. *Yeast filtration data table (1)*

<b>Filt. #</b>	<b>Feed</b>	<b>Cleaning</b>	<b>Initial PWP</b>	<b>Filtration Permeance</b>	<b>PWP after the cleaning</b>
22	Yeast 0.5 M NaCl 0.1 g/L PSBMA	Pure water	69	13	16
23			16	11	12
24			120	9	12
25	Yeast 0.5 M NaCl 0.2 g/L PSBMA	Pure water	113	22	29
26			29	15	23
27			23	14	21
28	Yeast 0.1 M NaCl	0.5 M NaCl	57	20	36
29			36	19	26
30			26	19	24
31			24	19	23
32			23	18	22
33			22	12	18

Table E.3. (Continued)

<b>Filt. #</b>	<b>R<sub>membrane</sub></b>	<b>R<sub>fouling</sub></b>	<b>R<sub>irr</sub></b>	<b>Irrevesibility %</b>	<b>Flux Recovery %</b>	<b>R%</b>
22	4±1	46±7	14±3	29±3	23	
23	17±5	37±5	5±2	13±4	77	100
24	22±7	42±6	2±1	5±3	97	
25	3	43	9	22	85	
26	13	38	4	10	81	100
27	16	36	2	4	91	
28	5±2	23±9	2±1	10±2	62	
29	7±4	22±8	2±2	8±4	74	
30	9±5	22±7	1±1	5±2	91	100
31	10±6	21±6	1±0	3±1	94	
32	11±6	20±8	1±0	3±2	98	
33	11±6	32±17	2±1	7±1	83	

Table E.4. *Yeast filtration data table (2)*

<b>Filt. #</b>	<b>Feed</b>	<b>Cleaning</b>	<b>Initial PWP</b>	<b>Filtration Permeance</b>	<b>PWP after the cleaning</b>
34			85	36	82
35			82	37	74
36	Yeast 0.1 M NaCl 0.1 g/L PSBMA	0.5 M NaCl	74	35	66
37			66	33	60
38			60	28	55
39			55	28	52
40	Yeast 0.1 M NaCl	0.5 M NaCl	75	17	37
41	0.2 g/L PSBMA		37	17	34
42			34	17	29
43	Yeast 0.1 M NaCl	0.5 M NaCl	43	13	33
44	0.1 g/L PSBMA	(20 min)	33	13	28
45			28	12	23
46	Yeast 0.1 M NaCl	0.5 M NaCl	142	31	53
47	(20 ml permeate)		53	27	40
48			40	26	34
49	Yeast 0.1 M NaCl	0.5 M NaCl	124	16	39
50	0.1 g/L PSBMA (20 ml permeate)		39	17	34
51			34	18	32

Table E.4. (Continued)

<b>Filt. #</b>	<b>R<sub>membrane</sub></b>	<b>R<sub>fouling</sub></b>	<b>R<sub>irr</sub></b>	<b>Irrevesibility %</b>	<b>Flux Recovery%</b>	<b>R%</b>
34	6±2	33±17	2±2	4±4	96	
35	8±3	32±15	1±1	4±0	91	
36	9±4	32±15	1±0	3±0	89	100
37	10±5	30±12	1±0	2±1	91	
38	10±4	30±9	0±0	1±2	92	
39	10±4	34±13	3±2	6±4	94	
40	4±1	40±2	6±1	14±1	50	
41	10±0	36±2	1±0	4±1	91	100
42	12±0	37±1	1±1	3±2	87	
43	8±1	65±16	6±3	8±3	76	
44	14±3	57±9	2±0	4±0	85	100
45	16±3	56±4	4±2	8±2	83	
46	3±0	24±2	5±0	20±0	37	
47	8±1	25±2	3±1	12±1	75	100
48	11±1	24±2	1±0	4±2	86	
49	3±0	43±0	7±0	15±0	31	
50	9±0	36±0	2±1	5±1	88	100
51	11±0	45±15	1±1	3±0	95	

*Yeast Filtrations using neat and P(SBMA) microgel deposited PES20 membranes*

Yeast filtrations were performed at room T and 2 bar TMP with stirring at 150 rpm using neat and P(SBMA) microgel deposited PES20 membranes, separately. 40 ml feed containing 1 g/L yeast was prepared in the absence of NaCl and 10 ml permeate was collected for each filtration.

Table E.5. *Yeast filtration data table using neat and P(SBMA) microgel deposited PES20 membranes*

<b>Filt. #</b>	<b>Feed</b>	<b>Cleaning</b>	<b>Initial PWP</b>	<b>Filtration Permeance</b>	<b>PWP after the cleaning</b>	<b>R<sub>deposition</sub></b>
52			91	42	68	-
53			68	38	60	-
54	Yeast (neat PES20)	0.5 M NaCl	60	35	55	-
55			55	33	52	-
56			52	36	48	-
57			59	42	70	3±1
58	Yeast (microgel deposited PES20)	0.5 M NaCl	70	49	70	2±1
59			70	50	68	2±1
60			68	50	68	2±1
61			66	50	61	2±1

Table E.5. (Continued)

<b>Filt. #</b>	<b>R<sub>membrane</sub></b>	<b>R<sub>fouling</sub></b>	<b>R<sub>irr</sub></b>	<b>Irrevesibility %</b>	<b>Flux Recovery %</b>	<b>R%</b>
52	4±0	13±1	1±0	9±1	75	
53	5±0	13±1	1±0	6±1	88	
54	6±0	14±1	1±0	5±1	92	100
55	6±0	14±2	0±0	3±0	93	
56	7±0	13±1	0±0	2±2	93	
57	4±0	17±3	2±0	9±0	119	
58	6±1	15±5	1±1	3±2	119	
59	6±1	14±4	0±0	2±1	116	100
60	7±1	14±5	0±0	2±0	113	
61	7±1	14±4	1±0	5±0	104	